

DESIGN AND ANALYSIS OF SPHERICAL CODES

BY

JON HAMKINS

B.S., California Institute of Technology, 1990

M.S., University of Illinois, 1993

THESIS

Submitted in partial fulfillment of the requirements
for the degree of Doctor of Philosophy in Electrical Engineering
in the Graduate College of the
University of Illinois at Urbana-Champaign, 1996

Urbana, Illinois

© Copyright by Jon Hamkins, 1996

DESIGN AND ANALYSIS OF SPHERICAL CODES

Jon Hamkins, Ph.D.
Department of Electrical and Computer Engineering
University of Illinois at Urbana-Champaign, 1996
Kenneth Zeger, Advisor

A spherical code is a finite set of points on the surface of a multidimensional unit radius sphere. This thesis gives two constructions for large spherical codes that may be used for channel coding and for source coding. The first construction “wraps” a finite subset of any sphere packing onto the unit sphere in one higher dimension. The second construction is analogous to the recursive construction of laminated lattices. Both constructions result in codes that are asymptotically optimal with respect to minimum distance, and the first construction can be efficiently used as part of a vector quantizer for a memoryless Gaussian source. Both constructions are structured so that codepoints may be identified without having to store the entire codebook. For several different rates, the distortion performance of the proposed quantizer is superior than previously published results of quantizers with equivalent complexities.

The construction techniques are motivated by the relationship between asymptotically large spherical codes and sphere packings in one lower dimension. It is shown that the asymptotically maximum density of a k -dimensional spherical code equals the maximum density of a sphere packing in \mathbb{R}^{k-1} . Similar relationships hold for the quantization coefficient and covering thickness. Previously published upper and lower bounds on the size of spherical codes of given minimum distances are analyzed and shown to be loose for asymptotically small minimum distances.

ACKNOWLEDGMENTS

I would like to thank my advisor Professor Ken Zeger for his excellent guidance and encouragement. I also would like to thank Professors Alexander Vardy, Bruce Reznick, Bruce Hajek, Dick Blahut, and Herbert Edelsbrunner for reading this thesis and serving on my committee. I thank Dakshi Agrawal for printing the thesis and depositing it for me. To my family, especially my parents, I owe a great deal. They have always encouraged me to strive for excellence. Finally, I would like to thank my fiancée, Meera Srinivasan, without whom this thesis would not have been possible.

TABLE OF CONTENTS

CHAPTER	PAGE
1 INTRODUCTION	1
2 PRELIMINARIES	4
2.1 Lattices	4
2.1.1 Lattice definition, generator matrices, and fundamental parallelotopes . .	4
2.1.2 The root lattices A_k , D_k , E_8 , and \mathbb{Z}^k	6
2.1.3 Spheres in k dimensions, packings, and density	7
2.1.4 Covering radius and covering thickness	10
2.1.5 Theta series	10
2.1.6 Voronoi regions, holes, and Delaunay cells	10
2.1.7 Dual lattices	11
2.1.8 Normalized second moment	12
2.1.9 Laminated lattices	12
2.2 Quantization	15
2.2.1 Vector quantization	15
2.2.2 Properties of optimal vector quantizers	17
2.2.3 Index assignment	18
2.2.4 Lattice quantization	18
2.3 Spherical Codes	19
3 BOUNDS ON THE DENSITY OF A SPHERICAL CODE	28
3.1 Asymptotic Spherical Code Density	28
3.2 Upper Bounds on Density	29
3.2.1 Fejes Tóth upper bound ($k = 3$)	29
3.2.2 Coxeter upper bound ($k \geq 4$)	31
3.3 Lower Bounds on Density	32
3.3.1 Yaglom lower bound	32
3.3.2 Wyner lower bound	33
3.3.3 Concatenated spherical codes	34
3.3.4 Spherical codes from binary codes	38
3.3.5 Apple-peeling spherical codes	39
3.3.6 Codes from other structures	40
3.3.7 Unstructured spherical codes	41
3.3.7.1 Physical model	41

3.3.7.2	Algorithm motivation and description	41
3.3.7.3	Implementation	43
3.3.7.4	Other algorithms for unstructured codes	44
3.4	Comparisons	46
3.5	Conclusions	47
4	WRAPPED SPHERICAL CODES	52
4.1	Introduction	52
4.2	Construction of Wrapped Spherical Codes	52
4.3	Asymptotic Density of the Wrapped Spherical Code	58
4.4	Decoding Wrapped Spherical Codes	62
4.5	Conclusions	64
5	LAMINATED SPHERICAL CODES	65
5.1	Introduction	65
5.2	Construction of Laminated Spherical Codes	66
5.3	Asymptotic Density of the Laminated Spherical Code	73
5.4	Decoding Laminated Spherical Codes	77
5.5	Conclusions	80
6	WRAPPED SPHERICAL CODES AS VECTOR QUANTIZERS FOR A MEMORYLESS GAUSSIAN SOURCE	81
6.1	Introduction	81
6.2	Properties of Vectors from a Memoryless Gaussian Source	82
6.3	A Wrapped Spherical Vector Quantizer	87
6.3.1	Structure of the codebook	87
6.3.2	Shape-gain rate allocation	88
6.3.3	Index assignment	90
6.4	Operational Complexity	91
6.5	Performance Analysis	92
6.6	Simulations and Comparisons	96
6.6.1	Average distortion computation	96
6.6.2	Confidence intervals of the simulations	97
6.6.3	Comparisons	98
6.7	Improvements and Extensions of the Basic Construction	100
6.7.1	Vector quantization of the gain	100
6.7.2	Allowing the shape codebook to depend on the gain	102
6.7.3	Allowing the gain codebook to depend on the shape	104
6.7.4	Non-Gaussian sources	105
6.8	Conclusions	106
7	CONCLUSIONS	108
	APPENDIX A GENERATOR MATRICES OF LATTICES	110

APPENDIX B THE ASYMPTOTIC NATURE OF PARAMETERS OTHER THAN DENSITY	114
B.1 Quantization Coefficient	114
B.2 Covering Thickness	116
APPENDIX C PROOF OF LEMMAS	118
C.1 Proof of Lemma 3.1	118
C.2 Proof of Lemma 3.7	121
C.3 Proof of Lemma 4.1	122
C.4 Proof of Lemma 6.2	124
C.5 Proof of Lemma 6.3	124
APPENDIX D PROOF OF THEOREM 5.1	128
REFERENCES	133
VITA	139

LIST OF TABLES

Table	Page
2.1 Properties of some well-known lattices.	8
3.1 Iterative spherical code optimization algorithm.	42
3.2 Three-dimensional code sizes at various minimum distances.	47
3.3 Four-dimensional code sizes at various minimum distances.	47
6.1 Algorithmic description of $W\Lambda$ -SVQ on a digital communication channel.	89
6.2 Comparison of the operating complexity of $W\Lambda_{24}$ -SVQ to other quantization schemes for a memoryless Gaussian source.	92
6.3 Optimization algorithm for construction of $W\Lambda$ -SVQ at rate R	96
6.4 Comparison of the performance of various quantization schemes for a memoryless Gaussian source.	100
6.5 Iterative algorithm to allocate number of points per shell.	104

LIST OF FIGURES

Figure	Page
2.1 Parameters of two lattices.	5
2.2 Part of the A_2 lattice packing.	9
2.3 (a) The first layer used to construct Λ_2 . (b) The first two layers of Λ_2 . A point of the second layer is directly above a hole of the first layer. (c) The first three layers of Λ_2	13
2.4 A quantizer in a digital communications system.	16
2.5 Output vs. input of a scalar quantizer.	16
2.6 The relationship between minimum distance d and minimum separating angle θ . . .	20
2.7 Sphere packing density and spherical code density.	22
2.8 The ratio of the asymptotic density of various spherical codes to that of wrapped spherical codes constructed from the densest known packings, as a function of dimension.	23
2.9 Eight shells of lattice A_2 , normalized to unit radius.	26
2.10 Eight shells of the face-centered cubic lattice (D_3), normalized to unit radius.	27
3.1 The density of a spherical code with minimal angle separation θ is at most the percentage of area covered in the spherical triangle formed by three mutually touching caps of angular radius $\theta/2$	30
3.2 Yaglom's mapping consists of taking the part of a lattice within Ω_{k-1} , shown at left, and projecting it out of the page onto the surface of Ω_k , shown at right.	32
3.3 A small section of the surface of the unit sphere.	43
3.4 The algorithm in action.	45
3.5 Comparison of three-dimensional spherical codes.	48
3.6 Comparison of four-dimensional spherical codes.	49
3.7 Comparison of eight-dimensional spherical codes.	50
4.1 Part of a wrapped code constructed from \mathbb{Z}^2	54
4.2 (a) Geometrical interpretation of $f(X)$. (b) Annuli.	54
4.3 Notation used in proof of Lemma 5.	57
5.1 (a) Eleven scaled one-dimensional spherical codes. (b) Two-dimensional code derived from the scaled one-dimensional codes by projecting codepoints up and down. (c) Five scaled two-dimensional codes. (d) Three-dimensional code derived from the two-dimensional codes by projecting codepoints out of the page, where codepoints are the centers of the caps.	67

5.2	The sphere is partitioned into annuli, buffer zones, and wasted regions.	69
5.3	Relation between r_i and r_{i-1}	70
5.4	(a) A finite subset of Λ_2 . (b) LSC(3, .3), before projection. (c) LSC(3, .3) after projection.	74
5.5	Comparison of apple-peeling, laminated, and wrapped spherical codes.	75
6.1	$X = (X_1, \dots, X_k)$ is formed from an i.i.d. $N(0, 1)$ source.	85
6.2	Comparison of VQs for the memoryless Gaussian source.	99
6.3	A universal quantizer.	105
C.1	Mapping part of Ω_k to \mathbb{R}^{k-1}	119

LIST OF SYMBOLS

A_k	k -dimensional zero-sum root lattice
B', B	buffer zones of a wrapped or laminated spherical code
\mathcal{C}	a spherical code or vector quantizer codebook
$\mathcal{C}(k, d)$	a k -dimensional spherical code with minimum distance d
$\mathcal{C}^A(k, d)$	apple-peeling code on Ω_k with minimum distance d
c_k	subcovering radius of laminated lattice Λ_k
$c(k, \phi)$	spherical cap on Ω_k with angular radius ϕ
$c_X(k, \phi)$	spherical cap centered at $X \in \Omega_k$ and with angular radius ϕ
\mathcal{D}	decoder component of a vector quantizer
D	average distortion of a vector quantizer
D_g	gain distortion of WA–SVQ
D_k	k -dimensional checkerboard root lattice
D_s	shape distortion of WA–SVQ
d	minimum distance between points of a set
d_Λ	minimum distance between points of lattice Λ
\mathcal{E}	encoder component of a vector quantizer
E_6, E_7, E_8	Gosset's root lattices
$F_n(t)$	student's t -distribution with n degrees of freedom
$F_k(\alpha)$	Schläfli's function
$f_X(Y)$	probability density function of a multidimensional Gaussian random vector
f', f	functions from Ω_k to \mathbb{R}^{k-1} used in defining the wrapped spherical code

$G(\Pi)$	normalized second moment of region Π
$G_{r,k}$	quantization coefficient of \mathbb{R}^k , under r th norm distortion measure
\mathcal{H}_m	Hadamard matrix of order m
$H(\mathcal{P})$	hole of the set \mathcal{P} lying within the convex hull of \mathcal{P}
$H_{r,k}$	quantization coefficient of Ω_k , under r th norm distortion measure
$h(X)$	hole associated with $X \in \Lambda_{k-1}^{(l)}$
l_k	layer number of laminated lattice Λ_k
$\text{LSC}(k, d)$	k -dimensional laminated spherical code with minimum distance d
$M(k, d)$	size of largest k -dimensional spherical code with minimum distance d
$O(\cdot)$	asymptotic notation
$Q(X)$	the output of a vector quantizer whose input is X
$Q(x)$	complementary error function defined by $Q(x) = \frac{1}{\sqrt{2\pi}} \int_x^\infty e^{-x^2/2} dx$
R_i	the i th encoder cell of a vector quantizer
S_k	$(k-1)$ -dimensional content (“surface area”) of Ω_k
$S(c(k, \theta))$	$(k-1)$ -dimensional content (“surface area”) of $c(k, \theta)$
V_k	k -dimensional content (“volume”) of Ω_k
$V(\Pi)$	volume of region Π
$\text{WA-SC}(k, d)$	k -dimensional wrapped spherical code with minimum distance d
WA-SVQ	wrapped spherical vector quantizer whose underlying lattice is Λ
Y_i	the i th output of a vector quantizer
$\alpha(x)$	a scaling factor used in the definition of f
$\beta(x, y)$	Beta function defined by $\beta(x, y) = \frac{\Gamma(x)\Gamma(y)}{\Gamma(x+y)}$
$\Delta_{\mathcal{C}}$	density of spherical code \mathcal{C}
Δ_k^{pack}	maximum density among all k -dimensional sphere packings
$\Delta_k^{\text{s.c.}}$	asymptotically maximum k -dimensional spherical coding density
$\Delta(k, d)$	maximum density over all $\mathcal{C}(k, d)$
$\Gamma(x)$	Gamma function defined by $\Gamma(x) = \int_0^\infty e^{-t} t^{x-1} dt$

Λ	a lattice
Λ_k	a k -dimensional laminated lattice
Λ_{24}	Leech lattice (24-dimensional laminated lattice)
$\Lambda_{k-1}^{(l)}$	l th layer within Λ_k ; a translation of Λ_{k-1}
Ω_k	k -dimensional unit sphere
ϕ_i	angular separation of i th annulus of a wrapped spherical code
$\overline{\phi}$	$\max\{\phi_i\}$
$\underline{\phi}$	$\min\{\phi_i\}$
τ	average kissing number of a lattice
Θ	covering thickness (density)
θ	minimum angular separation between points of a spherical code
ξ_i	latitude of i th annulus of a wrapped spherical code
$\overline{\xi}(x)$	smallest latitude greater than $ x $
$\underline{\xi}(x)$	largest latitude less than $ x $

CHAPTER 1

INTRODUCTION

This thesis concerns the design of spherical codes. A spherical code is a finite set of points on the surface of a multidimensional unit radius sphere. For a given code size, one may position the points on the sphere so as to maximize or minimize one of a number of parameters, including the minimum distance between points, the quantization coefficient, the covering radius, the probability of error, the integration error, the kissing number, and the indexing complexity. The choice of parameter to optimize depends on the application. Some examples include signaling on a Gaussian channel [30, 49]; spherical vector quantization [2]; efficient searches of k -dimensional space [3]; numerical evaluation of integrals on spheres [64]; and the computation of the minimum energy configuration of point charges on a sphere, for chemistry and physics applications [65].

Most spherical code research has concentrated on maximizing the minimum distance between codepoints, given the code size (or equivalently, maximizing the number of points that maintain a given minimum distance). This problem is sometimes referred to as *Tammes's Problem*, after the Dutch botanist who demonstrated experimentally that the pores on the spherical pollen grains of flowers were often located at the vertices of certain Platonic solids [86]. Since that time, much work has been done to find the best spherical codes, using mappings from binary codes [19–21], shells of lattices [1, 12, 81], permutations of a set of initial vectors [8, 80], simulated annealing or repulsion-energy methods [18, 51, 65], concatenations of lower dimensional codes [98], projections of lower dimensional objects [18, 95, 97], and other means [29, 30, 33–35, 49, 85]. Each of these codes provides a lower bound on the largest possible spherical code having a given minimum distance. Many upper bounds have also been found [5, 16, 17, 23, 48, 54, 55, 70, 74]. The problem of determining the maximum number of

equal-sized nonoverlapping spheres that can simultaneously touch a central sphere—the kissing number problem—is a special case of designing spherical codes.

The methods mentioned above have produced the best (largest) known spherical codes for a given minimum distance. However, none of the spherical coding methods above performs well in a fixed dimension as the minimum distance decreases. That is, the ratio of the largest code size provided by the methods above to the tightest upper bound on the code size does not approach one in the limit as the minimum distance approaches zero. This is unfortunate, since large code sizes become more practical as the speed and memory of computers increase.

This thesis makes four main contributions. The first, given in Chapter 3, is a characterization of asymptotically optimal k -dimensional spherical codes designed with respect to minimum distance. This characterization equates the asymptotically optimal k -dimensional spherical code density to the optimal sphere packing density in $k - 1$ dimensions. Previously known bounds on the size of spherical codes are recast in terms of the new characterization, which highlights the strength and weakness of each bound, asymptotically. Analogous characterizations of asymptotically optimal k -dimensional spherical codes with respect to quantization coefficient and covering thickness are included in Appendix B.

The second and third contributions, presented in Chapters 4 and 5, are two different designs of structured spherical codes that are asymptotically optimal with respect to the minimum distance parameter:

1. *Wrapped spherical codes.* A finite subset of any sphere packing in \mathbb{R}^{k-1} is mapped to the k -dimensional unit sphere in such a way that much of the structure of the sphere packing is preserved.
2. *Laminated spherical codes.* Techniques used to construct a laminated lattice in \mathbb{R}^{k-1} are exploited to construct codes on the k -dimensional sphere. The resulting spherical codes have much of the structure of laminated lattices.

Both wrapped and laminated spherical codes produce asymptotically optimal codes with respect to the minimum distance parameter. Each method has distinct advantages over the other, making neither method better than the other in all cases. This represents work previously published [38–42].

The fourth contribution of the thesis, presented in Chapter 6, is the demonstration that wrapped spherical codes make excellent quantizers. A scalar memoryless Gaussian source is blocked into k -dimensional vectors and encoded by a shape-gain vector quantizer. The shape codebook is the wrapped spherical code from Chapter 4. The gain codebook is iteratively generated by the Lloyd algorithm. In particular, the 24-dimensional Leech lattice is wrapped to \mathbb{R}^{25} to obtain the best performance known for quantizers of similar complexity at rates of 3 bits/sample or higher.

CHAPTER 2

PRELIMINARIES

This chapter reviews basic terminology and results regarding lattices, quantization, and spherical codes. Lattices are one of the fundamental building blocks of the spherical code constructions presented in Chapters 4 and 5. A basic understanding of quantization is necessary for the quantizer described in Chapter 6. There is little in this chapter that cannot be found in other sources; the definitions and summary of results contained in this chapter are included to make the thesis self-contained. The lattice and spherical code review closely follows the notation of [14], which has become a standard reference in this field. The review of quantization will follow the notation of [31].

2.1 Lattices

The definitions and summary of results in this section are extensively used in Chapters 4 to 6. The notation of [14] is followed closely.

2.1.1 Lattice definition, generator matrices, and fundamental parallelotopes

A *lattice* is the closure of a finite set of basis vectors $v_1, \dots, v_m \in \mathbb{R}^k$ under integer vector addition. The elements of a lattice are called *lattice points*. For example, the hexagonal lattice, denoted A_2 , can be defined as the set of vectors

$$\left\{ i(1, 0) + j \left(\frac{1}{2}, \frac{\sqrt{3}}{2} \right) : i, j \in \mathbb{Z} \right\},$$

and $(3, \sqrt{3})$ is a lattice point of A_2 . In this case, $v_1 = (1, 0)$ and $v_2 = (1/2, \sqrt{3}/2)$ are basis vectors of the two-dimensional lattice. The lattice contains an infinite number of lattice points;

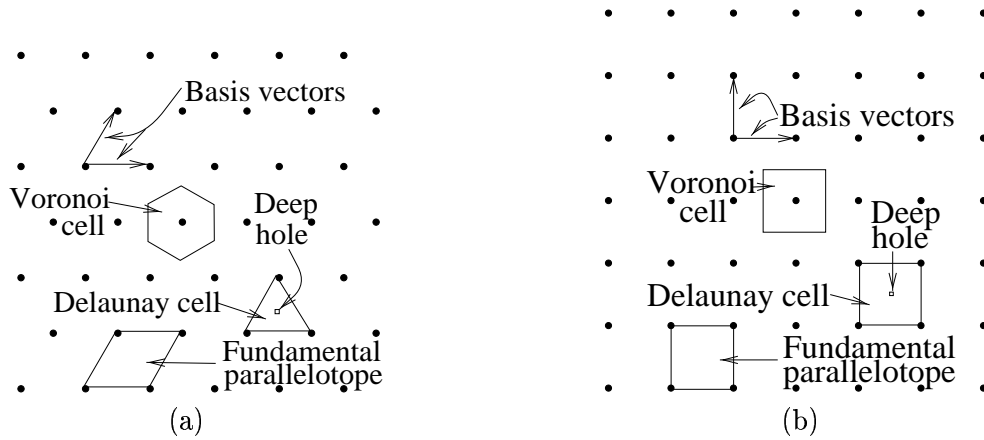


Figure 2.1 Parameters of two lattices. (a) The A_2 lattice. (b) The \mathbb{Z}^2 lattice.

a finite subset of this lattice is shown in Figure 2.1(a). If a subset of a lattice is itself a lattice (possibly of a lower dimension), then the subset is said to be a *sublattice*. For example, \mathbb{Z} is a sublattice of A_2 . The basis vectors may be placed in the rows of a matrix, called a *generator matrix*, so that when a row vector with integer coordinates premultiplies the matrix, the result is a lattice point. Thus, a generator matrix for A_2 is

$$M = \begin{bmatrix} 1 & 0 \\ \frac{1}{2} & \frac{\sqrt{3}}{2} \end{bmatrix},$$

and if $s = (i, j) \in \mathbb{Z}^2$, then sM is a point of A_2 . A lattice does not have a unique generator matrix. For example, the negation of a generator matrix is another generator matrix for the same lattice.

The *minimum distance* d_Λ of a lattice Λ is the smallest Euclidean distance between two distinct lattice points. If vectors v_1, \dots, v_k are a set of basis vectors for the lattice, then the set of points

$$\{t_1v_1 + \dots + t_kv_k : 0 \leq t_i < 1\}$$

is a *fundamental paralleloptope* of the lattice. Since there is no unique set of basis vectors for a lattice, there is no unique fundamental paralleloptope of the lattice. Nonetheless, every fundamental paralleloptope tiles the span of the basis vectors over the real field. That is, a fundamental paralleloptope repeated infinitely fills the whole space. A fundamental paralleloptope also contains exactly one lattice point. If M is a generator matrix for a lattice, then from linear

algebra, $\det(MM^T)$ is the square of the volume of a fundamental parallelotope; this squared volume is independent of the basis vectors used to construct the generator matrix M .

Altering the scale or orientation of a lattice leaves many of its properties unchanged. Consequently, two lattices are *equivalent* if one can be obtained from the other by a rotation and scale change. Because of this equivalence class, any lattice may be embedded in a higher-dimensional space. For example, the hexagonal lattice is also described by the generator matrix

$$M' = \begin{bmatrix} 1 & -1 & 0 \\ 0 & 1 & -1 \end{bmatrix}.$$

With this generator matrix, a point of the hexagonal lattice is an element of \mathbb{Z}^3 . If (x, y, z) is a lattice point, then $x + y + z = 0$; thus, using M' , the hexagonal lattice is contained in a plane of \mathbb{R}^3 . Also, the minimum distance between lattice points is two, while if M is used as defined above, the minimum distance is one. As a result, the squared volume of the fundamental region is also different. Although the lattices constructed by M and M' are equivalent, it will be important in the remainder of the thesis to fix a particular minimum distance for each lattice used, which will also fix the volume of a fundamental parallelotope.

2.1.2 The root lattices A_k , D_k , E_8 , and \mathbb{Z}^k

The definitions and basic properties of some well-known lattices are given here. The lattices A_k , D_k , E_k and \mathbb{Z}^k are called *root lattices* because of an association with the root systems of certain Lie algebras. An explanation of this association is not necessary to define these lattices, however, and is beyond the scope of this thesis. One way to define these lattices is by

$$\begin{aligned} \mathbb{Z}^k &\equiv \{(X_1, \dots, X_k) : X_k \in \mathbb{Z}\} \\ A_k &\equiv \{(X_1, \dots, X_{k+1}) \in \mathbb{Z}^{k+1} : X_1 + \dots + X_{k+1} = 0\} \\ D_k &\equiv \{(X_1, \dots, X_k) \in \mathbb{Z}^k : X_1 + \dots + X_k \text{ is even}\} \\ E_8 &\equiv \{(X_1, \dots, X_8) : \text{all } X_i \in \mathbb{Z} \text{ or all } X_i \in \mathbb{Z} + 1/2, \sum X_i \text{ is even}\}. \end{aligned}$$

The A_k lattice is called the *hexagonal lattice* for $k = 2$, the *face-centered cubic lattice* for $k = 3$, and in general, the *zero-sum root lattice*. The A_3^* lattice is called the *body-centered cubic lattice*, and is described in Section 2.1.7. The D_k lattice is called the *k-dimensional checkerboard lattice*. When $k = 3$, this lattice is equivalent to the face-centered cubic lattice. The E_8 lattice is called

the *Gosset lattice*. The properties of each of these lattices and their duals are included in Table 2.1. For completeness, the generator matrices for these important lattices are included in Appendix A.

2.1.3 Spheres in k dimensions, packings, and density

The surface of the unit radius k -dimensional Euclidean sphere is denoted by¹

$$\Omega_k \equiv \left\{ (x_1, \dots, x_k) \in \mathbb{R}^k : \sum_{i=1}^k x_i^2 = 1 \right\}.$$

The k -dimensional content, or “volume”, of Ω_k is defined by

$$V_k \equiv \int_{X \in \mathbb{R}^k : \|X\| \leq 1} dX.$$

It has been known at least since the 19th century [79] that $V_k = \frac{\pi^{n/2}}{\Gamma(\frac{n+2}{2})}$, where Γ is the usual Gamma function defined by $\Gamma(x) = \int_0^\infty e^{-t} t^{x-1} dt$. This may be rewritten as

$$V_k = \frac{\pi^{k/2}}{\Gamma(\frac{k+2}{2})} = \frac{2\pi^{k/2}}{k\Gamma(\frac{k}{2})} = \begin{cases} \frac{\pi^{k/2}}{(k/2)!} & \text{if } k \text{ even} \\ \frac{2^k \pi^{(k-1)/2} ((k-1)/2)!}{k!} & \text{if } k \text{ is odd.} \end{cases}$$

The last form avoids the use of the Gamma function. From the definition of V_k , it follows that a k -dimensional sphere of radius r has volume $V_k r^k$. The $(k-1)$ -dimensional content, or “surface area,” of Ω_k is given by

$$S_k \equiv \int_{\Omega_k} dX = kV_k.$$

Because the “volume” of an object in \mathbb{R}^k may be deemed the “surface area” of an object in \mathbb{R}^{k+1} , these terms are potentially confusing and will be avoided wherever possible; instead, the “ k -dimensional content” of an object will be used.

A *sphere packing* (or simply *packing*) is a set of mutually disjoint, equal radius, open spheres. A packing is a *lattice packing* if the centers of the spheres form a lattice. Hence, every lattice gives rise to a lattice packing and vice versa. The *packing radius* is the radius of the spheres in a packing; it is normally assumed that the packing radius is as large as possible such that the definition of packing is satisfied, i.e., such that there are tangent spheres in the packing but no overlapping spheres. As defined in [75], a packing is said to have *density* Δ if the ratio of the

¹The notation for the surface of the unit k -dimensional sphere varies somewhat in the literature, and Ω_k [5, 14, 17, 19, 21, 69, 81], S_k [96], and S^{k-1} [11, 48, 52] have all been used.

Table 2.1 Properties of some well-known lattices.

Lattice	Volume of fundamental region	Minimum distance	Covering radius	Density	Normalized second moment
\mathbb{Z}^k	1	1	$\frac{\sqrt{k}}{2}$	$V_k 2^{-k}$	$\frac{1}{12} \approx 0.833$
A_k	$\sqrt{k+1}$	$\sqrt{2}$	$\sqrt{\frac{\lfloor \frac{k+1}{2} \rfloor (k+1 - \lfloor \frac{k+1}{2} \rfloor)}{k+1}}$	$\frac{V_k 2^{-k/2}}{\sqrt{k+1}}$	$\frac{1}{(k+1)^{1/k}} \left[\frac{1}{12} + \frac{1}{6(k+1)} \right]$
A_k^*	$\frac{1}{\sqrt{k+1}}$	$\sqrt{\frac{k}{k+1}}$	$\sqrt{\frac{k(k+2)}{12(k+1)}}$	$\frac{V_k k^{k/2}}{2^k (k+1)^{(k-1)/2}}$	*
D_k	2	$\sqrt{2}$	$\frac{1}{\sqrt{k}}$ if $k = 3$ \sqrt{k} if $k \geq 4$	$V_k 2^{1-(k/2)}$	$\frac{1}{2^{2/k}} \left(\frac{1}{12} + \frac{1}{2k(k+1)} \right)$
D_k^*	$\frac{1}{2}$	$\frac{\sqrt{3}}{2}$ if $k = 3$ 1 if $k \geq 4$	$\frac{\sqrt{5}}{2}$ if $k = 3$ $2^{1-k} \sqrt{k/2}$ if k even $\frac{\sqrt{2k-1}}{2}$ if $k \geq 5$ and k odd	$\frac{V_{3^{3/2}}}{3^2}$ if $k = 3$ $\frac{V_k}{2^{k-1}}$ if $k \geq 4$	*
E_8	1	$\sqrt{2}$	1	$\frac{\pi^4}{384} \approx 0.2537$	$\frac{929}{12960} \approx 0.0716821$
Λ_{16}	16	2	$\sqrt{3}$	$\frac{\pi^8}{16 \cdot 8!} \approx 0.01471$	0.068299 ± 0.000027
Λ_{24}	1	2	$\sqrt{2}$	$\frac{\pi^{12}}{12!} \approx 0.001930$	0.065771 ± 0.000074

* The normalized second moment is described by a recurrence relation, omitted here for brevity.

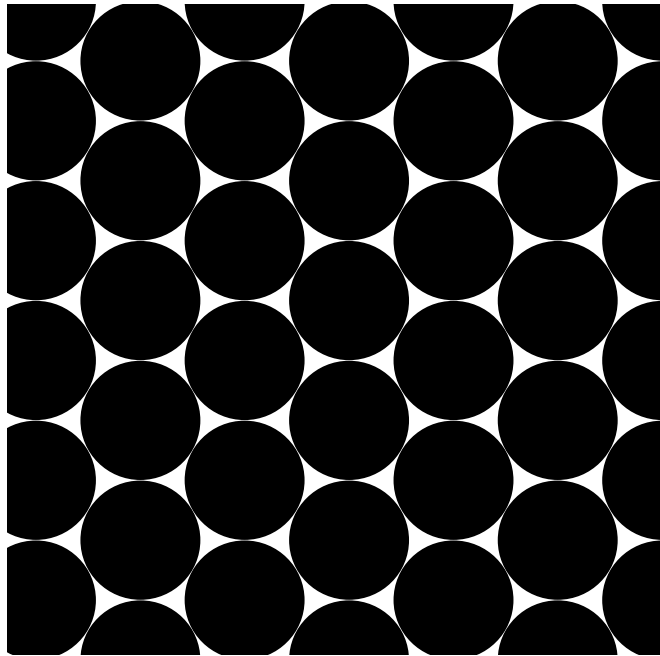


Figure 2.2 Part of the A_2 lattice packing.

volume of the part of a hypercube covered by the spheres of the packing to the volume of the whole hypercube tends to the limit Δ , as the side of the hypercube tends to infinity. That is, the density is the fraction of space occupied by the spheres of the packing. In two dimensions, a hypercube is a square; the density of the hexagonal lattice is illustrated in Figure 2.2. If the limit in the definition of density does not exist, then the density of the packing is not defined; such packings appear to be of limited interest and have not been extensively studied.

Every lattice packing has a density and this density can be calculated from its generator matrix, as follows. Suppose a lattice Λ has generator matrix M . Recall that a fundamental parallelotope tiles the space occupied by the lattice and it contains one lattice point. Hence, the density of the lattice packing— which is also referred to as the density of the lattice— is equal to the ratio of the volume of one sphere in the packing to the volume of the fundamental parallelotope. If the packing radius is r , then the volume of a sphere in the packing is $V_k r^k$. The volume of a fundamental parallelotope is $\sqrt{\det(MM^T)}$, or in the case of a square generator

matrix, $|\det(M)|$. Hence, the density of the lattice is

$$\Delta = \frac{V_k r^k}{\sqrt{\det(MM^T)}} = \frac{V_k r_k}{|\det(M)|},$$

where the last form may be used if M is a square matrix.

2.1.4 Covering radius and covering thickness

If the radius of the spheres in a packing in \mathbb{R}^k is increased above the packing radius, then the spheres in the packing overlap. If the new radius is sufficiently large, every point in \mathbb{R}^k will be inside at least one sphere. This is called a *cover* of \mathbb{R}^k , and the smallest radius that results in a cover of \mathbb{R}^k is the *covering radius* of the packing. The density of this covering, called the *covering thickness*, may be calculated as before except that the sphere packing radius is replaced by the covering radius. An important geometrical problem is to find the minimum covering thickness among all covers of \mathbb{R}^k .

2.1.5 Theta series

Associated with lattice Λ is a *theta series*, which indicates the number of lattice points at fixed distances from the origin. This can be written as a power series

$$\Theta_\Lambda(z) = \sum_{X \in \Lambda} q^{X \cdot X} = \sum_{m=0}^{\infty} N_m q^m,$$

where $q = e^{\pi i z}$ and where N_m is the number of points in Λ at a squared distance of m from the origin. In this thesis, Θ_Λ can be thought of as a formal power series in an indeterminate q ; in deeper investigations one must take $q = e^{\pi i z}$, where z is a complex variable. Since \mathbb{Z} has one lattice point at the origin and two points at every integral distance from the origin,

$$\Theta_{\mathbb{Z}} = \sum_{m=-\infty}^{\infty} q^{m^2} = 1 + 2q + 2q^4 + 2q^9 + 2q^{16} + \dots$$

It is beyond the scope of this thesis to derive the theta functions for other lattices used in the thesis. See [14, 81].

2.1.6 Voronoi regions, holes, and Delaunay cells

Given a set of points $P \subset \mathbb{R}^k$, a *nearest neighbor* to $X \in \mathbb{R}^k$ is a point of P closest to X . A *Voronoi region*, or *Voronoi cell*, of a point $Z \in P$ is the set Π of all points in \mathbb{R}^k for which Z is

a nearest neighbor. For certain pathological definitions of P , it is possible for a point $X \in \mathbb{R}^k$ to have no nearest neighbor. For example, if $P = \{2^{-i} : i \in \mathbb{Z}\}$, which is a subset of \mathbb{R} , then $X = -1$ has no nearest neighbor in P . This thesis will not consider such cases. When P is finite or forms a lattice, every point of \mathbb{R}^k has a nearest neighbor; thus, the union of all of the Voronoi regions is \mathbb{R}^k . A point that has more than one nearest neighbor belongs to more than one Voronoi region. Sometimes it is desirable to define the Voronoi regions so that they are disjoint and form a partition of the space. To do this, the definition is altered so that points that have more than one nearest neighbor in P are assigned to exactly one Voronoi region. Such points are often inconsequential for various applications, and in those cases the exact specification of the Voronoi regions can be arbitrary (i.e., left vague). If $f_P(X) = \min_{Z \in P} \|X - Z\|$, then a point $X \in \mathbb{R}^k$ is a *hole* if $f_P(X)$ is a local maximum and it is a *deep hole* if $f_P(X)$ is a global maximum. Note that the distance from a deep hole to the nearest point of P is equal to the covering radius of P . Also, every deep hole is a vertex of a Voronoi cell, although the converse is not always true. Each vertex of a Voronoi cell has an associated *Delaunay cell*, which consists of the convex hull of the points of P closest to that point. See Figure 2.1.

2.1.7 Dual lattices

If Λ is a lattice in \mathbb{R}^k , then the *dual* lattice of Λ is

$$\Lambda^* = \{X \in \mathbb{R}^k : X \cdot U \in \mathbb{Z} \text{ for all } U \in \Lambda\},$$

where $X \cdot U$ is the dot product of X and U . The asterisk will be used to indicate the dual, e.g., A_k^* is the dual of the A_k lattice. If M is a square generator matrix for a lattice Λ , then $(M^{-1})^T$ is a generator matrix for Λ^* ; thus,

$$\det \left((M^{-1})^T M^{-1} \right) = \det \left((MM^T)^{-1} \right) = (\det(MM^T))^{-1}.$$

Hence, given the density of a lattice, as computed by $\Delta_\Lambda = \frac{V_k r^k}{\sqrt{\det(MM^T)}}$, the density of the dual lattice is $\Delta_{\Lambda^*} = V_k (r^*)^k \sqrt{\det(MM^T)}$, where r^* is the covering radius of the dual lattice.

2.1.8 Normalized second moment

The normalized second moment of a k -dimensional lattice Λ with Voronoi region Π is defined by

$$G(\Pi) = \frac{\frac{1}{k-1} \int_{\Pi} X \cdot X dX}{V(\Pi)^{1+\frac{2}{k-1}}},$$

where $V(\Pi)$ is the k -dimensional content, or “volume” of Π . The Voronoi regions of the A_2 and \mathbb{Z}^2 lattices are shown in Figure 2.1. The normalized second moment of A_2 is $5/(36\sqrt{3}) \approx 0.080$, while it is $1/12 \approx 0.083$ for \mathbb{Z}^2 . The normalization factor in the definition above ensures that $G(\Pi)$ remains unchanged under any scaling of Λ .

2.1.9 Laminated lattices

The *laminated lattices* are useful for the code construction in Chapter 5. The one-dimensional laminated lattice is defined by

$$\Lambda_1 \equiv \mathbb{Z}.$$

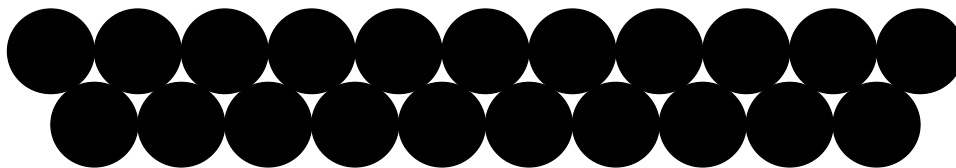
The notation Λ_k denotes the k -dimensional laminated lattice. Before giving the formal definition of Λ_k for $k > 1$, an informal construction technique is discussed.

In two dimensions, Λ_2 is constructed by stacking copies of Λ_1 , as shown in Figure 2.3. In order to produce the densest lattice, the layers are stacked so that a lattice point of one layer is directly above a hole of the previous layer. Because Λ_1 is a lattice, if one lattice point in a layer is directly above a hole of the previous layer, then all lattice points of that layer are above holes of the previous layer. Note that the second, fourth, sixth, etc. layers above a given layer are translations of the given layer along the last coordinate only. Thus, the layer number of Λ_2 is said to be two.

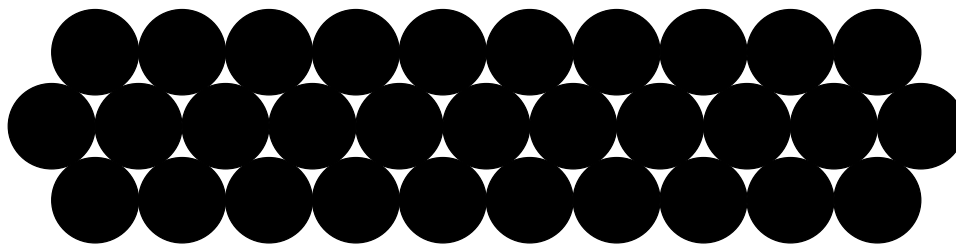
Similarly, Λ_3 is constructed by stacking up layers of Λ_2 . Without loss of generality, the orientation of the lattice may be fixed so every point in a given layer has an identical last (third) coordinate. Again, the lattice points of one layer are placed opposite to— that is, directly over, or differing in the last coordinate only— holes of the previous layer. In order to maintain the lattice property, namely, that the points of Λ_3 are closed under integer vector addition, the layer number of Λ_3 must be three. That is, the third, sixth, ninth, etc. layers are directly over the zeroth layer, i.e., a translation only in the last coordinate.



(a)



(b)



(c)

Figure 2.3 The first layer used to construct Λ_2 . It is a translation of Λ_1 . (b) The first two layers of Λ_2 . A point of the second layer is directly above a hole of the first layer. (c) The first three layers of Λ_2 .

This procedure can be repeated indefinitely. In each new dimension, layers of Λ_{k-1} are stacked as closely together as possible. More formally, For $k \geq 2$, a k -dimensional laminated lattice Λ_k , is a lattice whose minimum distance is one, whose sublattices include a $(k-1)$ -dimensional laminated lattice, and whose density is the highest possible under these conditions. Thus, Λ_k can be decomposed as

$$\Lambda_k = \bigcup_{l=-\infty}^{\infty} \Lambda_{k-1}^{(l)},$$

where $\Lambda_{k-1}^{(l)}$ is the l th layer of Λ_k i.e., a translation of Λ_{k-1} . Somewhat surprisingly, Λ_k is not unique for all k , although the density of Λ_k is unique.

In general,

$$l_k \equiv \min \left\{ i > 0 : \left(0, \dots, 0, i\sqrt{1 - c_{k-1}^2} \right) \in \Lambda_k \right\} \quad (2.1)$$

denotes the *layer number* of Λ_k . The layer number is the smallest number of consecutive layers of Λ_{k-1} stacked within Λ_k such that the top layer is “directly over” the bottom layer, i.e., differing in the last coordinate only. For example, $l_2 = 2$, $l_3 = 3$, and $l_4 = 2$.

In Λ_2 and Λ_3 , the points of one component layer are opposite deep holes of adjacent layers. Since the covering radius r of a layer is the distance from a deep hole to a lattice point, adjacent layers can be placed at a distance $\sqrt{1 - r^2}$ from each other to maintain a minimum distance of one between all points. Unfortunately, it is not a simple matter to show from the definition of laminated lattice that layers are separated by $\sqrt{1 - r^2}$ for higher dimensional laminated lattices. While this seems intuitively true, this question remains unproven for every $k > 12$, except 16, 24, 25, 26, and 32. As a result, the notion of subcovering radius is used. The *subcovering radius* c_{k-1} of Λ_{k-1} is defined such that $\sqrt{1 - c_{k-1}^2}$ is the distance between layers of Λ_k . Note that c_k is a lower bound on the covering radius of Λ_k . The values of c_k are known for $k \leq 47$, and are tabulated in [14, p. 158] for laminated lattices that are scaled by a factor of two. Since adjacent layers of Λ_k are separated by $\sqrt{1 - c_{k-1}^2}$ and the distance between distinct points of Λ_k is at least 1, it follows that $l_k \sqrt{1 - c_{k-1}^2} \geq 1$.

Corresponding to each point $X = (x_1, \dots, x_{k-1}) \in \Lambda_{k-1}^{(l)}$ is an associated unique hole $h(X)$ whose distance from X is c_{k-1} and that is opposite a lattice point in $\Lambda_{k-1}^{(l+1)}$. Let n_{k-1} denote the number of points of $\Lambda_{k-1}^{(l)}$ which are nearest lattice points of $h(X)$, and let $n(X)$ denote the lattice point of $\Lambda_{k-1}^{(l+1)}$ which is opposite $h(X)$. That is, $h(X)$ has n_{k-1} nearest neighbors in $\Lambda_{k-1}^{(l)}$, regardless of the choice of X (one of these nearest neighbors is X). These nearest

neighbor lattice points are denoted by $D(X)_1, \dots, D(X)_{n_{k-1}}$, and the convex hull of these points forms a Delaunay cell. For any finite set of points $\mathcal{P} \subset \mathbb{R}^k$, define

$$H(\mathcal{P}) \equiv \arg \max_{Y \in \text{CHULL}(\mathcal{P})} \min_{X \in \mathcal{P}} \|X - Y\|,$$

where it is understood that if there is not a unique argument Y which maximizes the expression above, any Y may be chosen. $H(\mathcal{P})$ is a hole of \mathcal{P} that lies within the convex hull of \mathcal{P} , and for each $X \in \mathcal{P}$,

$$h(X) = H(\{D(X)_1, \dots, D(X)_{n_{k-1}}\}).$$

2.2 Quantization

The definitions and summary of results in this section are extensively used in Chapter 6. The material in this section may be found in [31].

2.2.1 Vector quantization

A *vector quantizer* (VQ) is a mapping from \mathbb{R}^k into a set \mathcal{C} of output points

$$Q : \mathbb{R}^k \rightarrow \mathcal{C},$$

where $\mathcal{C} = \{Y_1, \dots, Y_M\}$ and $Y_i \in \mathbb{R}^k$ for $1 \leq i \leq M$. In the quantization literature, elements of \mathbb{R}^k are referred to both as *points* and as *vectors*. The set \mathcal{C} is a *codebook*, and each element of \mathcal{C} is a *codevector* or a *codepoint*. A vector quantizer may be decomposed into two mappings, an *encoder* $\mathcal{E} : \mathbb{R}^k \rightarrow \{1, \dots, M\}$ that maps the vectors of \mathbb{R}^k to distinct indices, and a *decoder* $\mathcal{D} : \{1, \dots, M\} \rightarrow \mathcal{C}$, where $\mathcal{D}(i) = Y_i$. Thus,

$$Q = \mathcal{D} \circ \mathcal{E}.$$

Associated with every k -dimensional vector quantizer is a partition of \mathbb{R}^k into disjoint encoder *cells* R_1, \dots, R_M , where for each $i \in \{1, \dots, M\}$,

$$R_i = \{x \in \mathbb{R}^k : \mathcal{E}(x) = i\}.$$

Figure 2.4 shows the operation of a quantizer in a digital communications system. This thesis will assume that the channel is error-free.



Figure 2.4 A quantizer in a digital communications system.

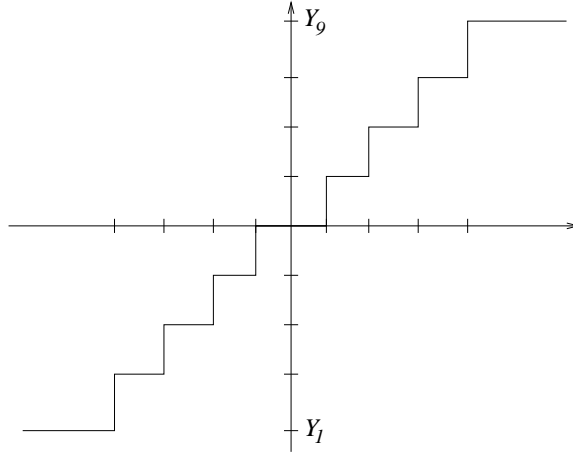


Figure 2.5 Output vs. input of a scalar quantizer.

A vector quantizer for which $k = 1$ is called a *scalar quantizer*, and is a function from \mathbb{R} to a finite subset of \mathbb{R} . Such a quantizer can be thought of as an analog to digital converter in which individual analog inputs are converted to one of M possible indexed output levels. See Figure 2.5.

A *distortion function* $\delta : \mathbb{R}^k \times \mathbb{R}^k \rightarrow \mathbb{R}$ is a measurable function that assigns to each pair of vectors in \mathbb{R}^k a nonnegative number describing the distortion between the two vectors. Given a random vector $X \in \mathbb{R}^k$, the average distortion D is defined as the expected distortion between X and its associated codevector $Q(X)$:

$$D = E[\delta(X, Q(X))].$$

The function δ is often chosen as the squared Euclidean distance measure, normalized by the dimension, so that $D = \frac{1}{k} E [\|X - Q(X)\|^2]$, although other distortion measures are sometimes used. In the remainder of the thesis, the distortion will be defined as the mean squared error per dimension.

Shannon's theorem for source coding with respect to a fidelity criterion [28] implies that for any source there is a fundamental lower bound on the mean squared error of an M -point

quantizer. This lower bound is expressed by the *distortion-rate function* $D(R)$, where $R = (1/k) \log_2 M$ is the *rate* of the vector quantizer, i.e., the average number of bits used to quantize each sample from the source. For example, for the Gaussian source, $D(R) = \sigma^2 2^{-2R}$. That is, if $X \sim N(0, \sigma^2)$, then any M -point vector quantizer for X must have a distortion of at least $\sigma^2 2^{-2R} = \sigma^2 M^{-2/k}$. The distortion-rate function for most other sources is not known explicitly, although numerical algorithms exist to calculate $D(R)$ [9].

The primary goal in designing an M -point vector quantizer is to choose the codebook \mathcal{C} and an associated partition of \mathbb{R}^k such that the average distortion D is as small as possible. By Shannon's theorem, the distortion must be at least as much as the distortion-rate function. Conversely, a vector quantizer can have distortion as close to the distortion-rate function as desired, provided the dimension of the vector quantizer is sufficiently large. Unfortunately, the proof of this latter fact uses a nonconstructive random coding argument. Furthermore, even an explicit construction of a vector quantizer is not useful if the complexity of its implementation is prohibitive. To effectively implement a vector quantizer, the operation of the encoder and decoder must have reasonable computational and storage complexities. Hence, suboptimal vector quantizers are useful if they are efficiently implementable and have good distortion performance. Chapter 6 presents a suboptimal vector quantizer that both performs well and is computationally efficient.

2.2.2 Properties of optimal vector quantizers

Two basic results in the theory of quantization lead to a remarkably simple and effective method for quantizer design. The first result states that, given a fixed codebook Y_1, \dots, Y_M , the optimal partition cells satisfy

$$R_i \subset \{X : \delta(X, Y_i) \leq \delta(X, Y_j) \text{ for } j = 1, \dots, M\},$$

for all $i = 1, \dots, M$. That is, $Q(X) = Y_i$ only if $\delta(X, Y_i) \leq \delta(X, Y_j)$, for all j . When $\delta(X, Y) \equiv \|X - Y\|^2$, a quantizer of this type satisfies the *nearest neighbor condition*. The second result states that, given a fixed partition R_1, \dots, R_M , the optimal codevectors satisfy

$$Y_i = E[X|X \in R_i],$$

for $i = 1, \dots, M$. That is, for each i , Y_i is the centroid of R_i . A quantizer for which this holds satisfies the *centroid condition*.

The optimality conditions above may be used to design a quantizer for any source distribution. The algorithm consists of repeating the following two steps.

1. Fix the codebook Y_1, \dots, Y_M . Use the nearest neighbor condition to define a new partition R_1, \dots, R_M .
2. Fix the partition R_1, \dots, R_M . Use the centroid condition to define a new codebook Y_1, \dots, Y_M .

For scalar quantizer design, this algorithm is called the *Lloyd-Max algorithm* [58, 63]. For vector quantizer design, it is called the *generalized Lloyd algorithm*. In both cases, the distortion is reduced or remains unchanged after each step. After many iterations, the distortion of the quantizer generally stops improving significantly, and the algorithm may be terminated. There is no guarantee that a codebook designed by this algorithm is optimal or near-optimal, because the centroid and nearest neighbor conditions are necessary but not sufficient conditions for optimal quantization. For the scalar quantization case, the two conditions can be shown to be sufficient if the probability density function of the source is log-concave, and in that case the Lloyd algorithm converges to the globally optimal scalar quantizer [27, 87]. A major drawback of the design approach is not its performance, which can be very good in some cases, but the implementation complexity of the resulting quantizer. The codebook is unstructured, and for fixed rate transmission systems, the complexity of encoding grows exponentially in the vector dimension.

2.2.3 Index assignment

In vector quantization, the encoder \mathcal{E} takes as input a vector $X \in \mathbb{R}^k$ and its output is a binary string representing a codevector. This binary string is transmitted across a channel. An efficient method is needed to map a codevector to a unique index and to map an index back to the original codevector.

2.2.4 Lattice quantization

Points of a k -dimensional lattice Λ are uniformly spread throughout \mathbb{R}^k , and thus a finite subset of Λ can be a good k -dimensional vector quantizer for a uniform source [32]. The primary advantage of the lattice quantizer is that source vectors can often be encoded by performing

a small constant number of operations, which allows both encoding and storage complexity to be very low. Although lattices have been previously proposed for quantization of nonuniform sources [47, 76], they have been usually reserved for uniform sources only.

If the size of the codebook is very large, the quantized output $Q(X)$ will be very close to the input X . This situation is termed *high resolution* quantization. In high resolution each encoder cell R_i is very small, and within the cell, the distribution of the source is approximately uniform. This approximation, called the *high resolution approximation*, leads to easy estimates for the distortion of some high resolution quantizers. For example, recall that $G(\Pi)$ is the normalized second moment of a Voronoi region of a $(k - 1)$ -dimensional lattice Λ , given by

$$G(\Pi) = \frac{\frac{1}{k-1} \int_{\Pi} X \cdot X dX}{V(\Pi)^{1+\frac{2}{k-1}}}.$$

The mean-squared error (MSE) obtained when the unscaled lattice Λ is used for quantization under high resolution is given by

$$E[\|X\|^2 | X \in \Pi] = \int_{\Pi} \frac{x \cdot x}{V(\Pi)} dx = (k - 1) \cdot G(\Pi) \cdot V(\Pi)^{2/(k-1)}.$$

When Λ is scaled to have minimum distance d , i.e., scaled by d/d_{Λ} , the MSE is scaled by $(d/d_{\Lambda})^2$. Hence, the MSE of the scaled lattice is

$$(k - 1) \cdot G(\Pi) \cdot V(\Pi)^{2/(k-1)} \cdot (d/d_{\Lambda})^2. \tag{2.2}$$

This will be useful in the analysis of the distortion of the quantizer developed in Chapter 6.

2.3 Spherical Codes

A k -dimensional *spherical code* is a finite set of points in \mathbb{R}^k that lie on the surface of the k -dimensional unit radius sphere Ω_k . The *minimum distance* of a k -dimensional spherical code $\mathcal{C} \subset \Omega_k$ is defined as

$$d \equiv \min_{\substack{X, Y \in \mathcal{C} \\ X \neq Y}} \|X - Y\|,$$

where $\|X - Y\|$ is the Euclidean distance in \mathbb{R}^k between codepoints X and Y . The minimum distance of a spherical code is directly related to the “quality” of the code in many channel coding applications. For channel codes, one generally desires to maximize the minimum distance for a given number of codepoints.

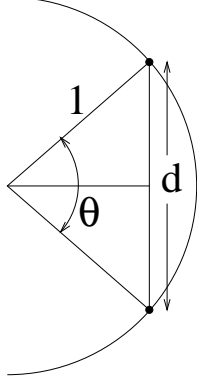


Figure 2.6 The relationship between minimum distance d and minimum separating angle θ .

As this thesis concentrates on asymptotically small d , it is important to clarify some notation. For a function $g(d)$, let $O(g(d))$ denote any function $f(d)$ for which there exists positive constants c and d_0 such that $0 \leq f(d) \leq cg(d)$ for all $d \in (0, d_0)$. Note that with this definition there are two inequalities involved, so that $f(d) = O(g(d))$ and $f(d) = -O(g(d))$ cannot both be true. The dimension k will be regarded as a constant in the asymptotic analysis.

The *angular separation* between two points (vectors) $X, Y \in \Omega_k$ is $\cos^{-1}(X \cdot Y)$. The *minimum angular separation* of spherical code \mathcal{C} (see Figure 2.6) is defined as

$$\theta \equiv 2 \sin^{-1}(d/2) \tag{2.3}$$

$$= d + \frac{d^3}{24} + O(d^5). \tag{2.4}$$

The set of points on Ω_k whose angular separation from a fixed point $X \in \Omega_k$ is less than ϕ is called a *spherical cap centered at X with angular radius ϕ* and is denoted by

$$c_X(k, \phi) \equiv \{Y \in \Omega_k : X \cdot Y > \cos \phi\}.$$

When the center X of a spherical cap is not relevant, the notation may be abbreviated as $c(k, \phi)$. If two spherical caps of angular radius $\theta/2$ are centered at different codepoints of a spherical code with minimum distance d and minimum angular separation θ , then the caps are

disjoint. The $(k-1)$ -dimensional content of $c(k, \theta/2)$ is given by

$$\begin{aligned}
S(c(k, \theta/2)) &= S_{k-1} \int_0^{\theta/2} \sin^{k-2} x \, dx \\
&= S_{k-1} \int_0^{\theta/2} (x - x^3/6 + O(x^5))^{k-2} \, dx \\
&= S_{k-1} \int_0^{\theta/2} (x^{k-2} - \frac{k-2}{6} x^k \pm O(x^{k+2})) \, dx \\
&= S_{k-1} \left(\frac{1}{k-1} (\theta/2)^{k-1} - \frac{k-2}{6(k+1)} (\theta/2)^{k+1} \pm O(\theta^{k+3}) \right) \tag{2.5}
\end{aligned}$$

$$= V_{k-1} (\theta/2)^{k-1} - O(\theta^{k+1}) \tag{2.6}$$

$$= V_{k-1} \left(\frac{d}{2} \right)^{k-1} + O(d^{k+1}) \tag{2.7}$$

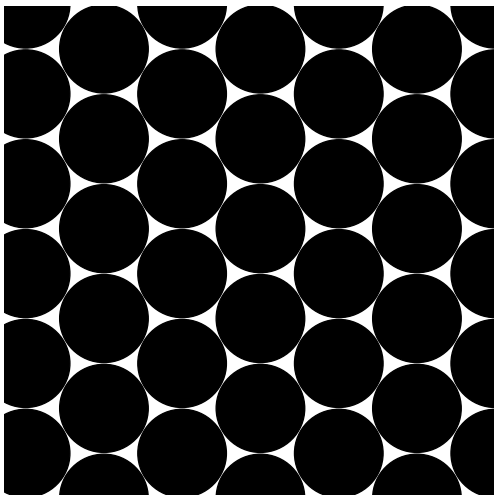
where (2.7) follows by using (2.4).

The *density* $\Delta_{\mathcal{C}}$ of a spherical code $\mathcal{C} \subset \Omega_k$ with minimum distance d is the ratio of the total $(k-1)$ -dimensional content of $|\mathcal{C}|$ disjoint spherical caps centered at the codepoints and with angular radius $\theta/2$, to the $(k-1)$ -dimensional content of Ω_k ; that is, $\Delta_{\mathcal{C}} = |\mathcal{C}| \cdot S(c(k, \theta/2))/S_k$. This definition is analogous to the definition of the density of a sphere packing. See Figure 2.7(b). Let $M(k, d)$ be the maximum cardinality of a k -dimensional spherical code with minimum distance d , and let $\Delta(k, d)$ be the maximum density among all k -dimensional spherical codes with minimum distance d . Then,

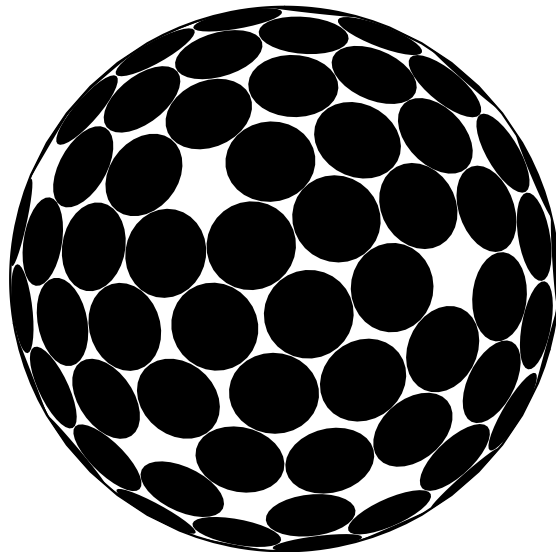
$$\Delta(k, d) \equiv \frac{M(k, d) S(c(k, \theta/2))}{S_k}. \tag{2.8}$$

The value of $M(k, d)$ is easy to compute for all d when $k = 2$: the maximum number of points on the unit circle with angular separation θ is $\lfloor \frac{2\pi}{\theta} \rfloor = \lfloor \frac{\pi}{\sin^{-1}(d/2)} \rfloor$. However, $M(k, d)$ is unknown for all $k \geq 3$ except for a handful of values of d , although a number of bounds have been given [5, 12, 16–20, 23, 35, 48, 74, 95, 97, 98]. For asymptotically small d , the tightest known upper bound on $M(k, d)$ is given in [23] for $k = 3$ and in [16] for $k \geq 4$, and a code construction in [18] provides the tightest known lower bound. However, there exists a nonvanishing gap between these upper and lower bounds as $d \rightarrow 0$.

A family of codes $\{\mathcal{C}(k, d)\}$ is *asymptotically optimal* if $|\mathcal{C}(k, d)|/M(k, d) \rightarrow 1$ as $d \rightarrow 0$, or equivalently, if $\Delta_{\mathcal{C}(k, d)}/\Delta(k, d) \rightarrow 1$ as $d \rightarrow 0$. It will be shown that $\lim_{d \rightarrow 0} \Delta_{\mathcal{C}(k, d)}$ cannot exceed the density of the densest $(k-1)$ -dimensional sphere packing. It will also be shown that this density is achieved by using the new constructions presented in this thesis. Hence,



(a)



(b)

Figure 2.7 Sphere packing density and spherical code density. (a) The sphere packing density is the percentage of the square that is shaded, as the length of the side of the square goes to infinity. (b) The spherical code density is the percentage of the unit sphere that is shaded.

given a densest packing in \mathbb{R}^{k-1} , asymptotically optimal k -dimensional spherical codes can be constructed from it. Figure 2.8 shows the asymptotic densities of the best spherical codes for up to 49 dimensions. For each dimension, the limiting density of spherical codes constructed by the various methods is computed. To emphasize the comparison to wrapped spherical codes, this limiting density is divided by the asymptotic density achieved by the wrapped spherical codes. Hence, in Figure 2.8, the wrapped code is identically 1, while any code whose asymptotic density is worse than the wrapped code is less than 1.

One way to construct a spherical code is to use the set of points of a lattice at a given radius r from the origin, normalized to the unit sphere: $\mathcal{C} = S_k \cap (\frac{1}{r}\Lambda)$. That is, the codebook is a *shell* of the lattice Λ . As an example of constructing a spherical code from a lattice, consider the points of D_4 at distance $r = \sqrt{6}$ from the origin. These is the set of 96 permutations of $(\pm 2, \pm 1, \pm 1, 0)$. The minimum distance between two points in this shell is the same as the minimum distance of D_4 , $\sqrt{2}$, as can be seen from $\|(2, 1, 1, 0) - (2, 1, 0, 1)\| = \sqrt{2}$. After scaling each coordinate by $1/r = 1/\sqrt{6}$, the minimum distance of the spherical code is determined to be $\sqrt{2}/\sqrt{6} = 1/\sqrt{3} \approx 0.577$.

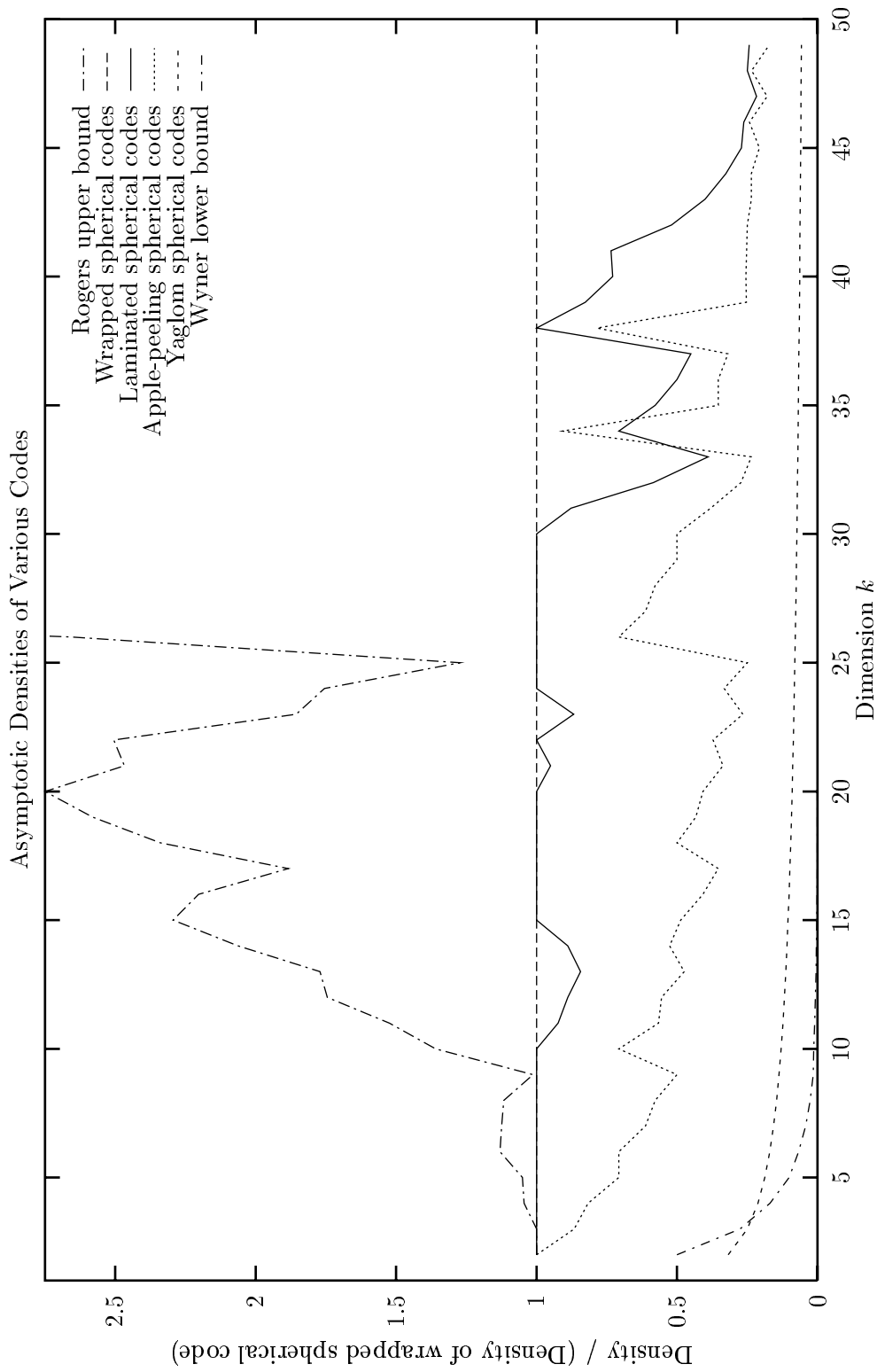


Figure 2.8 The ratio of the asymptotic density of various spherical codes to that of wrapped spherical codes constructed from the densest known packings, as a function of dimension. Except for the upper bound, all curves are below 1, indicating the wrapped spherical code's asymptotic superiority.

Recall that the number of lattice points on a shell of a lattice is determined by the theta function [14] of the lattice. The theta functions for a number of important lattices— including A_k , D_k , E_8 , the Leech lattice Λ_{24} , and their duals— are known and can be used to perform this count.

Although several authors have described how to obtain spherical codes from lattices and provided information about the number of points lying on each shell of various lattices, most notably [81], thus far there has been no formal theory for the resulting minimum distances between points on these shells. As a result, it is not known which shell of a lattice will result in the best spherical code. Indeed, it is not even known for which lattice it is best to begin searching shells. Clearly, the minimum distance between points on a shell of a lattice is no less than the minimum distance of the entire lattice, but the accuracy of this bound varies wildly. For example, the A_3 lattice has a minimum distance of $d_{A_3} = \sqrt{2}$. On the first shell, of radius $r = \sqrt{2}$, there are 12 points and a minimum distance of 1, in agreement with d_{A_3}/r . On the second shell, of radius 2, there are 6 points at radius $r = 2$ and a minimum distance of $\sqrt{2}$, whereas $d_{A_3}/r = 1/\sqrt{2}$. For the comparisons made in Chapter 3, the *exact* minimum distances are computed for the first 1000 shells of the A_k , D_k , E_8 , and \mathbb{Z}^k lattices.

For the quantization problem, shells of the cubic lattice [24], Gosset lattice [78], and Leech lattice [1] have been proposed as quantizers. The encoding complexity has been shown to be reasonable for certain cases, but the choice of the rate at which to operate is limited. It has been reported in [1] that 11 different rates between 0.733 and 2.106 bits/sample are possible by using the first 16 shells of the Leech lattice. It is unclear, however, whether the complexity of the encoding will be small when larger shells of the Leech lattice are used.

As is the case for minimum distance calculations, there is little formal theory about the performance of shells of lattices when used as vector quantizers for sources uniformly distributed on the surface of a sphere. From Section 2.1.8, the figure of merit for a high resolution lattice quantizer is the normalized second moment of its Voronoi region; however there is no known general method to calculate this figure of merit for quantizers formed from shells of lattices, and it is not known which lattice is best, or even which shell of a given lattice is best for a given rate. Indeed, many different shells of a lattice have the same number of codepoints, but may have vastly different performances. Among all shells containing a given number of points, the smallest radius shell might result in a small encoding complexity, but it often does not give

the best performance. For example, among the first eight shells of the hexagonal lattice A_2 that result in different codebook sizes, seven give suboptimal MSE performance for a source uniformly distributed on the circle, and the same seven are outperformed by larger shells of the lattice which contain the same number of points. Even these larger shells are suboptimal, however. For the A_3 lattice, the results are similar. See Figures 2.9 and 2.10.

The conclusion is that although a k -dimensional lattice may be a very dense lattice or a very good quantizer for a uniform source in \mathbb{R}^k , this alone does not imply that shells of this lattice will be very dense spherical codes or that the spherical code will be good for quantizing a uniform source on the sphere Ω_k .

Intuitively, it should be expected that for an optimal codebook in high resolution, the codepoints on a small $(k-1)$ -dimensional “patch” on the surface of Ω_k should be in an arrangement very similar to the best $(k-1)$ -dimensional packing for quantizing a uniform source in \mathbb{R}^{k-1} . This thesis exploits this intuition.

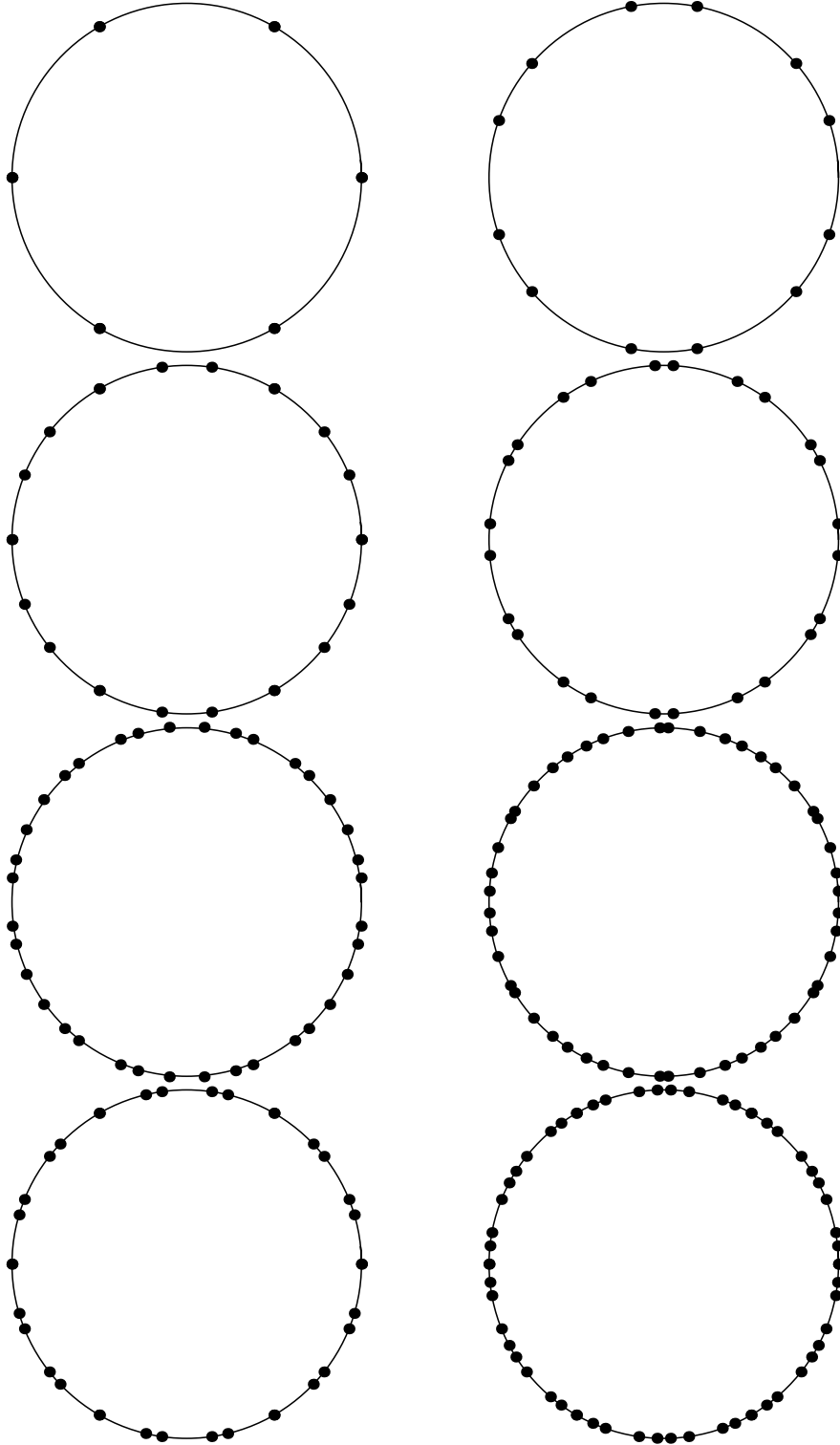


Figure 2.9 Eight shells of lattice A_2 , normalized to unit radius. Unnormalized, each shell is the smallest radius shell of A_2 which contains the given number of points. These squared radii are 1, 7, 49, 91, 637, 1729, 2401, and 8281, resulting in spherical codes of sizes 6, 12, 18, 24, 36, 48, 30, and 54, respectively. Only the code of size 6 has an optimal arrangement for minimum distance or quantization coefficient.

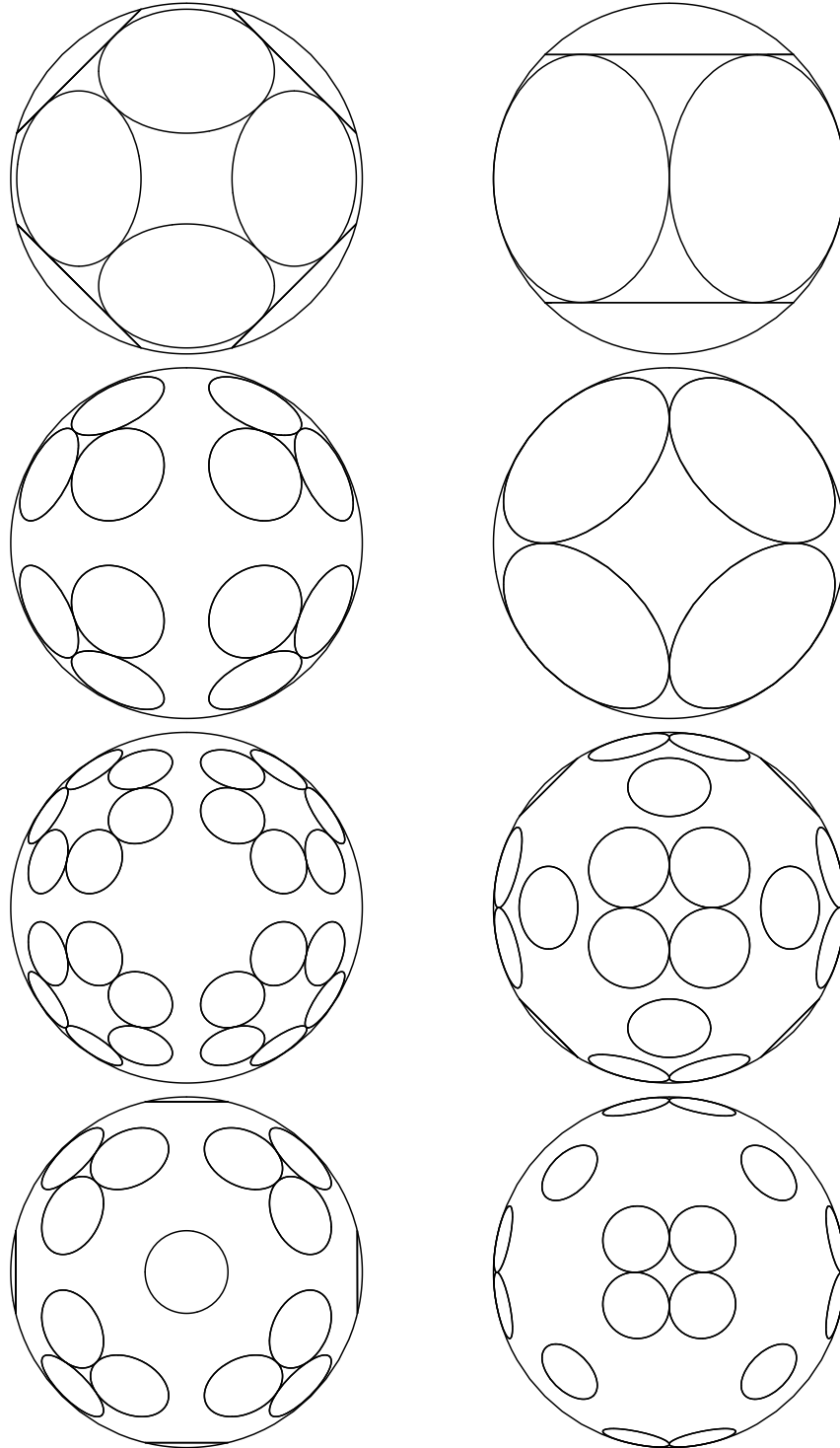


Figure 2.10 Eight shells of the face-centered cubic lattice (D_3), normalized to unit radius. Lattice points are located at the center of the spherical caps shown, which are drawn at the largest size such that they are nonoverlapping. Unnormalized, each shell is the smallest radius shell of D_3 which contains the given number of points. The unnormalized squared radii are 1, 2, 3, 6, 7, 9, 18, and 54, resulting in spherical codes of sizes 12, 6, 24, 8, 48, 36, 30, and 32, respectively. Only three of the eight codes have an optimal arrangement of points for minimum distance or quantization coefficient.

CHAPTER 3

BOUNDS ON THE DENSITY OF A SPHERICAL CODE

This chapter begins with a lemma that states that the maximum density of a k -dimensional spherical code, asymptotically as the minimum distance shrinks, equals the maximum density of a $(k - 1)$ -dimensional sphere packing. There is intuitive justification for this relationship, and similar relationships hold for parameters other than density. Two other parameters are explored in Appendix B.

When designing for minimum distance, the best k -dimensional spherical code with minimum distance d is the one which has the largest number of codepoints, namely, $M(k, d)$. Consequently, most previous authors have used $M(k, d)$ as the figure of merit for a spherical code. Using Equation (2.8), any bound on the code size $M(k, d)$ may be converted to a bound on the code density $\Delta(k, d)$. Whereas the code size increases without bound as d becomes small, the density is always a number in the interval $[0, 1]$. Therefore, for small minimum distances the bounds are more easily compared if they are expressed in terms of density. Additionally, using density as the figure of merit instead of code size allows one to compare the quality of codes with different minimum distances. Conversion of the bounds from statements about $M(k, d)$ to statements about $\Delta(k, d)$ also highlights the gap between the existing upper and lower bounds, and brings to light the fact that some of the best bounds known are not asymptotically tight.

3.1 Asymptotic Spherical Code Density

The following lemma shows that as $d \rightarrow 0$, the density of the densest k -dimensional spherical code approaches that of the densest sphere packing in $k - 1$ dimensions.¹ Let the *asymptotically*

¹For $k = 3$, the densest covering of Earth with dimes would look like the hexagonal lattice packing A_2 to someone standing on the Earth.

maximum spherical coding density be defined by

$$\Delta_k^{s.c.} \equiv \lim_{d \rightarrow 0} \Delta(k, d),$$

where $\Delta(k, d)$ is the maximum density of a k -dimensional spherical code with minimum distance d , as defined in (2.8). Let Δ_k^{pack} denote the density of the densest k -dimensional sphere packing.

Lemma 3.1 $\Delta_k^{s.c.} = \Delta_{k-1}^{pack}$.

Proof: See Appendix C.1

The proof of Lemma 3.1 gives a technique to create spherical codes that are asymptotically optimal, as $d \rightarrow 0$. However, the performance of these codes for moderately large d may be poor. Also, no efficient decoding technique for these spherical codes is known. The wrapped and laminated spherical codes presented in later chapters perform well for moderate sizes of d and are efficiently decodable.

Note that since $\Delta_2^{pack} = \frac{\pi}{2\sqrt{3}}$, the maximum asymptotic density possible for a three-dimensional spherical code is $\frac{\pi}{2\sqrt{3}}$. The densest sphere packing is not known for $k > 2$, however.² From Lemma 3.1, upper bounds on asymptotic sphere packing densities give upper bounds on spherical code densities. For example, Rogers's bound [75] on sphere packing densities is used to provide the upper bound in Figure 2.8.

3.2 Upper Bounds on Density

3.2.1 Fejes Tóth upper bound ($k = 3$)

For small d , the smallest known upper bound on $M(3, d)$ is given by Fejes Tóth [23], who proved that disjoint spherical caps with angular radius $\theta/2$ cannot be packed on the sphere Ω_3 in a denser configuration than that of three mutually tangent spherical caps with angular radius $\theta/2$ (see Figure 3.1). As a result, the minimal angular separation was shown to be bounded as

$$\theta \leq \cos^{-1} \left[\frac{\cot^2 \left(\frac{M(3, d)\pi}{6M(3, d) - 12} \right) - 1}{2} \right], \quad (3.1)$$

from which the following lemma is obtained.

²In 1991 W.-Y. Hsiang announced a proof [43] (later published in [44]) of Kepler's conjecture, dating back to 1611, that the face-centered cubic packing is the densest packing in three dimensions. However, the validity of the proof has been questioned [37]. Hsiang has published a rejoinder [45].

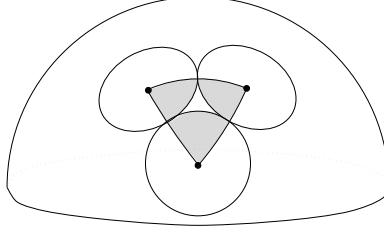


Figure 3.1 The density of a spherical code with minimal angle separation θ is at most the percentage of area covered in the spherical triangle formed by three mutually touching caps of angular radius $\theta/2$.

Lemma 3.2 *The density of any three-dimensional spherical code \mathcal{C} with minimum distance $d > 0$ is less than $\frac{\pi}{2\sqrt{3}}$. Asymptotically, the density is bounded above as $\Delta_{\mathcal{C}} \leq \frac{\pi}{2\sqrt{3}} - O(d^2)$.*

Proof: Combining (2.3) and (3.1) gives

$$d \leq \sqrt{3 - \cot^2 \left(\frac{\pi}{6 - 12/M(3, d)} \right)}$$

or equivalently

$$M(3, d) \leq 2 \cdot \left[1 - \frac{\pi/6}{\cot^{-1} \sqrt{3 - d^2}} \right]^{-1}$$

Using

$$S(c(3, \theta/2)) = S_2 \int_0^{\theta/2} \sin x \, dx = 2\pi(1 - \cos \theta/2) = 2\pi(1 - \sqrt{1 - d^2/4})$$

and (2.8),

$$\begin{aligned} \Delta(3, d) &\leq \frac{2 \cdot \left[1 - \frac{\pi/6}{\cot^{-1} \sqrt{3 - d^2}} \right]^{-1} \cdot 2\pi(1 - \sqrt{1 - d^2/4})}{4\pi} \\ &= \frac{1 - \sqrt{1 - d^2/4}}{1 - \frac{\pi/6}{\cot^{-1} \sqrt{3 - d^2}}} \end{aligned} \quad (3.2)$$

Some elementary (but laborious) calculus reveals that the supremum of (3.2) is $\frac{\pi}{2\sqrt{3}}$, which occurs as $d \rightarrow 0$. A Taylor expansion about $d = 0$ gives $\Delta(3, d) \leq \frac{\pi}{2\sqrt{3}} - O(d^2)$. ■

Since $\Delta_2^{pack} = \frac{\pi}{2\sqrt{3}}$, Lemma 3.2 agrees with Lemma 3.1, and implies the following.

Corollary 3.1 *The Fejes Tóth bound is asymptotically tight.*

Proof: From Lemma 3.1, it follows that $\Delta_3^{s.c.} = \Delta_2^{pack} = \frac{\pi}{2\sqrt{3}}$. The Fejes Tóth bound implies $\Delta_3^{s.c.} = \lim_{d \rightarrow 0} \Delta(3, d) \leq \frac{\pi}{2\sqrt{3}}$. ■

3.2.2 Coxeter upper bound ($k \geq 4$)

Böröczky [10] proved that in a k -dimensional space of constant curvature, the density of a packing of equal radii k -dimensional spheres cannot exceed the density of $k + 1$ such spheres that mutually touch one another. This verified Coxeter's conjecture [16] that spherical caps on Ω_k can be packed no denser than k spherical caps on Ω_k that simultaneously touch one another. The centers of these caps lie on the vertices of a regular spherical simplex, which is a generalization of the Fejes Tóth bound for $k = 3$. Coxeter's bound is given by

$$M(k, d) \leq \frac{2F_{k-1}(\alpha)}{F_k(\alpha)},$$

where α is given by

$$\sec 2\alpha = \frac{2}{2 - d^2} + k - 2,$$

and where $F_k(\alpha)$ is Schlafli's function given by the recursive relation

$$F_k(\alpha) = \frac{2}{\pi} \int_{\sec^{-1} \frac{k-1}{2}}^{\alpha} F_{k-2}(\beta) d\theta,$$

with $\sec 2\beta = (\sec 2\theta) - 2$, and the initial conditions $F_0(\alpha) = F_1(\alpha) = 1$. Unfortunately, the computational complexity of evaluating the bound is high for $k > 3$, as it involves a $\lfloor k/2 \rfloor$ -fold integral.

Coxeter's bound was motivated by an argument of Rogers, who showed that the density of a simplex is an upper bound on the density of a sphere packing, despite the fact that simplices cannot tile \mathbb{R}^k [75]. Coxeter's bound uses a similar argument, except that \mathbb{R}^k is replaced by Ω_k and simplices are replaced by spherical simplices. (A similar argument was used for a proposed bound on the quantization coefficient in \mathbb{R}^k [13].) Thus, when Coxeter's bound on $M(k, d)$ is translated to a bound on $\Delta(k, d)$, it becomes a statement about the density of a spherical simplex of edge-length d . As $d \rightarrow 0$, the density of the spherical simplex of edge-length d on Ω_k approaches the density of a regular simplex in \mathbb{R}^{k-1} , which gives us the following lemma.

Lemma 3.3 *Coxeter's upper bound on asymptotic spherical coding density $\Delta_k^{s.c.}$ equals Rogers's upper bound on sphere packing density Δ_{k-1}^{pack} .*

Corollary 3.2 *Coxeter's upper bound on $\Delta_k^{s.c.}$ is tight if and only if Rogers's upper bound on Δ_{k-1}^{pack} is tight. In particular, Coxeter's bound is not asymptotically optimal for $k = 4$.*

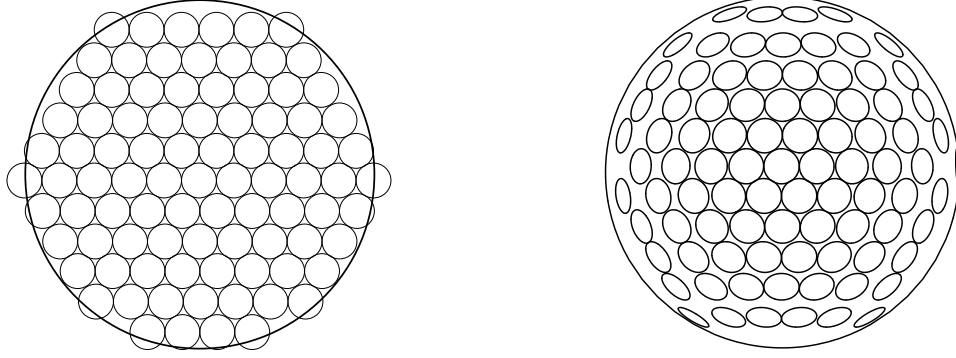


Figure 3.2 Yaglom’s mapping consists of taking the part of a lattice within Ω_{k-1} , shown at left, and projecting it out of the page onto the surface of Ω_k , shown at right.

Proof: The first statement follows from Lemmas 3.1 and 3.3. The second statement follows because Rogers’s bound of $\Delta_3^{pack} \leq 0.7796$ has been improved to $\Delta_3^{pack} \leq 0.7784$ [57]. ■

3.3 Lower Bounds on Density

3.3.1 Yaglom lower bound

Any spherical code can be described by the projection of its codepoints to the interior of a sphere of one less dimension via the mapping $(x_1, \dots, x_{k-1}, \sqrt{1 - \sum_{i=1}^{k-1} x_i^2}) \rightarrow (x_1, \dots, x_{k-1})$. Conversely, a k -dimensional spherical code may be obtained by placing codepoints in the interior of Ω_{k-1} and projecting each codepoint onto Ω_k using the reverse mapping. This simple mapping was used by Yaglom [97] to map a $(k - 1)$ -dimensional lattice Λ onto Ω_k . Specifically, Yaglom proves this method implies

$$M(k, d) \geq \left(\frac{2}{d}\right)^{k-1} \Delta_{k-1}^{pack}.$$

In particular, for $k = 3$ this method implies that $M(3, d) \geq \frac{\pi}{2\sqrt{3}d^2}$. The distortion created by mapping Λ to Ω_k gives poor asymptotic spherical code densities, even if Λ is the densest lattice in $k - 1$ dimensions, as summarized in Figure 2.8. This is due to the “warping” effect on the codepoints near the boundary, as illustrated in Figure 3.2.

Converting Yaglom’s bound on $M(k, d)$ to a bound on $\Delta(k, d)$ is accomplished by noting that points initially are located on and inside of Ω_{k-1} , and are mapped to the surface of Ω_k . This implies the following lemma. The Beta function, defined by $\beta(x, y) = \frac{\Gamma(x)\Gamma(y)}{\Gamma(x+y)}$, is used in the lemma.

Lemma 3.4 $\Delta(k, d) \geq \frac{V_{k-1} \Delta_{k-1}^{pack}}{S_k} = \frac{\Delta_{k-1}^{pack}}{(k-1)\beta(\frac{k}{2}, \frac{1}{2})}$

Corollary 3.3 *Spherical codes constructed from Yaglom's mapping are not asymptotically optimal. Furthermore, the ratio of the asymptotic density of these codes in k dimensions to the maximum asymptotic spherical coding density $\Delta_k^{s.c.}$ tends to 0 as $k \rightarrow \infty$.*

Proof: The first statement follows from Lemmas 3.1 and 3.4 and the fact that $(k-1)\beta(\frac{k}{2}, \frac{1}{2}) > 1$ for all $k > 1$, and the second statement follows from the fact that this quantity tends to ∞ as $k \rightarrow \infty$. ■

3.3.2 Wyner lower bound

Wyner [95] gives a nonconstructive lower bound. The largest k -dimensional code with minimum distance d has the property that there is no point on Ω_k that is more than distance d away from its nearest codepoint; otherwise, such a point could be added to the code. Thus, if $M(k, d)$ caps of angular radius $\theta/2$ are nonoverlapping, increasing the angular radius of each cap to θ causes them to cover the sphere. Wyner used this to show a general bound in k dimensions:

$$M(k, d) \geq \frac{k}{k-1} \cdot \frac{\sqrt{\pi} \Gamma(\frac{k+1}{2})}{\Gamma(\frac{k+2}{2})} \cdot \left[\int_0^{2 \sin^{-1}(d/2)} \sin^{k-2} \phi d\phi \right]^{-1}.$$

When $k = 3$, the result is that $M(3, d) \geq \frac{4}{d^2}$. The bound is written more concisely in our notation:

$$M(k, d) \geq \frac{S_k}{S(c(k, \theta))},$$

which together with Equation (2.8) gives us the following lemma.

Lemma 3.5 $\Delta(k, d) \geq \frac{S(c(k, \theta/2))}{S(c(k, \theta))}$

Using Equation (2.6), the asymptotic nature (as $d \rightarrow 0$) of Wyner's bound is $\Delta_k^{s.c.} \geq 2^{1-k}$. How well does this compare with the true answer of $\Delta_k^{s.c.} = \Delta_{k-1}^{pack}$, as proved in Lemma 3.1? Even for moderately large k , the result is very weak. For example, when $k = 25$, Wyner's bound is $\Delta_k^{s.c.} \geq 2^{-24} \approx 5.96 \times 10^{-8}$, whereas the Leech lattice implies $\Delta_k^{s.c.} = \Delta_{k-1}^{pack} \geq 0.001930$. In fact, for all $k \leq 25$, $\Delta_{k-1}^{pack} \gg 2^{1-k}$. On the other hand, for very large k , Minkowski's bound of $\Delta_{k-1}^{pack} \geq 2^{1-k}$ is still the best bound known.

Corollary 3.4 *The Wyner bound is not asymptotically tight for $1 \leq k \leq 25$.*

3.3.3 Concatenated spherical codes

An M -ary *phase-shift-keying* (MPSK) code is a set of points equally spaced about a circle in \mathbb{R}^2 . MPSK codes $\mathcal{C}_1, \dots, \mathcal{C}_m$ may be concatenated to yield a $2m$ -dimensional spherical code $\mathcal{C}_1 \times \dots \times \mathcal{C}_m$. Concatenated codes have the desirable property that they are not only formed from codepoints of constant energy, but also every pair of coordinates in the code is constant energy as well. In general, the codes being concatenated need not be two-dimensional. Using the same method and notation, l -dimensional codes may be concatenated. Let M_i and r_i be the number of codepoints and the norm of codepoints of \mathcal{C}_i (radius of the sphere containing \mathcal{C}_i), respectively, and let $r_i d_i$ be the distance between points of \mathcal{C}_i , i.e., so that d_i is the minimum distance when \mathcal{C}_i is scaled to the unit sphere (circle, for MPSK codes).

A concatenation of m of these l -dimensional codes is said to be an *optimal concatenation* if no other concatenation of m such l -dimensional codes has the same number of codepoints and a larger minimum distance. Underlying codes of differing radii and number of codepoints may be used in the concatenation [98]. For example, a four-point MPSK code on a circle with radius $1/2$ may be concatenated with a 16-point MPSK code on a radius $\sqrt{3}/2$ circle to form a 64-point four-dimensional spherical code. This gives $d = 2\frac{\sqrt{3}}{2} \sin(\frac{\pi}{16}) \approx 0.338$.

Lemma 3.6 *Let a $(2m)$ -dimensional spherical code with M^m codepoints be formed by the concatenation of m two-dimensional codes of radii r_1, \dots, r_m and sizes M_1, \dots, M_m , respectively. The code is an optimal concatenation if $M_1 = M_2 = \dots = M_m = M$ and $r_1 = r_2 = \dots = r_m = \sqrt{1/m}$.*

Proof: The concatenated code is subject to the constraints

$$\prod_{i=1}^m M_i = M^m, \text{ and} \tag{3.3}$$

$$\sum_{i=1}^m r_i^2 = 1. \tag{3.4}$$

First, it is shown that every optimal concatenation satisfies $d = r_1 d_1 = r_2 d_2 = \dots = r_m d_m$. By definition, $d = \min\{r_i d_i\}$. By way of contradiction, suppose there were an optimal concatenation with i and j such that $d = r_i d_i < r_j d_j$. Choose $\delta > 0$ such that $r_i d_i < r_j d_j - \delta$. Construct a new concatenated code by increasing the radius of code i by some small $\epsilon > 0$ (to be determined

shortly), and decreasing the radius of code j by another amount. This is indicated using the prime notation for the new concatenation parameters

$$\begin{aligned} r'_i &= r_i + \epsilon \\ r'_j &= \sqrt{r_j^2 - 2\epsilon r_i - \epsilon^2}. \end{aligned}$$

Note that under this change the constraints (3.3) and (3.4) are still met. However, it follows that

$$\begin{aligned} r'_i d'_i &= (r_i + \epsilon) d_i > r_i d_i, \\ r'_j d'_j &= \sqrt{r_j^2 - 2\epsilon r_i - \epsilon^2} d_j > r_j d_j - \delta, > r_i d_i \end{aligned}$$

for sufficiently small ϵ . Thus, the minimum distance of the concatenation has been improved, a contradiction.

Each component code of an optimal concatenation is optimal; M_i points equally spread about a unit circle give a minimum distance of $d_i = 2 \sin(\pi/M_i)$, for all i . Suppose an optimal concatenation exists such that for some i and j , $M_i > M_j + 1$. A new concatenated code is constructed by adjusting the size and radii of the i th and j th codes as follows:

$$\begin{aligned} M'_i &= M_i - 1 \\ M'_j &= M_j + 1 \\ r'_i &= \frac{r_i d_i}{2 \sin\left(\frac{\pi}{M_i - 1}\right)} \\ r'_j &= \frac{r_j d_j}{2 \sin\left(\frac{\pi}{M_j + 1}\right)} \\ d'_i &= 2 \sin\left(\frac{\pi}{M_i - 1}\right) \\ d'_j &= 2 \sin\left(\frac{\pi}{M_j + 1}\right). \end{aligned}$$

The minimum distance of the new code is equal to that of the old code, since $r'_i d'_i = r_i d_i$ and $r'_j d'_j = r_j d_j$. The new code has more points, since $M'_i M'_j = (M_i - 1)(M_j + 1) = M_i M_j + M_i - M_j - 1 > M_i M_j$. To meet constraint (3.3), any M^m of the points are retained and the rest are discarded. Next it is shown that constraint (3.4) holds. Note that if $\sum_{i=1}^m r_i^2 < 1$, then all codes may have their radius increased, which would meet constraint (3.4) and increase the minimum

distance. Hence, it need only be shown that $(r'_i)^2 + (r'_j)^2 \leq r_i^2 + r_j^2$, or equivalently,

$$\frac{(r_i d_i)^2}{4 \sin^2\left(\frac{\pi}{M_i-1}\right)} + \frac{(r_j d_j)^2}{4 \sin^2\left(\frac{\pi}{M_j+1}\right)} \leq \frac{(r_i d_i)^2}{4 \sin^2\left(\frac{\pi}{M_i}\right)} + \frac{(r_j d_j)^2}{4 \sin^2\left(\frac{\pi}{M_j}\right)}.$$

Recall, $r_i d_i = r_j d_j$, and hence, it suffices to show that

$$f(M) = \frac{1}{\sin^2\left(\frac{\pi}{M}\right)} - \frac{1}{\sin^2\left(\frac{\pi}{M-1}\right)} = \underbrace{\left(\frac{1}{\sin\left(\frac{\pi}{M}\right)} + \frac{1}{\sin\left(\frac{\pi}{M-1}\right)}\right)}_{g(M)} \underbrace{\left(\frac{1}{\sin\left(\frac{\pi}{M}\right)} - \frac{1}{\sin\left(\frac{\pi}{M-1}\right)}\right)}_{h(M)}$$

is a nondecreasing function in M . It is easy to see that $g(M)$ is increasing in M . Elementary calculus shows that $1/\sin(\pi/M)$ is convex; thus,

$$\frac{1}{\sin\left(\frac{\pi}{M+1}\right)} + \frac{1}{\sin\left(\frac{\pi}{M-1}\right)} - \frac{2}{\sin\left(\frac{\pi}{M}\right)} \geq 0.$$

The left-hand side is equal to $h(M+1) - h(M)$; therefore, $h(M)$ is increasing in M . Since $g(M)$ and $h(M)$ are increasing in M , $f(M)$ is increasing in M . Thus, the new concatenated code meets the size and radius constraints. Since it has the same number of points as the old code and its minimum distance did not decrease, it is also an optimal concatenation. Note that the difference between the number of points of the i th and j th codes is strictly less than before. This process may be repeated until the component code sizes are equal or differ by one. Thus, there exist $a \geq 0$ and $l \in [0, m]$, such that l component codes are of size a and $m-l$ component codes are of size $a+1$, and such that the concatenation is optimal. Since the number of codepoints in the concatenation is M^m , it follows that $a^l(a+1)^{m-l} = M^m$. Thus,

$$a^m \leq a^l(a+1)^{m-l} = M^m \leq (a+1)^m.$$

This implies $a \leq M \leq a+1$. Since $M \in \mathbb{Z}$, either $M = a$ or $M = a+1$. In the first case, $a^m = a^l(a+1)^{m-l}$ and l must be m ; in the second case $a^l(a+1)^{m-l} = (a+1)^m$ and l must be 0. In either case, then, the component codes are all the same size (either all size a or all size $a+1$). Thus, there is an optimal code with $M_1 = \dots = M_m$. Since $d_i = 2 \sin(\pi/M_i)$, it follows that $r_1 = \dots = r_m$ as well. ■

Corollary 3.5 *Optimal concatenation of MPSK codes implies*

$$M(k, d) \geq \left(\frac{\pi}{\sin^{-1}\left(d\sqrt{\frac{k}{8}}\right)} \right)^{k/2},$$

for k even.

Proof: Lemma 3.6 implies $r_1 = 1/\sqrt{m} = \sqrt{\frac{2}{k}}$ and $d_i = 2 \sin\left(\frac{\pi}{M^{2/k}}\right)$. Since $d = r_1 d_1$, it follows that $d = 2\sqrt{\frac{2}{k}} \sin\left(\frac{\pi}{M^{2/k}}\right)$, from which the result follows. ■

Corollary 3.6 *For k even, the optimal concatenation of MPSK codes does not result in asymptotically optimal spherical codes. In fact, the density of these codes tends to 0 as $d \rightarrow 0$.*

Proof: From Equation (2.8), it suffices to show that $\lim_{d \rightarrow 0} \left(\frac{\pi}{\sin^{-1}\left(d\sqrt{\frac{k}{8}}\right)} \right)^{k/2} \cdot S(c(k, \theta/2)) \rightarrow 0$.

This follows directly from Equation (2.7), which implies $S(c(k, \theta/2)) = O(d^{k-1})$, and from

$$\left(\frac{\pi}{\sin^{-1}\left(d\sqrt{\frac{k}{8}}\right)} \right)^{k/2} = O(d^{-k/2}). \blacksquare$$

Lemma 3.6 allows one to plot an upper bound on minimum distances attainable for concatenated codes, for no concatenated code will perform better than the code formed by concatenations of (hypothetical) codes which meet the Coxeter upper bound. That is, any l -dimensional spherical code may be rescaled by dividing it by \sqrt{m} and concatenated with m copies of itself to obtain a $(2ml)$ -dimensional code having a minimum distance smaller by a factor of \sqrt{m} . In general, even the size of these hypothetical codes compares unfavorably to other construction techniques. For example, consider a spherical code in three dimensions of minimum distance 0.83. For the sake of argument, suppose this code met the Coxeter upper bound of 20 codepoints. (In fact, the best code known with this minimum distance has only 18 points.) A concatenation of the code with itself gives a six-dimensional 400-point code with $d = 0.830/\sqrt{2} \approx 0.587$. On the other hand, there exist six-dimensional codes of size more than 720 points that meet this minimum distance.

This result is not entirely surprising, for embedded in every spherical code obtained by concatenating l -dimensional codes is the constraint that every l components of each codepoint form a vector of some fixed norm; this severely limits the position of codepoints on the larger dimensional sphere of the code.

3.3.4 Spherical codes from binary codes

To obtain a spherical code from a binary code of blocklength k , every 0 is changed to 1 and every 1 to -1, and every coordinate is rescaled by $1/\sqrt{k}$. For example,

$$\begin{aligned} 01111101 &\rightarrow \frac{1}{\sqrt{8}}(1, -1, -1, -1, -1, -1, 1, -1), \text{ and} \\ 11110000 &\rightarrow \frac{1}{\sqrt{8}}(-1, -1, -1, -1, 1, 1, 1, 1). \end{aligned}$$

Hamming distance d_H between two codewords of length k corresponds to Euclidean distance $2\sqrt{d_H/k}$ between the corresponding spherical code codepoints. In the example, Hamming distance 4 corresponds to Euclidean distance $\sqrt{2}$.

There does not exist a family of asymptotically optimal k -dimensional spherical codes that are constructed from binary codes using the method described in this section. In fact, the density of these codes tends to 0 as $d \rightarrow 0$. This is implied by the simple fact that a binary code of blocklength k is limited to at most 2^k codewords, a finite number, and thus no asymptotically large spherical code may be formed, for fixed k , from the binary code.

How do nonasymptotic spherical codes from binary codes perform? If we restrict attention to linear codes, the Singleton bound implies that a linear binary code of blocklength k , size M , and minimum Hamming distance d_H , must satisfy

$$d_H \leq 1 + k - \log M,$$

and using $d = 2\sqrt{d_H/k}$, the corresponding spherical code satisfies

$$M \leq 2^{k(1-d^2/4)+1}.$$

Using Equation (2.8), the density Δ of a spherical code constructed from a linear binary code is at most

$$\Delta = \frac{M \cdot S(c(k, \theta/2))}{S_k} \leq \frac{2^{k(1-d^2/4)+1} (V_{k-1}(\frac{d}{2})^{k-1} + O(d^{k+1}))}{S_k} = \frac{4 \cdot 2^{-kd^2/4} V_{k-1}}{k V_k}.$$

Thus, for a given k and d , $\Delta \leq \frac{4V_{k-1}}{kV_k} = \frac{4}{k\beta(\frac{k}{2}, \frac{1}{2})}$. This quantity is significantly less than Δ_{k-1}^{pack} for $1 \leq k \leq 9$, as can be verified from known lower bounds on Δ_{k-1}^{pack} .

3.3.5 Apple-peeling spherical codes

Prior to this thesis, the best spherical codes known for asymptotically small d were the so-called apple-peeling codes due to El Gamal et al. [18]. Their technique resembles peeling an apple in three dimensions, and is described below for comparison purposes.

Let $\mathcal{C}^*(k-1, d)$ denote any $(k-1)$ -dimensional spherical code with minimum distance d , whose codepoints are indexed from 1 to $|\mathcal{C}^*(k-1, d)|$. The *apple-peeling spherical code* $\mathcal{C}^A(k, d)$ on Ω_k with respect to $\mathcal{C}^*(k-1, \cdot)$ is defined in [18] as the set of points

$$\{(x_1(i, j) \cos \eta(i), \dots, x_{k-1}(i, j) \cos \eta(i), \sin(\eta(i)))\}$$

such that

$$i \in \{l \in \mathbb{Z} : -\pi/2 \leq \eta(l) \leq \pi/2\} \quad (3.5)$$

$$j \in \{1, \dots, |\mathcal{C}^*(k-1, d/\cos \eta(i))|\}$$

$$\eta(i) \equiv (i + 1/2)\theta$$

$$X(i, j) = (x_1(i, j), \dots, x_{k-1}(i, j)) \text{ is the } j\text{th} \quad (3.6)$$

codeword of $\mathcal{C}^*(k-1, d/\cos \eta(i))$.

It is verified in [18] that the apple-peeling code has minimum distance d .

Summing over all admissible values of i in (3.5) and choosing $\mathcal{C}^*(k-1, d/\cos \eta(i))$ to be a maximum size code for all i give the lower bound

$$M(k, d) \geq 2 \cdot \sum_{i=0}^{\lfloor \frac{\pi}{2\theta} - \frac{1}{2} \rfloor} M(k-1, d/\cos \eta(i)). \quad (3.7)$$

Lemma 3.7 *The density of the densest k -dimensional apple-peeling spherical code $\mathcal{C}^A(k, d)$ approaches $\frac{1}{2} \cdot \Delta_{k-2}^{pack} \beta(\frac{k}{2}, \frac{1}{2})$, as $d \rightarrow 0$.*

Proof: See Appendix C.2.

Corollary 3.7 *For all $k \geq 3$, the k -dimensional apple-peeling code is not asymptotically optimal. Further, the ratio of the asymptotic density of apple-peeling codes in k -dimensions to the maximum asymptotic spherical coding density $\Delta(k)$ tends to 0 as $k \rightarrow \infty$.*

Proof: This follows from the facts that $\frac{1}{2} \cdot \beta(\frac{k}{2}, \frac{1}{2})$ is less than 1 for all $k \geq 3$ and that this quantity approaches 0 as k tends to ∞ . ■

The numeric values of $M(k-1, d)$ for $k \geq 4$ are not presently known, except for a handful of values of d ; hence, $\Delta_{\mathcal{C}^A(k,d)}$ cannot be easily evaluated using (3.7). Also, Δ_{k-2}^{pack} is not known for $k \geq 5$, and so the asymptotic performance is also difficult to evaluate. However, the numerical values of the asymptotic density of the best realizable apple-peeling codes, given the current state of knowledge of $M(k-1, d)$, can be determined as follows. If, in (3.6), $\mathcal{C}^*(k-1, d/\cos \eta(i))$ is chosen to be the best code known with the given parameters, then a lower bound on $\Delta(k, d)$ can be computed. By Lemma 3.1, the density of $\mathcal{C}(k-1, d/\cos \eta(i))$ can be as high as the density of the best sphere packing known in \mathbb{R}^{k-2} . The asymptotic density of the best apple-peeling codes currently realizable is given by replacing Δ_{k-2}^{pack} in the formula for the density in Lemma 3.7 with the density of the best sphere packing *known* in \mathbb{R}^{k-2} . This apple-peeling code asymptotic density is shown in Figure 2.8, using a table [14] of the best sphere packings known, along with recent improvements from [90] and [15]. The asymptotic density of the wrapped spherical codes is equal or higher in every dimension.

3.3.6 Codes from other structures

The vertices, midpoints of edges, or centers of the faces of any regular polytope may be used to derive spherical codes. For example, the vertices of a dodecahedron are each the same distance to the center of the dodecahedron, and these form a spherical code of size 20. The midpoints of the edges or centers of the faces result in codebooks of size 30 and 12, respectively. In fact, the vertices of the octahedron, tetrahedron, and icosahedron result in spherical codes with optimally high d .

Permutation groups also may be used. If (x_1, \dots, x_k) is a k -tuple, then any permutation of its components has the same norm. The k -tuples of a permutation may be scaled to form a spherical code [8].

Some success in generating spherical codes with large d has been reported in [21]. The codes are constructed from symmetric sets of equally spaced points on the real line.

3.3.7 Unstructured spherical codes

In this section, a method is described to construct spherical codes with excellent minimum distance properties, using an iterative design technique. The method is motivated by a physical model of charges on a sphere. The implementation is similar to the simulated annealing method of [18]. This method requires a substantial computational effort, and does not produce asymptotically optimal spherical codes. However, the algorithm in this section has produced many codes that improve upon those of [18] for specific minimum distances.

3.3.7.1 Physical model

Imagine a metal sphere on which a single charge is placed. When a force acts upon the charge, the charge moves through the metal, always confined to the sphere’s interior or surface. If M equal charges are placed on the surface of the sphere and there are no external forces, the net force on any particular charge depends only on the contributions of force from the other $M - 1$ charges. Since the charges all repel each other, none of the $M - 1$ contributing forces has a component directed to the interior of the sphere, and thus the charges will remain on the surface of the sphere as they move about. The charges will continue to move until some stable configuration is reached.

The goal is to find the final stable configuration of charges. In a sense the algorithm presented in this section seeks to mimic nature, where each “charge” represents a codepoint of a spherical code, and the “forces” between codepoints are determined by computer simulation.

3.3.7.2 Algorithm motivation and description

The physical analogy of the design procedure is intuitively interesting, although it is not a perfect analogy. Whereas the value of the minimum distance d can be determined directly from the nearest neighbor distances of the M codepoints (the smallest one), the potential energy is a sum involving *all* of the distances between pairs of points. To coarsely account for this difference, the algorithm only considers the force exerted by a charge’s *nearest neighbor*. This has the additional advantage of easing the computation, reducing $M - 1$ force computations to one.

Table 3.1 Iterative spherical code optimization algorithm.

Step 1. Populate the k -dimensional sphere with M codepoints at random positions.

Step 2. Repeat the following, until the minimum distance stops improving:

- A.** Develop a “goal” minimum distance g for the codebook, based on how fast the algorithm has improved the codebook in recent iterations. The value of g is assigned a value slightly larger than the minimum distance of the best codebook obtained thus far.
- B.** Pick a codepoint X at random.
- C.** Move X directly toward or away from its nearest neighbor, according to the modified force law (3.8).

Another difference is that charges on a sphere may arrange themselves in a locally stable configuration that is not the best configuration. A modification of the usual inverse square law for force helps to avoid this problem. Whereas the magnitude of the natural repelling force between two charges at locations X and Y is proportional to

$$\frac{1}{\|X - Y\|^2},$$

the algorithm uses a modified force law in which the repelling force is proportional to

$$\frac{\|X - Y\|^2 - g^2}{\|X - Y\|^2}, \quad (3.8)$$

where g is a goal minimum distance of the codebook. Indeed, suppose g is the desired minimum distance, X is the codepoint for which the force is to be determined, and Y is the nearest neighbor of X . If $\|X - Y\| < g$, it is important that X move away from Y — all codepoints should be at a distance at least g from each other. On the other hand, if $\|X - Y\| > g$, it is *not* important that X move away from Y , since X meets the goal distance g without moving. In fact, it is desirable for X to move *toward* Y , so that X is packed next to Y at or close to a distance g from Y , and a gap is opened where X was before it was moved. This gap may prove useful for other codepoints, as is illustrated in Figure 3.3. The algorithm is summarized in Table 3.1.

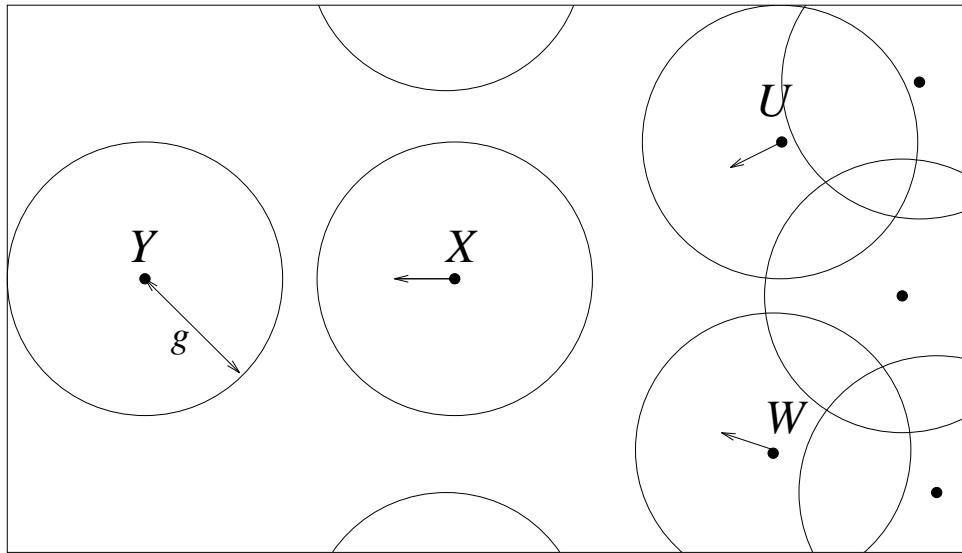


Figure 3.3 A small section of the surface of the unit sphere. Codepoints have a cap of radius g around them. If no caps intersect, then the minimum distance is greater than g . The algorithm moves X toward its nearest neighbor Y , not away. This allows U and W to make use of the resulting gap.

3.3.7.3 Implementation

The algorithm has been implemented on an HP Apollo Series 700. The codebook is stored as a linked list, sorted by the first coordinate of the codepoints. When a codepoint is perturbed, it is reinserted at the proper point in the list, and the new minimum distance of the codebook is computed. Each codepoint's nearest neighbor is tracked at all times. This involves, after each perturbation, finding the new nearest neighbor of the perturbed codepoint and determining whether the perturbed codepoint has become the nearest neighbor of any other codepoint.

Efficient methods for determining nearest neighbors were used. To find the nearest neighbor of codepoint X , the algorithm begins by computing the distance d^* to the codepoint next to X in the sorted linked list. Then, the list is searched backward and forward from X for a nearer codepoint to X , aborting any partial distance calculation when it exceeds d^* , and ending the entire search when a codeword Y in the list is reached that differs from X by more than d^* in the first coordinate alone. In this way, much of the codebook is never involved in the distance calculation. This method has also been used elsewhere [31, p. 479-480].

For each dimension and number of codepoints considered, one to three million perturbations were performed, requiring anywhere from a few minutes to a few hours of computation time, depending on the dimension and number of codepoints.

The program has produced codes remarkably better than those from lattices, binary codes, and other means. In particular, one spherical code produced in a few minutes of computation has larger minimum distance than that published in [35], a paper devoted solely to developing a spherical code with $M = 19$ and $k = 3$. Figure 3.4 shows the front and back of a three-dimensional sphere with the placement of 19 points on it after iterations one to one million. The final minimum distance obtained by our algorithm is 0.807, while [35] achieves 0.804.

This unstructured spherical code search has been improved in [69, 82]. The iterative algorithm described above converges to a locally optimal solution, but the locally optimal configuration will not be obtained exactly after a finite number of iterations. Instead, the algorithm may be terminated and a system of equations may be solved to yield this locally optimum configuration. This improves many of the solutions and has yielded the best known spherical codes in three dimensions for codesizes up to 33,002 [82].

3.3.7.4 Other algorithms for unstructured codes

The algorithm presented above strikes a balance between mimicking nature faithfully and running each iteration quickly, but it does not prove that better unstructured spherical codes are impossible. Could some other method do better, while still having a reasonable running time? There is not much room for improvement, since the method presented here already closely approaches the upper bounds on the minimum distance.

Nonetheless, a few other ideas were investigated. Testing showed that whether the force law was an inverse square, inverse cube, etc. made very little difference in the resulting minimum distance. Keeping track of more than one nearest neighbor of each codepoint and computing the forces based on those sets of points results in a faster convergence rate *per iteration*, but a much slower convergence rate per hour of computer time, because more computation is required per iteration.

Another approach is to randomly populate the sphere with points as before, except that thousands or millions more points than are actually desired for the final codebook must be created. Then, the codepoint having the closest nearest neighbor is identified and deleted.

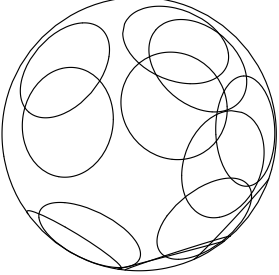
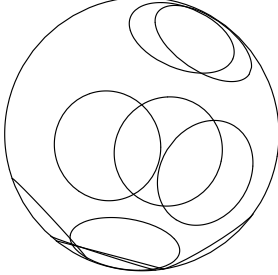
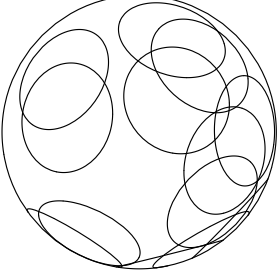
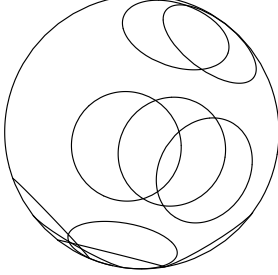
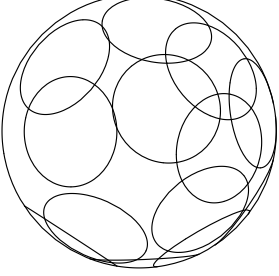
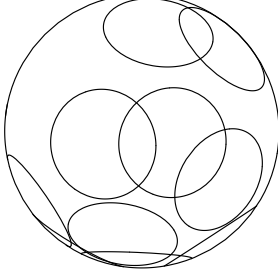
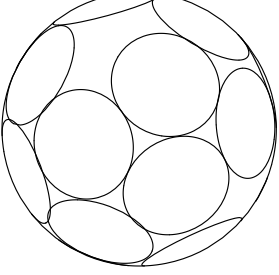
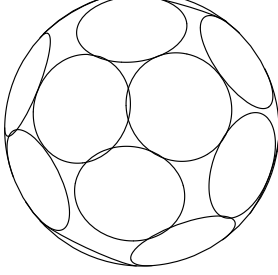
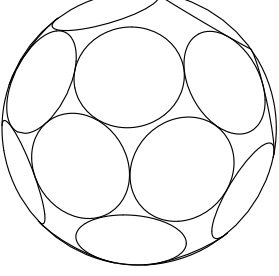
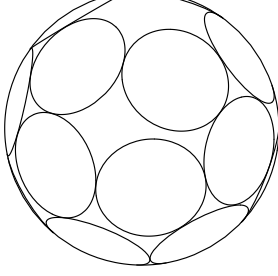
Iteration	d	Front	Back
1	0.061		
100	0.301		
1,000	0.519		
10,000	0.777		
1,000,000	0.807		

Figure 3.4 The algorithm in action.

From this new codebook, again the codepoint having the closest nearest neighbor is found and deleted. This process is repeated until the desired number of codepoints remains. At each stage, the minimum distance increases or remains unchanged. Also, the algorithm is less complex than the one above. Unfortunately, this approach resulted in codebooks with minimum distances that are substantially lower than those of the original algorithm.

3.4 Comparisons

For dimensions three, four, and eight, Figures 3.5, 3.6, and 3.7, respectively, show the relative performance of the spherical codes constructed by the methods in this section. Numerical values are given in Tables 3.2 and 3.3. In dimensions three and four, the density of various spherical codes divided by the upper bound on density is plotted versus the minimum distance.

Recall that the minimum distance between points on these shells is at least as large as the minimum distance of the lattice, but could be much larger. To make a fair comparison, the exact minimum distances were calculated with the aid of a computer. It was found that minimum distances could be 50% higher, or more, than the minimum distance of the lattice. Whereas previous work has compared spherical codes using the lower figure [98], this thesis appears to be the first work in which an exact minimum distance has been computed. The first 1000 shells of lattices were used to construct spherical codes.

For minimum distances larger than about 0.5, shells of lattices often produce very good spherical codes. For example, a shell of each of A_3 , A_3^* and \mathbb{Z}^3 produces the optimal three-dimensional spherical code with twelve points and minimum distance one. Shells of lattices also produce the (conjectured optimal) four-dimensional spherical code with 24 points and minimum distance one. A shell of E_8 produces the best known eight-dimensional code with minimum distance one. A few codes constructed by Ericson and Zinoviev also have good performances for large minimum distances. The performance for smaller minimum distances is worse, however. For minimum distances below about 0.1, the wrapped and laminated spherical codes perform better than the shells of lattices.

The codes compiled by (and in many cases constructed by) Hardin and Sloane [82] represent the best known spherical codes in three dimensions for minimum distances larger than about 0.02 and in four dimensions for minimum distances larger than about 0.6. These codes were

Table 3.2 Three-dimensional code sizes at various minimum distances.

d	Coxeter upper bound	laminated code	wrapped code	apple-peeling code
10^{-1}	1450	1294	1070	1236
10^{-2}	145,103	134,422	130,682	125,504
10^{-3}	1.45×10^7	1.43×10^7	1.40×10^7	1.26×10^7
10^{-4}	1.45×10^9	1.45×10^9	1.44×10^9 *	1.26×10^9
10^{-5}	1.45×10^{11}	1.45×10^{11}	1.45×10^{11} *	1.26×10^{11}

* estimated

Table 3.3 Four-dimensional code sizes at various minimum distances. The Coxeter upper bound is not asymptotically tight: using the best known upper bound on packing density in three dimensions and Lemma 1 of [1], an asymptotic upper bound of $2.79 \times 10^{3n+1}$ is achieved, for $d = 10^{-n}$ and large n .

d	Coxeter upper bound	laminated code	wrapped code	apple-peeling code
10^{-1}	29,364	16,976	17,198	22,740
10^{-2}	2.94×10^7	2.31×10^7	2.31×10^7 *	2.28×10^7
10^{-3}	2.94×10^{10}	2.59×10^{10}	2.59×10^{10} *	2.28×10^{10}
10^{-4}	2.94×10^{13}	2.72×10^{13}	2.72×10^{13} *	2.28×10^{13}
10^{-5}	2.94×10^{16}	2.77×10^{16}	2.77×10^{16} *	2.28×10^{16}

* estimated

constructed by an iterative algorithm which would not be suitable for extremely large spherical codes with small minimum distances. Codes from the iterative technique presented in this chapter are included in Figures 3.5, 3.6, and 3.7 as well.

The performances of the wrapped spherical codes and laminated spherical codes are included in the plots as well, and will be discussed more in Chapters 4 and 5.

3.5 Conclusions

The surface of the k -dimensional sphere “looks” like \mathbb{R}^{k-1} , in the sense that the maximum packing density, minimum quantization coefficient, and thinnest covering in \mathbb{R}^{k-1} equal the maximum asymptotic spherical coding density, minimum asymptotic spherical quantization coefficient, and thinnest asymptotic covering of Ω_k , respectively.

Previous bounds on the size of spherical codes have been converted to bounds on the density of spherical codes. This brings to light the fact that Yaglom’s spherical codes, Wyner’s lower bound, concatenated MPSK codes, spherical codes from binary codes, and apple-peeling codes

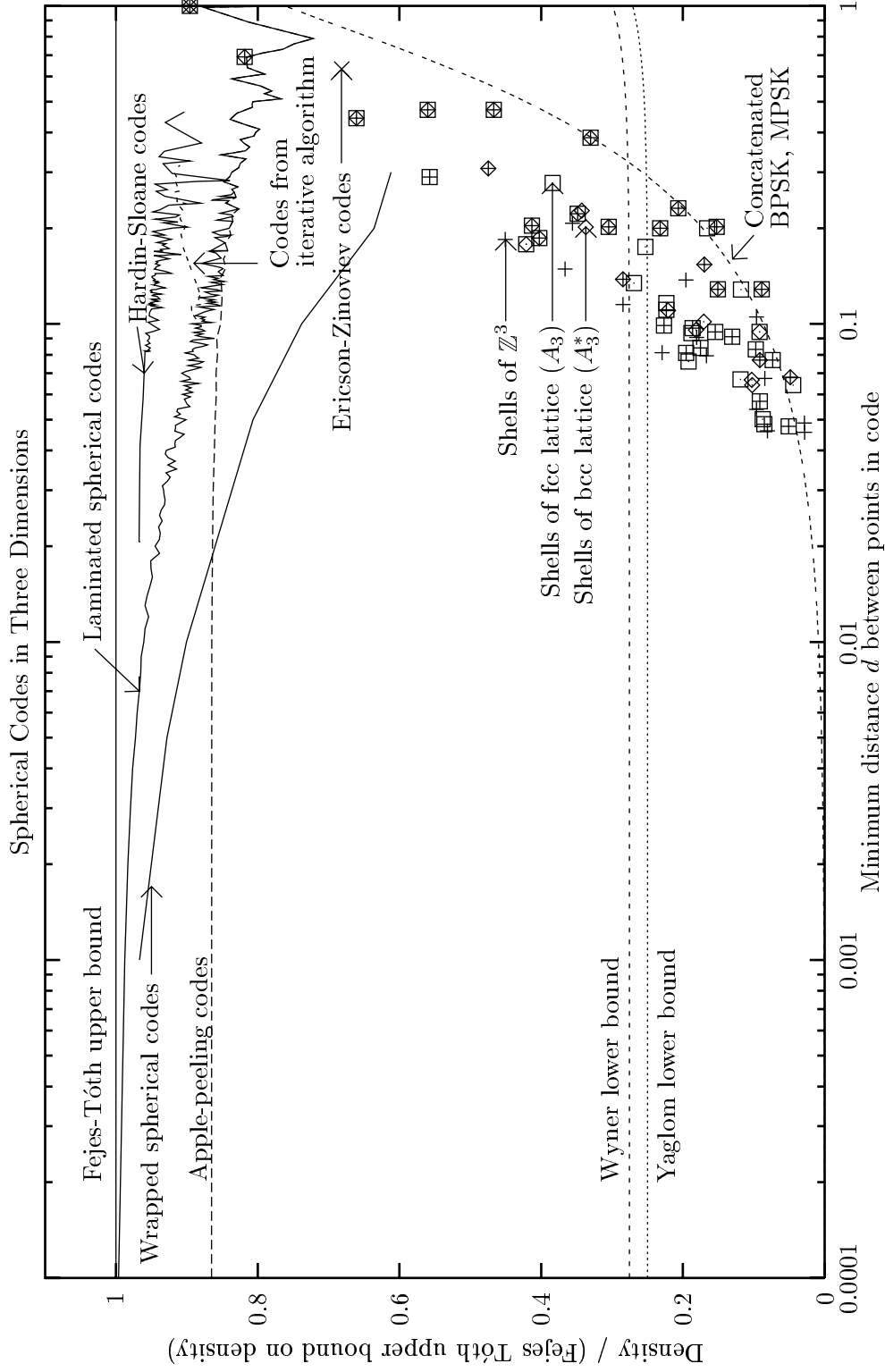


Figure 3.5 Comparison of three-dimensional spherical codes.

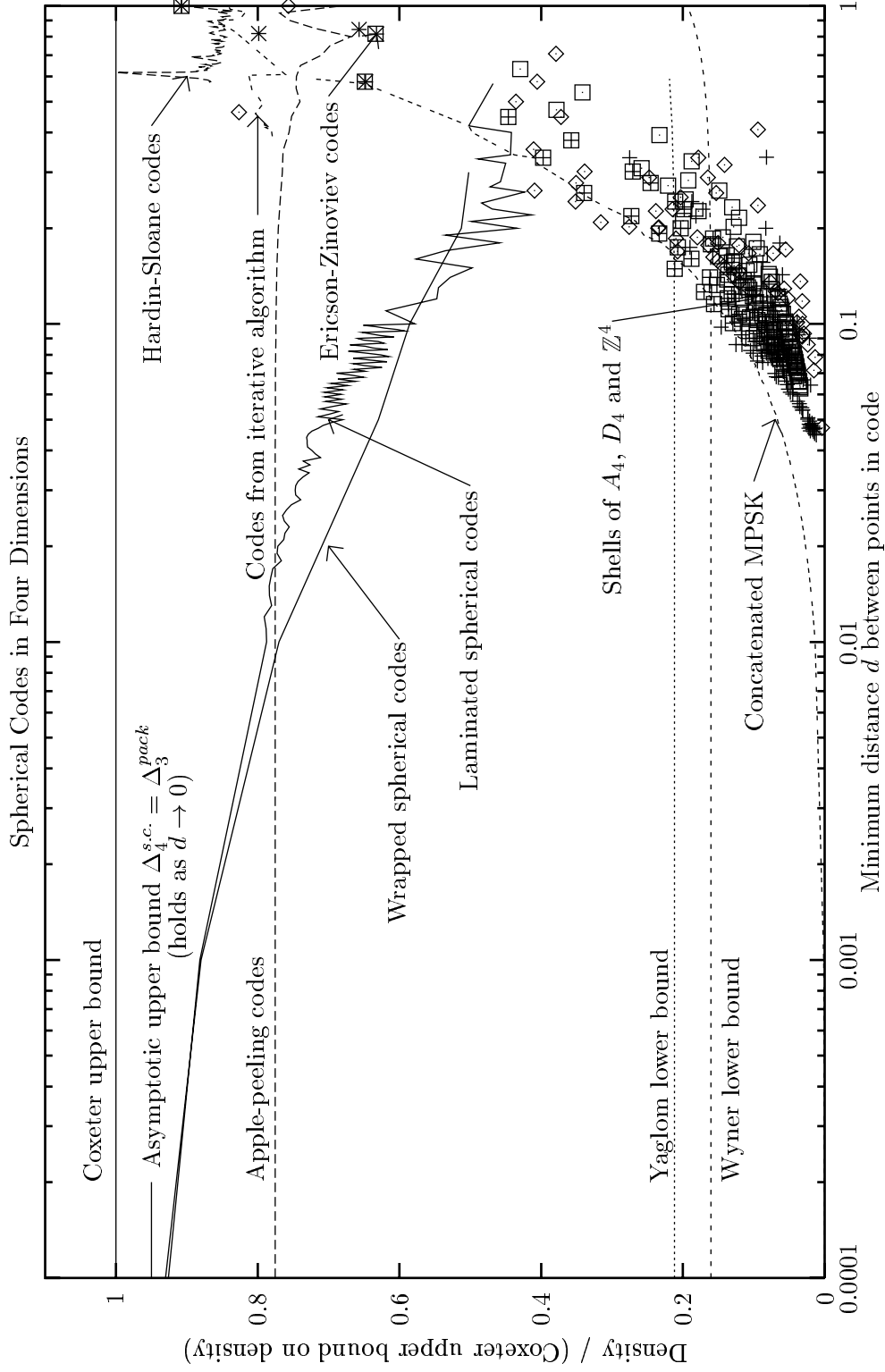


Figure 3.6 Comparison of four-dimensional spherical codes.

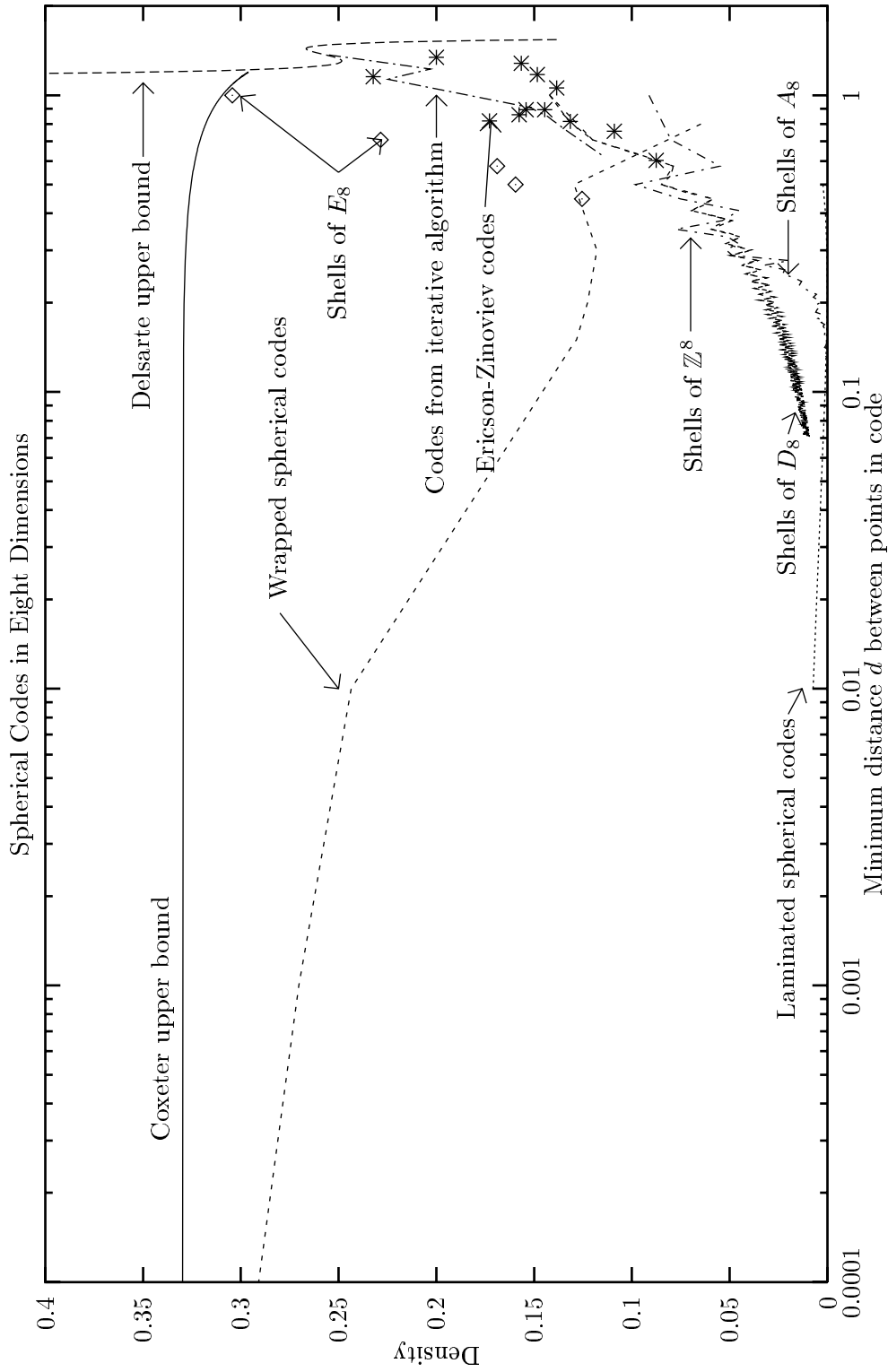


Figure 3.7 Comparison of eight-dimensional spherical codes.

are not asymptotically optimal. Unstructured codes can be asymptotically optimal, but finding them requires a computer optimization that is not feasible for large codebooks. The spherical code constructions of the next two chapters each produce asymptotically optimal spherical codes.

CHAPTER 4

WRAPPED SPHERICAL CODES

4.1 Introduction

In this chapter, a mapping is introduced which effectively “wraps” any packing in \mathbb{R}^{k-1} around Ω_k (actually into a finite subset of Ω_k); hence, the spherical codes it constructs are referred to as wrapped spherical codes. This technique creates codes of any size and thus provides a lower bound on achievable minimum distance as a function of code size. It will be shown that the spherical code density approaches the density of the underlying packing, as $d \rightarrow 0$.

4.2 Construction of Wrapped Spherical Codes

Let Λ be a sphere packing in \mathbb{R}^{k-1} with minimum distance d and density Δ_Λ . Λ may be either a lattice packing or a nonlattice packing. Let $0 = \xi_0 < \dots < \xi_N = 1$, and for $x \in [-1, 1]$, let $\underline{\xi}(x) \equiv \max\{\xi_i : \xi_i \leq |x|\}$ and $\bar{\xi}(x) \equiv \min\{\xi_i : \xi_i > |x|\}$. The real numbers ξ_0, \dots, ξ_N are referred to as *latitudes* and will be chosen later to yield a large code size. The i th *annulus* is defined as the set of points $(x_1, \dots, x_k) \in \Omega_k$ that satisfy $\xi_i \leq x_k < \xi_{i+1}$ (i.e., points between consecutive latitudes). Define the many-to-one function $f': \Omega_k \rightarrow \mathbb{R}^{k-1}$ by

$$f'(x_1, \dots, x_k) = \alpha(x_k) \cdot \frac{(x_1, \dots, x_{k-1})}{\sqrt{1 - x_k^2}} \quad (4.1)$$

where

$$\alpha(x_k) = \left(\sqrt{1 - \underline{\xi}(x_k)^2} - \sqrt{(|x_k| - \underline{\xi}(x_k))^2 + \left(\sqrt{1 - \underline{\xi}(x_k)^2} - \sqrt{1 - x_k^2} \right)^2} \right)_+,$$

and where $(x)_+ = \max(0, x)$. If $X = (x_1, \dots, x_k)$ and $Y = f'(X) \neq 0$, then

$$\left\| \left(\sqrt{1 - \underline{\xi}(x_k)^2}, \underline{\xi}(x_k) \right) - \left(\sqrt{1 - x_k^2}, |x_k| \right) \right\| = \sqrt{1 - \underline{\xi}(x_k)^2} - \|Y\|,$$

which is shown geometrically in Figure 4.2. Define the *buffer region* as the set

$$B' = \left\{ (x_1, \dots, x_k) \in \Omega_k : (|x_k| - \underline{\xi}(x_k))^2 + \left(\sqrt{1 - \underline{\xi}(x_k)^2} - \sqrt{1 - x_k^2} \right)^2 < d^2 \right\}.$$

A useful spherical code with respect to Λ is defined by $\text{WA-SC} = (f')^{-1}(\Lambda \setminus \{0\}) \setminus B'$.

Let

$$f(x_1, \dots, x_k) = \begin{cases} f'(x_1, \dots, x_{k-2}, x_{k-1}, x_k) & \text{if } |x_k| \leq 1/\sqrt{2} \\ f'(x_1, \dots, x_{k-2}, x_k, x_{k-1}) & \text{if } |x_k| > 1/\sqrt{2} \end{cases},$$

and let

$$B = B' \cup \left\{ (x_1, \dots, x_k) \in \Omega_k : \left(|x_k| - \frac{1}{\sqrt{2}} \right)^2 + \left(\frac{1}{\sqrt{2}} - \sqrt{1 - x_k^2} \right)^2 < d^2 \right\}.$$

The *wrapped spherical code* with respect to a packing Λ having minimum distance d is defined by

$$\text{WA-SC} = f^{-1}(\Lambda \setminus \{0\}) \setminus B.$$

Figure 4.1 illustrates part of a wrapped spherical code constructed with this mapping. Note that WA-SC depends on those latitudes ξ_i that satisfy $\xi_i \leq 1/\sqrt{2}$. Geometrically, WA-SC is identical to \hat{C}^Λ for points whose last coordinate has magnitude at most $1/\sqrt{2}$, and is a reflection of \hat{C}^Λ by $\pi/2$ for the remaining points. In the following two sections, it will be shown that WA-SC has good asymptotic density properties and has an efficient decoding algorithm.

As this thesis is chiefly concerned with asymptotic performance, discussion on small codebook improvements possible for moderately large minimum distances will be limited. A number of simple improvements are possible. One such improvement involves the buffer regions B' and B , which are included in the code definitions solely to insure the minimum distance requirement is met. For a particular value of d , a careful choice of a latitudes $\{\xi_i\}$ may make much of the buffer region unnecessary.

The inverse mapping $(f')^{-1}$ may be computed using the following lemma.

Lemma 4.1 *For every $Y \in \mathbb{R}^{k-1} \setminus \{0\}$, $(f')^{-1}(Y)$ is given by*

$$\left\{ \frac{g_i Y}{\|Y\|} \pm (0, \dots, 0, \sqrt{1 - g_i^2}) : 0 \leq h_i < \sqrt{(\xi_{i+1} - \xi_i)^2 + \left(\sqrt{1 - \xi_i^2} - \sqrt{1 - \xi_{i+1}^2} \right)^2} \right\},$$

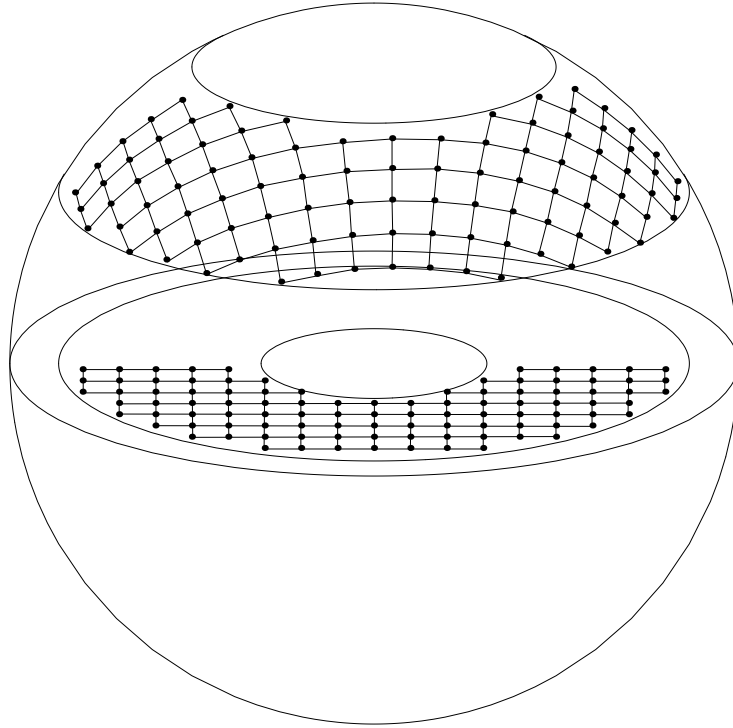


Figure 4.1 Part of a wrapped code constructed from \mathbb{Z}^2 . The slightly distorted grid above is the inverse image of the grid formed from \mathbb{Z}^2 below. Codepoints are located at the intersections of the distorted grid lines.

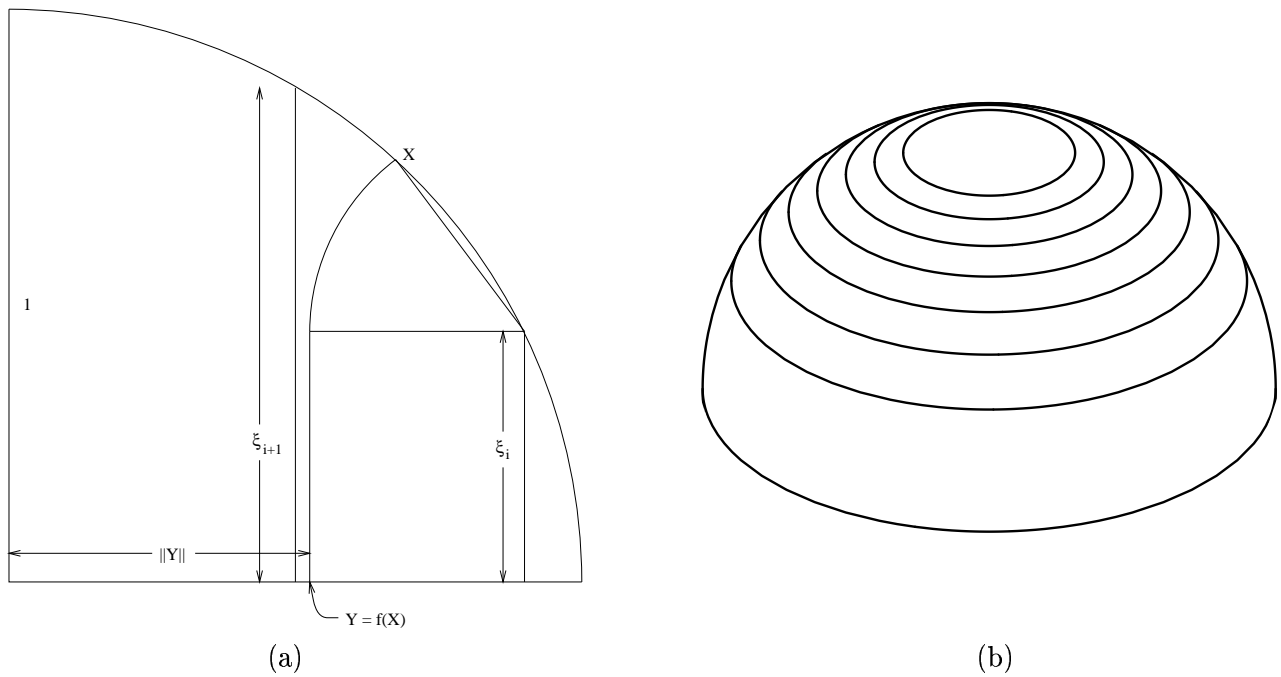


Figure 4.2 (a) Geometrical interpretation of $f(X)$. (b) Annuli.

where $h_i = \sqrt{1 - \xi_i^2} - \|Y\|$ and $g_i = \left(1 - \frac{h_i^2}{2}\right) \sqrt{1 - \xi_i^2} - \frac{h_i \xi_i}{2} \sqrt{4 - h_i^2}$.

Proof: See Section C.3

Lemma 4.1 also allows f^{-1} to be calculated, via

$$f^{-1}(Y) = \left\{ (x_1, \dots, x_k) \in (f')^{-1}(Y) : x_k \leq 1/\sqrt{2} \right\} \\ \cup \left\{ (x_1, \dots, x_{k-2}, x_k, x_{k-1}) \in (f')^{-1}(Y) : x_k > 1/\sqrt{2} \right\}.$$

Note that $\|f'(X)\| \leq \sqrt{1 - \underline{\xi}(x_k)^2}$ for any point $X = (x_1, \dots, x_k) \in \Omega_k$, with equality if and only if $x_k = \underline{\xi}(x_k)$. This may be verified directly from (4.1). In fact, $\|f'(X)\| \leq \|(x_1, \dots, x_{k-1})\|$. Since the norm $\|f'(X)\|$ depends only on x_k and the orientation $f'(X)/\|f'(X)\| = (x_1, \dots, x_{k-1})$, f' maps points in Ω_k with a constant k th coordinate (i.e., constant latitude) to points on a $(k-1)$ -dimensional sphere in \mathbb{R}^{k-1} . The image under f' of an annulus in Ω_k is a region bounded by two concentric $(k-1)$ -dimensional spheres in \mathbb{R}^{k-1} .

Lemma 4.2 *If $X = (x_1, \dots, x_k) \in \Omega_k$ and $Y = (y_1, \dots, y_k) \in \Omega_k$ belong to the same annulus of \hat{C}^Λ , then*

$$\|f'(X) - f'(Y)\|^2 \leq \|X - Y\|^2.$$

If, additionally, $\xi_i = \sin(i\sqrt{d})$, $x_k, y_k \leq 1/\sqrt{2}$, and $\|f'(X) - f'(Y)\| \leq d$, then

$$\|X - Y\|^2 - 3d^{5/2} + O(d^3) \leq \|f'(X) - f'(Y)\|^2.$$

Proof: Let $X' = (x_1, \dots, x_{k-1})$ and $Y' = (y_1, \dots, y_{k-1})$, and note that $\underline{\xi}(x_k) = \underline{\xi}(y_k)$ and $\bar{\xi}(x_k) = \bar{\xi}(y_k)$. Then

$$\begin{aligned} \|f'(X) - f'(Y)\|^2 &= \sum_{i=1}^{k-1} \left(\frac{\alpha(x_k)}{\|X'\|} x_i - \frac{\alpha(y_k)}{\|Y'\|} y_i \right)^2 \\ &= \alpha(x_k)^2 + \alpha(y_k)^2 - \frac{\alpha(x_k)\alpha(y_k)}{\|X'\| \cdot \|Y'\|} 2X' \cdot Y' \\ &= (\alpha(x_k) - \alpha(y_k))^2 + \frac{\alpha(x_k)\alpha(y_k)}{\|X'\| \cdot \|Y'\|} \left(\|X' - Y'\|^2 - (\|X'\| - \|Y'\|)^2 \right) \end{aligned} \quad (4.2)$$

$$\leq (x_k - y_k)^2 + (\|X'\| - \|Y'\|)^2 \quad (4.3)$$

$$\begin{aligned} &+ \frac{\alpha(x_k)\alpha(y_k)}{\|X'\| \cdot \|Y'\|} \left(\|X' - Y'\|^2 - (\|X'\| - \|Y'\|)^2 \right) \\ &= (x_k - y_k)^2 + \|X' - Y'\|^2 \\ &+ \left(\frac{\alpha(x_k)\alpha(y_k)}{\|X'\| \cdot \|Y'\|} - 1 \right) \left(\|X' - Y'\|^2 - (\|X'\| - \|Y'\|)^2 \right) \\ &\leq \|X - Y\|^2, \end{aligned} \quad (4.4)$$

where (4.3) follows because

$$\begin{aligned}
(\alpha(x_k) - \alpha(y_k))^2 &= \left\{ \left[\sqrt{1 - \underline{\xi}(x_k)^2} - \left\| \left(\sqrt{1 - x_k^2}, x_k \right) - \left(\sqrt{1 - \underline{\xi}(x_k)^2}, \underline{\xi}(x_k) \right) \right\| \right] \right. \\
&\quad \left. - \left[\sqrt{1 - \underline{\xi}(y_k)^2} - \left\| \left(\sqrt{1 - y_k^2}, y_k \right) - \left(\sqrt{1 - \underline{\xi}(y_k)^2}, \underline{\xi}(y_k) \right) \right\| \right] \right\}^2 \\
&= \left\{ \left\| \left(\sqrt{1 - y_k^2}, y_k \right) - \left(\sqrt{1 - \underline{\xi}(y_k)^2}, \underline{\xi}(y_k) \right) \right\| - \right. \\
&\quad \left. \left\| \left(\sqrt{1 - x_k^2}, x_k \right) - \left(\sqrt{1 - \underline{\xi}(x_k)^2}, \underline{\xi}(x_k) \right) \right\| \right\}^2 \\
&\leq \left\| \left(\sqrt{1 - x_k^2}, x_k \right) - \left(\sqrt{1 - y_k^2}, y_k \right) \right\|^2, \text{ by the triangle inequality} \\
&= (x_k - y_k)^2 + (\|X'\| - \|Y'\|)^2.
\end{aligned}$$

Also, (4.4) follows since

$$\alpha(x_k) \leq \left(\sqrt{1 - \underline{\xi}(x_k)^2} - \sqrt{0 + \left(\sqrt{1 - \underline{\xi}(x)^2} - \sqrt{1 - x_k^2} \right)^2} \right)_+ = \|X'\|,$$

(and similarly $\alpha(y_k) \leq \|Y'\|$) and

$$\|X' - Y'\|^2 - (\|X'\| - \|Y'\|)^2 \geq 0, \text{ (by Cauchy-Schwarz)}.$$

Note that equality holds in both (4.3) and (4.4) if and only if either $X = Y$ or $x_k = y_k = \underline{\xi}(x_k)$.

This proves the first part of the lemma.

Now suppose that $\xi_i = \sin(i\sqrt{d})$, $x_k, y_k \leq 1/\sqrt{2}$, and $\|f'(X) - f'(Y)\| \leq d$. A lower bound on $(\alpha(x_k) - \alpha(y_k))^2$ will be found. Without loss of generality, suppose $y_k \geq x_k \geq 0$ and let

$$\begin{aligned}
\tilde{X} &= \left(\sqrt{1 - x_k^2}, x_k \right) \\
\tilde{Y} &= \left(\sqrt{1 - y_k^2}, y_k \right) \\
\tilde{E} &= \left(\sqrt{1 - \underline{\xi}(x_k)^2}, \underline{\xi}(x_k) \right).
\end{aligned}$$

Let $c = \|\tilde{X} - \tilde{Y}\|$, $e = \|\tilde{X} - \tilde{E}\|$, $g = \|\tilde{Y} - \tilde{E}\|$, $\beta = \angle \tilde{Y} O \tilde{X}$, $\gamma = \angle \tilde{X} O \tilde{E}$, and $\phi = \beta + \gamma$, as illustrated in Figure 4.3. It follows that

$$\beta = 2 \sin^{-1} \frac{c}{2} \tag{4.5}$$

$$\gamma = \phi - \beta \tag{4.6}$$

$$e = 2 \sin \frac{\gamma}{2} \tag{4.7}$$

$$g = 2 \sin \frac{\phi}{2}. \tag{4.8}$$

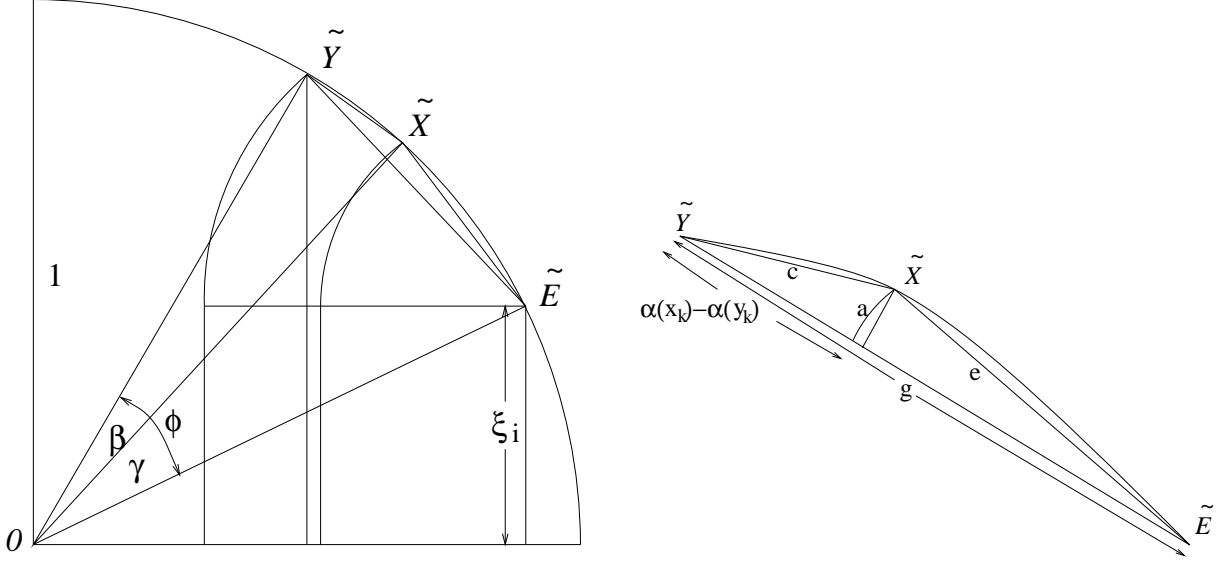


Figure 4.3 Notation used in proof of Lemma 5. The triangle $\tilde{X}\tilde{Y}\tilde{E}$ at left is shown enlarged at right.

Combining (4.5)-(4.8) gives

$$\begin{aligned}
|\alpha(x_k) - \alpha(y_k)| &= g - e \\
&= 2 \sin \frac{\phi}{2} - 2 \sin \left(\frac{\phi - 2 \sin^{-1}(c/2)}{2} \right) \\
&= \phi - \frac{\phi^3}{24} + O(\phi^5) - \phi + 2 \sin^{-1}(c/2) - \frac{(\phi - 2 \sin^{-1}(c/2))^3}{24} + O(\phi^5) \quad (4.9) \\
&= c - \frac{\phi^3}{12} - \frac{c\phi^2}{8} - \frac{c^2\phi}{8} + O(\phi^5) + O(c^3) \\
&\geq c - \frac{d^{3/2}}{12} - O(d^2), \quad (4.10)
\end{aligned}$$

where (4.9) follows from a Taylor expansion, and (4.10) follows since $\phi \leq \sqrt{d}$ and $c = O(d)$.

Thus,

$$(\alpha(x_k) - \alpha(y_k))^2 \geq c^2 - \frac{d^{5/2}}{6} + O(d^3) = (x_k - y_k)^2 + \|X' - Y'\|^2 - \frac{d^{5/2}}{6} + O(d^3).$$

Since $\|X'\| \geq 1/\sqrt{2}$, it also follows that

$$1 \geq \frac{\alpha(x_k)}{\|X'\|} \geq \frac{\|X'\| - \sqrt{d}}{\|X'\|} \geq 1 - \sqrt{2d}, \quad (4.11)$$

and similarly,

$$1 \geq \frac{\alpha(y_k)}{\|Y'\|} \geq 1 - \sqrt{2d}. \quad (4.12)$$

Hence, (4.2) may be rewritten as

$$\begin{aligned}
\|f'(X) - f'(Y)\|^2 &= (\alpha(x_k) - \alpha(y_k))^2 + \frac{\alpha(x_k)\alpha(y_k)}{\|X'\|\|Y'\|} \left(\|X' - Y'\|^2 - (\|X'\| - \|Y'\|)^2 \right) \\
&\geq (x_k - y_k)^2 + \|X' - Y'\|^2 - \frac{d^{5/2}}{6} + O(d^3) \\
&\quad + \frac{\alpha(x_k)\alpha(y_k)}{\|X'\|\|Y'\|} \left(\|X' - Y'\|^2 - (\|X'\| - \|Y'\|)^2 \right) \\
&= \|X - Y\|^2 - \frac{d^{5/2}}{6} + O(d^3) \\
&\quad + \left(\frac{\alpha(x_k)\alpha(y_k)}{\|X'\|\|Y'\|} - 1 \right) \left(\|X' - Y'\|^2 - (\|X'\| - \|Y'\|)^2 \right) \\
&\geq \|X - Y\|^2 - \frac{d^{5/2}}{6} + O(d^3) + \left((1 - \sqrt{2d})^2 - 1 \right) \|X - Y\|^2 \\
&= \|X - Y\|^2 (1 - \sqrt{2d})^2 - \frac{d^{5/2}}{6} + O(d^3) \\
&= \|X - Y\|^2 (1 - 2\sqrt{2d} + 2d) - \frac{d^{5/2}}{6} + O(d^3) \\
&\geq \|X - Y\|^2 - (2\sqrt{2} + 1)d^{5/2} + O(d^3) \\
&> \|X - Y\|^2 - 3d^{5/2} + O(d^3),
\end{aligned} \tag{4.13}$$

$$\begin{aligned}
&\tag{4.14} \\
&= \|X - Y\|^2 (1 - \sqrt{2d})^2 - \frac{d^{5/2}}{6} + O(d^3) \\
&= \|X - Y\|^2 (1 - 2\sqrt{2d} + 2d) - \frac{d^{5/2}}{6} + O(d^3) \\
&\geq \|X - Y\|^2 - (2\sqrt{2} + 1)d^{5/2} + O(d^3) \\
&> \|X - Y\|^2 - 3d^{5/2} + O(d^3),
\end{aligned}$$

where (4.13) follows from (4.10) and (4.14) follows from (4.11) and (4.12). ■

Note that if $\xi_i = 1/\sqrt{2}$ for some i , then Lemma 4.2 also holds when f' is replaced by f .

Corollary 4.1 *If Λ is a sphere packing with minimum distance d , then the minimum distance of the wrapped spherical code $W\Lambda$ -SC is also d .*

Proof: If distinct $X, Y \in W\Lambda$ -SC belong to the same annulus, then $\|X - Y\| \geq \|f(X) - f(Y)\| \geq d$, since the minimum distance of Λ is d . If X and Y belong to different annuli, then the definition of B guarantees their separation is d . ■

4.3 Asymptotic Density of the Wrapped Spherical Code

Let $\{\xi_i^{(d)}\}$ be the partition of $[0, 1/\sqrt{2}]$ used in the definition of a wrapped spherical code $W\Lambda$ -SC that has minimum distance d . Let $\phi_i = \sin^{-1} \xi_{i+1}^{(d)} - \sin^{-1} \xi_i^{(d)}$ denote the *angular separation* of the i th annulus. Next it is shown that if the maximum angular separation between annuli, $\bar{\phi} \equiv \max_i \phi_i$ approaches 0 as $d \rightarrow 0$ and the minimum angular separation $\underline{\phi} \equiv \min_i \phi_i$

does not approach zero too quickly, then the density of the wrapped code approaches the density of Λ .

Theorem 4.1 *Let Λ be a $(k-1)$ -dimensional sphere packing with minimum distance d . Let $W\Lambda$ -SC be a wrapped spherical code with respect to Λ and with latitudes ξ_0, \dots, ξ_N . If the maximum and minimum annulus angular separations satisfy $\lim_{d \rightarrow 0} [\bar{\phi} + (d/\underline{\phi})] = 0$, then the asymptotic density of $W\Lambda$ -SC approaches the density of Λ , i.e., $\lim_{d \rightarrow 0} \Delta_{W\Lambda\text{-SC}} = \Delta_\Lambda$.*

Proof: It will be shown that the density of codepoints within each annulus is close to Λ . It suffices to concentrate on the annuli with latitudes at most $1/\sqrt{2}$, i.e., where f is equivalent to f' . Let $T_i(d)$ be the i th annulus and let $R_i(d) = f(T_i(d))$. Let $S_{T_i(d)}$ and $S_{R_i(d)}$ denote the $(k-1)$ -dimensional contents of $T_i(d)$ and $R_i(d)$, respectively. For ease of notation, let $\underline{\xi} = \xi_i^{(d)}$ and let $\bar{\xi} = \xi_{i+1}^{(d)}$. Abbreviate $T_i(d)$ and $R_i(d)$ as T and R , respectively. As in Equation (2.3), the angular separation ϕ_i may also be expressed as a Euclidean distance (thickness), by

$$2 \sin(\phi_i/2) = \sqrt{(\bar{\xi} - \underline{\xi})^2 + \left(\sqrt{1 - \underline{\xi}^2} - \sqrt{1 - \bar{\xi}^2} \right)^2}$$

Throughout this proof, constants encompassed by $O(\cdot)$ notation do not depend on i . First S_T and S_R are computed.

$$\begin{aligned} S_T &= S_{k-1} \int_{\sin^{-1} \underline{\xi}}^{\sin^{-1} \bar{\xi}} \cos^{k-2} x \, dx \\ &= S_{k-1} \int_{\sin^{-1} \underline{\xi}}^{\sin^{-1} \bar{\xi}} \left[(1 - \underline{\xi}^2)^{\frac{k-2}{2}} - O(x - \sin^{-1} \underline{\xi}) \right] dx \\ &= S_{k-1} (1 - \underline{\xi}^2)^{\frac{k-2}{2}} \phi_i - O(\phi_i^2), \end{aligned} \tag{4.15}$$

where (4.15) follows from the Taylor expansion of $\cos^{k-2} x$ about $\sin^{-1} \underline{\xi}$. The $(k-1)$ -dimensional content of R is the difference between the $(k-1)$ -dimensional contents of two concentric $(k-1)$ -dimensional spheres, namely, a sphere of radius $\sqrt{1 - \underline{\xi}^2}$ and a sphere of radius

$$\sqrt{1 - \underline{\xi}^2} - \sqrt{(\bar{\xi} - \underline{\xi})^2 + \left(\sqrt{1 - \underline{\xi}^2} - \sqrt{1 - \bar{\xi}^2} \right)^2}.$$

Thus,

$$S_R = V_{k-1} \left[(1 - \underline{\xi}^2)^{\frac{k-1}{2}} - \left(\sqrt{1 - \underline{\xi}^2} - \sqrt{(\bar{\xi} - \underline{\xi})^2 + \left(\sqrt{1 - \underline{\xi}^2} - \sqrt{1 - \bar{\xi}^2} \right)^2} \right)^{k-1} \right] \quad (4.16)$$

$$= V_{k-1} \left[(1 - \underline{\xi}^2)^{\frac{k-1}{2}} - \sum_{i=0}^{k-1} (-1)^i \binom{k-1}{i} (1 - \underline{\xi}^2)^{\frac{k-1-i}{2}} \left((\bar{\xi} - \underline{\xi})^2 + \left(\sqrt{1 - \underline{\xi}^2} - \sqrt{1 - \bar{\xi}^2} \right)^2 \right)^{\frac{i}{2}} \right] \quad (4.17)$$

$$= V_{k-1} \left[(k-1) (1 - \underline{\xi}^2)^{\frac{k-2}{2}} \sqrt{(\bar{\xi} - \underline{\xi})^2 + \left(\sqrt{1 - \underline{\xi}^2} - \sqrt{1 - \bar{\xi}^2} \right)^2} - O \left((\bar{\xi} - \underline{\xi})^2 + \left(\sqrt{1 - \underline{\xi}^2} - \sqrt{1 - \bar{\xi}^2} \right)^2 \right) \right] \quad (4.18)$$

$$= V_{k-1} \left[(k-1) (1 - \underline{\xi}^2)^{\frac{k-2}{2}} \phi_i - O(\phi_i^2) \right]$$

$$= S_{k-1} (1 - \underline{\xi}^2)^{\frac{k-2}{2}} \phi_i - O(\phi_i^2),$$

where (4.16) follows because the $(k-1)$ -dimensional content of a $(k-1)$ -dimensional sphere of radius r is $V_{k-1} r^{k-1}$ and (4.17) follows from the binomial theorem. The zeroth term in the summation in (4.17) cancels the term outside the summation, and the remaining terms are higher powers of the Euclidean thickness of the annulus, which are expressed in $O(\cdot)$ notation. The Euclidean thickness is expressed as an angular separation by

$$\sqrt{(\bar{\xi} - \underline{\xi})^2 + \left(\sqrt{1 - \underline{\xi}^2} - \sqrt{1 - \bar{\xi}^2} \right)^2} = 2 \sin(\phi_i/2) = \phi_i - \phi_i^3/24 + O(\phi_i^5)$$

which gives (4.18), and (4.19) follows from $S_{k-1} = (k-1)V_{k-1}$. Thus,

$$S_T - O(\phi_i^2) \leq S_R \leq S_T + O(\phi_i^2). \quad (4.19)$$

Next, $|\Lambda \cap R|$ and $|\text{WA-SC} \cap T|$ are computed.

$$|\Lambda \cap R| = \frac{\Delta_\Lambda(S(R) - O(d))}{V_{k-1}(d/2)^{k-1}},$$

where the $O(d)$ term appears because the density of lattice points in R may be lower than Δ_Λ in a region within distance d of the boundary of R , and the $(k-1)$ -dimensional content of this

boundary region is $O(d)$. Also,

$$\begin{aligned}
|\text{W}\Lambda\text{-SC} \cap T| &= |\Lambda \cap R \setminus \{0\}| - |\Lambda \cap R \cap f(B') \setminus \{0\}| \\
&= \frac{\Delta_\Lambda(S(R) - O(d))}{V_{k-1}(d/2)^{k-1}} - \frac{\Delta_\Lambda O(d)}{V_{k-1}(d/2)^{k-1}} \\
&= \frac{\Delta_\Lambda(S(R) - O(d))}{V_{k-1}(d/2)^{k-1}}.
\end{aligned}$$

Thus,

$$\begin{aligned}
\Delta_T &= \frac{|\text{W}\Lambda\text{-SC} \cap T| S(c(k, \theta/2))}{S_T} \\
&= \frac{\left[\frac{\Delta_\Lambda(S(R) - O(d))}{V_{k-1}(d/2)^{k-1}} \right] V_{k-1}(\frac{d}{2})^{k-1} (1 + O(d^2))}{S_T} \\
&= \frac{\Delta_\Lambda(S_R - O(d))(1 + O(d^2))}{S_T} \\
&\geq \frac{\Delta_\Lambda(S_T - O(\phi_i^2 + d))(1 + O(d^2))}{S_T} \tag{4.20} \\
&= \Delta_\Lambda \left(1 - O\left(\frac{\phi_i^2 + d}{S_T}\right) \right) (1 + O(d^2)) \\
&= \Delta_\Lambda \left(1 - O\left(\phi_i + \frac{d}{\phi_i}\right) \right) (1 + O(d^2)) \\
&= \Delta_\Lambda \left(1 - O\left(\bar{\phi} + \frac{d}{\underline{\phi}}\right) \right) (1 + O(d^2)) \\
&= \Delta_\Lambda - O\left(\bar{\phi} + \frac{d}{\underline{\phi}}\right), \tag{4.21}
\end{aligned}$$

where (4.20) follows from the left-hand inequality of (4.19). Using the right-hand inequality of (4.19), the inequality sign of (4.20) reverses if ϕ_i^2 is replaced by $-\phi_i^2$, which gives

$$\Delta_T \leq \Delta_\Lambda + O(\bar{\phi}). \tag{4.22}$$

Since (4.21) and (4.22) do not depend on i ,

$$\Delta_\Lambda - O\left(\bar{\phi} + \frac{d}{\underline{\phi}}\right) \leq \Delta_{\text{W}\Lambda\text{-SC}} \leq \Delta_\Lambda + O(\bar{\phi}). \tag{4.23}$$

Since $\lim_{d \rightarrow 0} [\bar{\phi} + (d/\underline{\phi})] = 0$ and each term inside the limit is nonnegative, $\lim_{d \rightarrow 0} \bar{\phi} = 0$. ■

Equation (4.21) also suggests a choice of $\{\xi_i\}$ that will provide a fast rate of convergence, and implies the following corollary.

Corollary 4.2 *Let Λ be a $(k-1)$ -dimensional sphere packing with minimum distance d , and let $\text{W}\Lambda\text{-SC}$ be a wrapped spherical code with respect to Λ and with latitudes given by $\xi_i = \sin(i\sqrt{d})$ for $0 \leq i \leq \pi/(2\sqrt{d})$. Then the spherical code density satisfies $|\Delta_{\text{W}\Lambda\text{-SC}} - \Delta_\Lambda| \leq O(\sqrt{d})$.*

Proof: The result follows immediately from (4.23), since $\bar{\phi} = \underline{\phi} = \sqrt{d}$. ■

The performances of the wrapped spherical codes in dimensions three, four, and eight are shown in Figures 3.5, 3.6, and 3.7, respectively. In three dimensions, the wrapped spherical code has a higher density than shells of \mathbb{Z}^3 , A_3 , and A_3^* for minimum distances less than 0.3. As the minimum distance shrinks, the convergence of the density to the upper bound is evident.

The wrapped spherical codes are outperformed by the laminated spherical codes in dimensions three and four. For higher dimensions, however, the wrapped spherical codes perform better. For example, in dimension 8 shown in Figure 3.7, the wrapped code is dramatically better than the laminated spherical code. The wrapped spherical code outperforms most other codes for minimum distances less than about 0.4.

4.4 Decoding Wrapped Spherical Codes

An important question in channel decoding and quantization encoding is how to efficiently find the nearest codepoint to an arbitrary point in \mathbb{R}^k [30, 31, 59, 67, 89]. Often, an advantage of a structured code is that codepoints themselves need not be stored explicitly.

If the k -dimensional signal $X \in \text{WA-SC}$ is sent across an additive white Gaussian noise (AWGN) channel, then the received signal is $R = X + N$, where N is a zero-mean Gaussian random vector with variance σ^2 . The maximum likelihood decoder is a minimum distance decoder, i.e., given R , the decoder output is $\tilde{X} = \arg \min_{X \in \text{WA-SC}} \|X - R\|$, the closest codepoint to R . For any $R \in \mathbb{R}^k$ and any spherical code $\mathcal{C}(k, d)$, the nearest codepoint of $\mathcal{C}(k, d)$ to R is the same as the nearest codepoint of $\mathcal{C}(k, d)$ to $R/\|R\|$. Hence, in the following, it is assumed that $R \in \Omega_k$.

The performance of an efficient suboptimal decoding method can now be evaluated. Given a received vector $R \in \Omega_k$, let the decoder output be

$$\hat{X} = \arg \min_{X \in \text{WA-SC}} \|f(X) - f(R)\|.$$

Note that $X \in \text{WA-SC}$ implies $f(X) \in \Lambda$. Let Y be a nearest neighbor of $f(R)$ in Λ . There is at most one candidate in the set $f^{-1}(Y)$ which could be a nearest neighbor to R , namely, the element E which is in the same annulus as R . However, because of the buffer region B , E might not be in WA-SC . This happens with probability $O(\sqrt{d})$ or less, for B covers $O(\sqrt{d})$

of the sphere. (Such an E exists provided $\|Y\| \leq 1$ and R is not within d of the border of an annulus, which holds with probability $1 - O(\sqrt{d})$.) Thus, with probability $1 - O(\sqrt{d})$,

$$\hat{X} \in f^{-1} \left(\arg \min_{Y \in \Lambda} \|Y - f(R)\| \right),$$

which involves only f , f^{-1} , and the decoding algorithm for Λ .

It is known that when points from the packing Λ with minimum distance d are used on an AWGN channel, the probability of symbol error is $\tau Q(\frac{d}{2\sigma})$ (see, e.g., [14]), where τ is the average number of codepoints at distance d from a codepoint and where Q is the complementary error function defined by $Q(x) = \frac{1}{\sqrt{2\pi}} \int_x^\infty e^{-x^2/2} dx$. The following theorem shows that the performance of efficiently decoding $W\Lambda$ -SC is asymptotically close to the performance of Λ .

Theorem 4.2 *Let Λ be a $(k-1)$ -dimensional packing with minimum distance d , and let $W\Lambda$ -SC be a wrapped spherical code with respect to Λ and with latitudes $\xi_i = \sin(i\sqrt{d})$. Let P_e be the probability of symbol error when $W\Lambda$ -SC is used on an AWGN channel with equiprobable inputs and the decoder output is $\hat{X} = \arg \min_{X \in W\Lambda\text{-SC}} \|f(X) - f(R)\|$. Then $P_e \leq \tau Q\left(\frac{d}{2\sigma}(1 - O(d^{1/4}))\right)$.*

Proof: Given a received vector $R \in \Omega^k$, a decoding error occurs if \hat{X} is not a nearest neighbor codepoint of R , i.e., if there exist $X, Y \in W\Lambda$ -SC such that $\|X - R\|^2 < \|Y - R\|^2$ and $\|f(X) - f(R)\|^2 > \|f(Y) - f(R)\|^2$. Together with Lemma 4.2, these inequalities would imply

$$\begin{aligned} \|Y - R\|^2 &> \|X - R\|^2 \\ &\geq \|f(X) - f(R)\|^2 \\ &> \|f(Y) - f(R)\|^2 \\ &> \|Y - R\|^2 - 3d^{5/2} + O(d^3). \end{aligned}$$

Hence,

$$0 \leq \|f(X) - f(R)\|^2 - \|f(Y) - f(R)\|^2 \leq 3d^{5/2} + O(d^3).$$

That is, in \mathbb{R}^{k-1} , $f(R)$ is within $\sqrt{3d^{5/2} + O(d^3)} = \sqrt{3}d^{5/4} + O(d^{7/4})$ of the bisecting hyperplane between $f(X)$ and $f(Y)$. Since $f(X)$ and $f(Y)$ differ by at least d , by the union bound the probability of symbol error is

$$P_e \leq \tau Q \left(\frac{d - 6d^{5/4} + O(d^{7/4})}{2\sigma} \right) = \tau Q \left(\frac{d}{2\sigma} (1 - O(d^{1/4})) \right).$$

■

4.5 Conclusions

A new technique was presented that constructs wrapped spherical codes in any dimension and with any minimum distance. The construction is performed by defining a map from \mathbb{R}^{k-1} to Ω_k . Although any set of points in \mathbb{R}^{k-1} may be wrapped to Ω_k using our technique, if the densest packing in \mathbb{R}^{k-1} is used the wrapped spherical codes are asymptotically optimal, in the sense that the ratio of the code size of the constructed code to the upper bound approaches one as the minimum distance decreases. This demonstrates the tightness of the upper bound in [23] for three dimensions, asymptotically, and that previous lower bounds are not asymptotically optimal.

CHAPTER 5

LAMINATED SPHERICAL CODES

5.1 Introduction

Chapter 4 described a technique to map any packing Λ onto the unit k -dimensional sphere Ω_k . In this chapter, a new technique is introduced to construct spherical codes called laminated spherical codes. Whereas wrapped spherical codes were described by an explicit function that maps \mathbb{R}^{k-1} onto the unit sphere Ω_k for any $k \in \mathbb{Z}_+$, laminated spherical codes will be defined in a recursive manner using terminology and techniques from laminated lattice constructions. The laminated spherical codes improve upon previously known codes, and for low dimensions and many code sizes have higher minimum distances than the wrapped spherical codes described in Chapter 4. Most of the known best performing spherical codes in three dimensions with less than about 30,000 codepoints and in four and five dimensions with less than about 150 codepoints are due to Hardin and Sloane [82]. For codes larger than the Hardin-Sloane codes or for dimensions greater than three, the laminated spherical codes introduced in this chapter often give the best known performance.

As explained in Section 3.3.1, any spherical code can be described by the projection of its codepoints from Ω_k to \mathbb{R}^{k-1} , via the mapping $(x_1, \dots, x_{k-1}, x_k) \rightarrow (x_1, \dots, x_{k-1})$. Conversely, a k -dimensional spherical code may be obtained by placing codepoints on concentric $(k-1)$ -dimensional spheres and projecting each codepoint onto Ω_k . If the projected codepoints are constrained to lie on a small number of radii $\left(\sum_{i=1}^{k-1} x_i^2\right)^{1/2}$, then a structured packing can be obtained. This idea is exploited by packing the concentric spheres closely. The codepoints of one sphere are placed at the radial extension of the holes of codepoints of the next smaller radius sphere, and use a method similar to that for constructing laminated lattices (e.g., [14])

to construct new spherical codes, which is denoted by LSC. This is illustrated for $k = 2$ and $k = 3$ in Figure 5.1. This method is similar to those of [97] and [18] in that a projection from $k - 1$ dimensions to k dimensions is used; the difference lies in the placement of points prior to the projection. The new technique creates codes of any size and thus provides a lower bound on achievable minimum distance as a function of code size. The spherical code density approaches the density of the laminated lattice Λ_{k-1} , as $d \rightarrow 0$.

5.2 Construction of Laminated Spherical Codes

Let $k \leq 49$ and $d \in (0, 1]$. For $k = 2$, a largest spherical code with minimum distance d is obvious (although not unique); it is denoted by $\text{LSC}(2, d)$. For $k \geq 3$, the k -dimensional *laminated spherical code* $\text{LSC}(k, d)$ with minimum distance d is recursively defined as follows.

$$\text{LSC}(k, d) \equiv \left\{ \left(x_1, \dots, x_{k-1}, \pm \sqrt{1 - \sum_{i=0}^{k-1} x_i^2} \right) : (x_1, \dots, x_{k-1}) \in \bigcup_{i=0}^N r_i \mathcal{C}_i(k-1, d/r_{s(i)}) \right\}, \quad (5.1)$$

where

$$\begin{aligned} r(i, b) &\equiv \frac{r_{i-1} \left(1 - \frac{d^2}{2}\right) \sqrt{1 - b \left(\frac{c_{k-2}d}{r_{s(i-1)}}\right)^2} + d \sqrt{(1 - r_{i-1}^2) \left(1 - \frac{d^2}{4} - b \left(\frac{r_{i-1}c_{k-2}}{r_{s(i-1)}}\right)^2\right)}{1 - b \left(\frac{r_{i-1}c_{k-2}d}{r_{s(i-1)}}\right)^2} \\ r_i &\equiv \begin{cases} id & \text{if } i = 0 \text{ or } i = 1 \\ r(i, 0) & \text{if } i > 1 \text{ and } \lfloor r_{i-1}d^{-2/k} \rfloor \neq \\ & \lfloor \max(r(i, 1), r(i - l_{k-1}, 0))d^{-2/k} \rfloor \\ \max(r(i, 1), r(i - l_{k-1}, 0)) & \text{otherwise} \end{cases} \\ g(i) &\equiv \min\{j : r_j > id^{2/k}\} \\ s(i) &\equiv g(\max\{j : r_{g(j)} \leq r_i\}) \\ N &\equiv \max\{i : r_i \leq \sqrt{1 - d^2/4}\} \\ w_l(X) &\equiv n(w_{l-1}(f^{-1}(X))) \\ L(X) &\equiv \{w_{l-1}^{-1}(D(w_{l-1}(X))_i) : 1 \leq i \leq n_{k-2}\} \\ f(X) &\equiv \frac{H(L(X))}{\|H(L(X))\|} \\ \mathcal{C}_{g(j)+l}(k-1, d) &\equiv \begin{cases} \text{LSC}(k-1, d) & \text{if } l = 0 \\ f(\mathcal{C}_{g(j)+l-1}(k-1, d)) & \text{if } 1 \leq l \leq g(j+1) - g(j) - 1 \end{cases} \end{aligned} \quad (5.2)$$

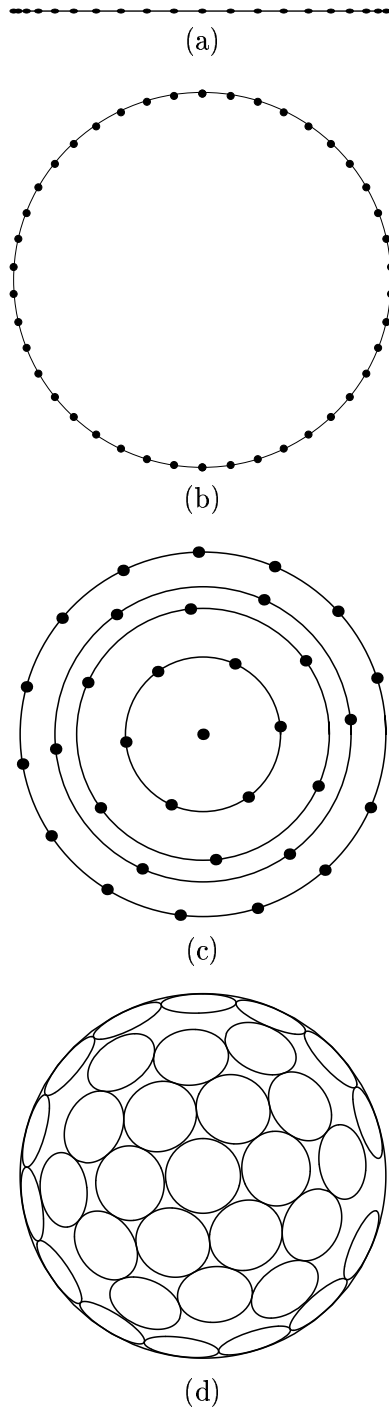


Figure 5.1 (a) Eleven scaled one-dimensional spherical codes. (b) Two-dimensional code derived from the scaled one-dimensional codes by projecting codepoints up and down. (c) Five scaled two-dimensional codes. (d) Three-dimensional code derived from the two-dimensional codes by projecting codepoints out of the page, where codepoints are the centers of the caps.

Remarks:

- The sequence $\{r_i\}$ satisfies $0 = r_0 < \dots < r_N \leq \sqrt{1 - d^2/4}$.
- $\{r_i\}$ and $s(i)$ are defined in terms of each other, but each is well-defined. In particular, $s(i - 1)$ and r_i each depend only on r_0, \dots, r_{i-1} .
- $w_l(X): \mathcal{C}_{g(j)+l}(k - 1, d) \rightarrow \Lambda_{k-1}^l$ associates each point from a spherical code with a point on a laminated lattice
- $L(X)$ associates $X \in \mathcal{C}_{g(j)+l}(k - 1, d)$ with a subset of $\mathcal{C}_{g(j)+l}(k - 1, d)$ that is used to determine a point on the shell with radius $r_{g(j)+l+1}$.
- l_k is defined in (2.1) and c_k , $H(\cdot)$, and $n(\cdot)$ are defined in Section 2.1.9.

The following definitions are also used in the code construction:

$$\begin{aligned}
\textit{ith shell:} & \quad r_i \mathcal{C}_i(k - 1, d/r_{s(i)}) \\
\textit{ith gap:} & \quad T_i \equiv \left\{ (x_1, \dots, x_k) \in \Omega_k : \sqrt{\sum_{i=1}^{k-1} x_i^2} \in (r_{i-1}, r_i] \right\} \\
\textit{ith annulus:} & \quad A_i \equiv \bigcup_{j=g(i)+1}^{g(i+1)-1} T_j \\
\textit{ith buffer zone:} & \quad B_i \equiv \left\{ (x_1, \dots, x_k) \in \Omega_k : \sqrt{\sum_{i=1}^{k-1} x_i^2} \in (r_{g(i)-1}, r_{g(i)}] \right\} \\
& \quad W_1 \equiv \left\{ (x_1, \dots, x_k) \in \Omega_k : \sqrt{\sum_{i=1}^{k-1} x_i^2} < d^{1/k} \right\} \\
& \quad W_2 \equiv \left\{ (x_1, \dots, x_k) \in \Omega_k : \sqrt{\sum_{i=1}^{k-1} x_i^2} > 1 - d^{1/k} \right\} \\
\textit{wasted region:} & \quad W \equiv W_1 \cup W_2 \\
& \quad T \equiv \bigcup_{i=0}^{\lceil d^{-2/k} \rceil - 1} A_i \\
& \quad B \equiv \bigcup_{i=1}^{\lceil d^{-2/k} \rceil - 1} B_i.
\end{aligned}$$

The i th shell *shell* is a $(k - 1)$ -dimensional spherical code scaled to a sphere of radius r_i . The points between the spheres of the $(i - 1)$ th and i th shells constitute the i th *gap*. The i th *annulus* is the set of points in \mathbb{R}^{k-1} whose distance to the origin is in the interval $(r_{g(i)}, r_{g(i+1)-1}]$. That is, an annulus is a collection of consecutive gaps. Note that $s(i)$ is the smallest integer for which the set of all points whose magnitude is in the interval $(r_{s(i)}, r_i]$ lies in a single annulus. The

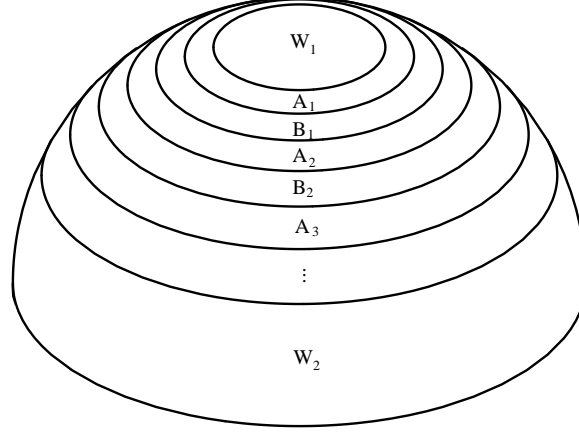


Figure 5.2 The sphere is partitioned into annuli, buffer zones, and wasted regions. In general, W_1 and W_2 may contain one or more annuli.

i th buffer zone is the set of points lying between the $(i - 1)$ th and i th annuli. Shells, gaps, annuli, and buffer zones that are projected onto the unit k -dimensional sphere Ω_k are again called shells, gaps, annuli, and buffer zones, respectively. The sets W_1 and W_2 are referred to as “wasted” regions, in which codepoints are not necessarily as tightly packed as the rest of the sphere. The radii $\{r_i\}$ and the sets W , T , and B are determined by the parameters k and d . For any k and d , it follows that $\Omega_k = W \cup T \cup B$, as seen in Figure 5.2.

Each point in $LSC(k, d)$ corresponds to a unique point on the lattice Λ_{k-1} , since each point in the shell $\mathcal{C}_{g(j)+l-1}(k - 1, d)$ corresponds to a unique point on the lattice $\Lambda_{k-2}^{(l-1)}$, via the function $w_{l-1}(\cdot)$. Recall that a point $X \in \Lambda_{k-2}^{(l-1)}$ gives rise to the point $n(X) \in \Lambda_{k-2}^{(l)}$ via the hole $H(D(X)_1, \dots, D(X)_{n_{k-1}})$. Likewise, a point $X \in \mathcal{C}_{g(j)+l-1}(k - 1, d)$ gives rise to a point in $\mathcal{C}_{g(j)+l}(k - 1, d)$ via the hole of the codepoints of $\mathcal{C}_{g(j)+l-1}(k - 1, d)$ which correspond to $D(X)_1, \dots, D(X)_{n_{k-1}}$, namely, $L(X)$. Thus, $\mathcal{C}_{g(j)+l}(k - 1, d)$ is equal to a set of the (properly normalized) holes arising from $\mathcal{C}_{g(j)+l-1}(k - 1, d)$, and $w_l(\cdot)$ is now also defined. For $k = 3$, the two-dimensional code layers can explicitly be written as

$$\mathcal{C}_{g(j)+i}(2, d) \equiv \begin{cases} \{(\cos(i\theta_{g(j)+i}), \sin(i\theta_{g(j)+i}))\} & \text{if } i \text{ even} \\ \{(\cos((i + \frac{1}{2})\theta_{g(j)+i}), \sin((i + \frac{1}{2})\theta_{g(j)+i}))\} & \text{if } i \text{ odd} \end{cases}$$

where $\theta_m \equiv 2 \sin^{-1} \left(\frac{d}{2r_{s(m)}} \right)$, $j \in \{0, \dots, \lfloor 2\pi/\theta_i \rfloor - 1\}$ and $i \in \{0, \dots, N\}$.

The laminated spherical code construction ensures that each $(k - 1)$ -dimensional code has minimum distance d . The sequence $\{r_i\}$ must be defined such that codepoints from different shells are at least distance d from each other. This constraint is analogous to the separation of

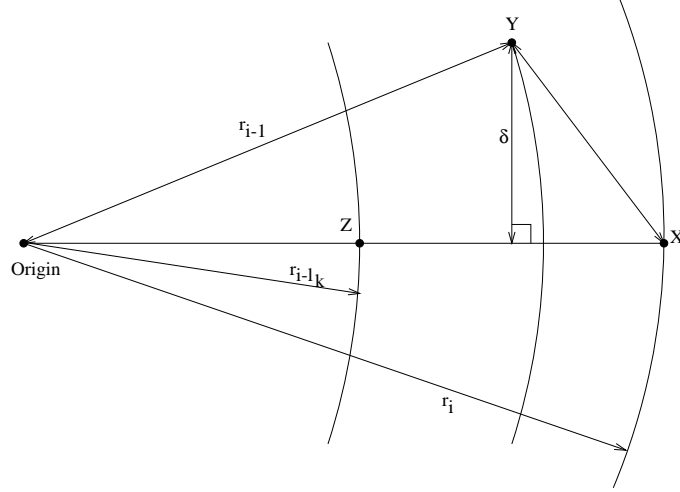


Figure 5.3 Relation between r_i and r_{i-1} .

layers of Λ_{k-2} in Λ_{k-1} , except that here there is the added complication that each layer (i.e., $(k-1)$ -dimensional spherical code) is projected onto Ω_k .

The radius r_i is recursively chosen as small as possible and yet large enough so that the points at radius r_i are at least distance d from the points at radius r_{i-1} , after the projection. Suppose r_0, \dots, r_{i-1} have been determined. Then r_i is defined as the smallest positive number such that for each $X \equiv (x_1, \dots, x_{k-1}) \in r_i \mathcal{C}_i(k-1, d/r_{s(i)})$ and $Y \equiv (y_1, \dots, y_{k-1}) \in r_{i-1} \mathcal{C}_{i-1}(k-1, d/r_{s(i)})$, the distance between the corresponding codepoints $X' = \left(x_1, \dots, x_{k-1}, \sqrt{1 - \sum_{i=1}^{k-1} x_i^2}\right)$ and $Y' = \left(y_1, \dots, y_{k-1}, \sqrt{1 - \sum_{i=1}^{k-1} y_i^2}\right)$ in $\text{LSC}(k, d)$ is at least d (see Figure 5.3). That is, r_i is chosen such that $\|X' - Y'\| \geq d$.

Let δ be the distance from Y to the hole associated with Y . Note that $\mathcal{C}_{i-1}(k-1, d/r_{s(i-1)})$ and $\mathcal{C}_{s(i)}(k-1, d/r_{s(i)})$ each have codepoints with angular separation θ_i . Thus, the distance from Y to its associated hole is $\frac{r_{i-1}}{r_{s(i-1)}}$ times greater than the distance from a point in $\mathcal{C}_{s(i)}$ to its associated hole. Hence,

$$\delta \geq \frac{r_{i-1} c_{k-2} d}{r_{s(i-1)}}, \quad (5.3)$$

where the inequality comes from the fact that $c_{k-2} d$ is less than or equal to the distance from a point of $\mathcal{C}_{s(i)}(k-1, d)$ to its associated hole. Therefore, r_i is chosen such that

$$\begin{aligned} d^2 &\leq \|X' - Y'\|^2 \\ &= \left(r_i - \sqrt{r_{i-1}^2 - \delta^2}\right)^2 + \delta^2 + \left(\sqrt{1 - r_{i-1}^2} - \sqrt{1 - r_i^2}\right)^2. \end{aligned}$$

Rearranging terms gives

$$\sqrt{(1 - r_{i-1}^2)(1 - r_i^2)} \leq 1 - d^2/2 - r_i \sqrt{r_{i-1}^2 - \delta^2}$$

which upon squaring both sides and solving the quadratic for r_i give

$$r_i \geq \frac{\left(1 - \frac{d^2}{2}\right) \sqrt{r_{i-1}^2 - \delta^2} + \sqrt{(1 - r_{i-1}^2)(d^2 - \frac{d^4}{4} - \delta^2)}}{1 - \delta^2}. \quad (5.4)$$

The negative solution for the quadratic equation is smaller than r_{i-1} and is omitted. Taking the derivative of the right-hand side of (5.4) with respect to δ reveals that it is a decreasing function of δ when δ is in the range for which (5.4) produces a real value. Thus, using (5.3) and setting

$$r_i = \frac{r_{i-1} \left(1 - \frac{d^2}{2}\right) \sqrt{1 - \left(\frac{c_{k-2}d}{r_{s(i-1)}}\right)^2} + d \sqrt{(1 - r_{i-1}^2) \left(1 - \frac{d^2}{4} - \left(\frac{r_{i-1}c_{k-2}}{r_{s(i-1)}}\right)^2\right)}}{1 - \left(\frac{r_{i-1}c_{k-2}d}{r_{s(i-1)}}\right)^2} \quad (5.5)$$

ensure that $\|X' - Y'\| \geq d$.

The recursion for r_i in (5.5) is used only when Y belongs to the same annulus as X . If r_{i-1} is the radius of the outermost shell in an annulus, then r_i is defined such that every point on $r_i\Omega_{k-1}$ is at least a distance d from every point on the circle of radius r_{i-1} . This is equivalent to taking $\delta = 0$ in the solution above (i.e., when \overrightarrow{YX} is directed radially outward), and gives

$$r_i = r_{i-1} \left(1 - \frac{d^2}{2}\right) + d \sqrt{(1 - r_{i-1}^2) \left(1 - \frac{d^2}{4}\right)}. \quad (5.6)$$

While (5.5) ensures that the minimum distance between codepoints in a pair of adjacent shells is no more than d , it does not insure this condition for codepoints in nonadjacent shells. It is possible that (5.5) would result in codepoints from shell i and shell $i + l_{k-1}$ which are closer than d . Let X' , Y' , and Z' , respectively, be the projections of X , Y , and Z shown in Figure 5.3, onto Ω_k . Then $Y', X' \in \text{LSC}(k, d)$. If $\|Z' - X'\| < d$, then (5.5) is not used, in which case r_i is set to the value which produces $\|Z' - X'\| = d$ and from (5.6) gives

$$r_i = r_{i-l_{k-1}} \left(1 - \frac{d^2}{2}\right) + d \sqrt{(1 - r_{i-l_{k-1}}^2) \left(1 - \frac{d^2}{4}\right)}. \quad (5.7)$$

In summary, the r_i 's may be determined by the following algorithm:

```

 $r_0 := 0;$ 
 $i := 1;$ 
 $r_s := r_1 := d;$ 
while  $r_i \leq \sqrt{1 - d^2/4}$  {
   $i := i + 1;$ 
  if  $\lfloor r_{i-1} d^{-2/k} \rfloor \neq \lfloor \max(r(i, 1), r(i - l_{k-1}, 0)) d^{-2/k} \rfloor$ 
    then  $r_s := r_i := r(i, 0);$  /* begin new annulus */
    else  $r_i := \max(r(i, 1), r(i - l_{k-1}, 0));$  /* regular solution */
}
 $N := i - 1;$ 

```

Example of a Laminated Spherical Code

The construction of a laminated spherical code is illustrated for $k = 3$ and $d = 0.3$. First, the radii $\{r_i\}$ are determined. Since in Λ_2 lattice points in one layer differ in the second coordinate from lattice points two layers away, it follows that $l_2 = 2$. In Λ_1 , holes are a distance $1/2$ from two lattice points, and hence $c_1 = 1/2$, and $n_1 = 2$. An iteration of the algorithm above gives $(r_0, \dots, r_N) = (0, .3, .569, .752, .872, .978)$, $(s(0), \dots, s(5)) = (0, 1, 2, 2, 2, 5)$, and $(g(0), \dots, g(3)) = (0, 1, 2, 5)$. Next, the two-dimensional spherical codes to be projected onto Ω_3 are determined.

$$i = 0: \mathcal{C}_i(k-1, d/r_{s(i)}) = \mathcal{C}_0(2, \infty) = \mathcal{C}_{g(0)+0}(2, \infty) = \text{LSC}(2, \infty) = \{(1, 0)\}.$$

$$i = 1: \mathcal{C}_i(k-1, d/r_{s(i)}) = \mathcal{C}_{g(1)+0}(2, 1) = \text{LSC}(2, 1) = \{(\cos(i\pi/3), \sin(i\pi/3)) : 0 \leq i \leq 5\}.$$

$$i = 2: \mathcal{C}_i(k-1, d/r_{s(i)}) = \mathcal{C}_{g(2)+0}(2, .527). \text{ Thus, } \theta_i = 2 \sin^{-1}(.527/2) = .533, \text{ and}$$

$$\mathcal{C}_i(k-1, d/r_{s(i)}) = \{(\cos(.533i), \sin(.533i)) : 0 \leq i \leq 10\}.$$

$$i = 3: \mathcal{C}_i(k-1, d/r_{s(i)}) = \mathcal{C}_{g(2)+1}(2, .527) = f(\mathcal{C}_i(2, .527)) = \left\{ \frac{H(L(X))}{\|H(L(X))\|} : X \in f(\mathcal{C}_i(2, .527)) \right\}.$$

If $Y \in \Lambda_1^0$, then $D(Y)_1 = Y$, $D(Y)_2 = Y + (1, 0)$, and so $n(Y) = H(D(Y)_1, D(Y)_2) + (0, \sqrt{1 - c_{k-2}^2}) = Y + (1/2, \sqrt{3}/2)$. Let $X = (\cos(.533i), \sin(.533i)) \in \mathcal{C}_2(2, .527)$. Then $w_0(X) \equiv (i, 0)$, and hence

$$\begin{aligned} L(X) &= \{w_0^{-1}(i, 0), w_0^{-1}(i+1, 0)\} \\ &= \{(\cos(.533i), \sin(.533i)), (\cos(.533(i+1)), \sin(.533(i+1)))\}. \end{aligned}$$

From this, it follows that $H(L(X))/\|H(L(X))\| = (\cos(.533(i + 1/2)), \sin(.533(i + 1/2)))$.

In the next shell, the fact that $w_1(X) = (i + 1/2, \sqrt{3}/2)$ is used. Letting X range over $\mathcal{C}_2(2, .527)$ gives $\mathcal{C}_i(k - 1, d/r_{s(i)}) = \{(\cos(.533(i + 1/2)), \sin(.533(i + 1/2))) : 0 \leq i \leq 10\}$.

$i = 4$: $\mathcal{C}_i(k - 1, d/r_{s(i)}) = \mathcal{C}_{g(2)+2}(2, .527) = \{(\cos(.533i), \sin(.533i)) : 0 \leq i \leq 10\}$.

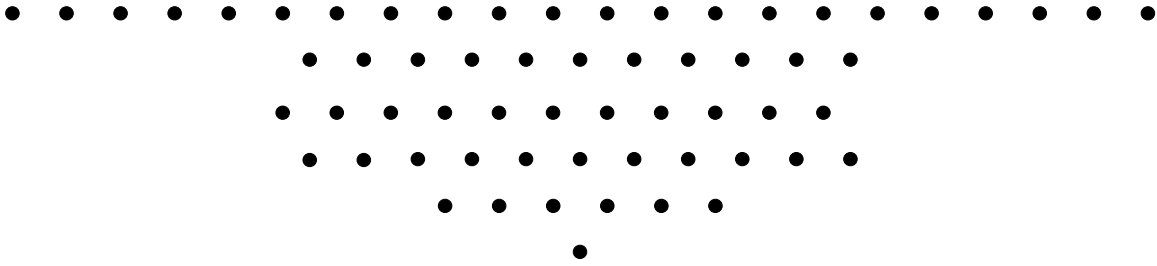
$i = 5$: A new annulus begins with $\mathcal{C}_{g(3)+0}(2, .307)$. Thus, $\theta_i = 2 \sin^{-1}(.307/2) = .308$, and $\mathcal{C}_i(k - 1, d/r_{s(i)}) = \{(\cos(.308i), \sin(.308i)) : 0 \leq i \leq 19\}$.

The resulting code $\text{LSC}(3, .3)$ is defined using (5.1) and has six shells. The shells contain 1, 6, 11, 11, 11, and 20 points, respectively, and thus, the entire code has 120 points. The subset of Λ_2 used is shown in Figure 5.4(a). The unprojected two-dimensional codes are shown in Figure 5.4(b). The spherical caps of the final code $\text{LSC}(3, .3)$ are shown in Figure 5.4(c). As d approaches 0, the advantage of the laminating technique becomes more apparent. The apple-peeling spherical code $\mathcal{C}^A(3, 0.05)$ is compared to the laminated spherical code $\text{LSC}(3, 0.05)$ in Figure 5.5.

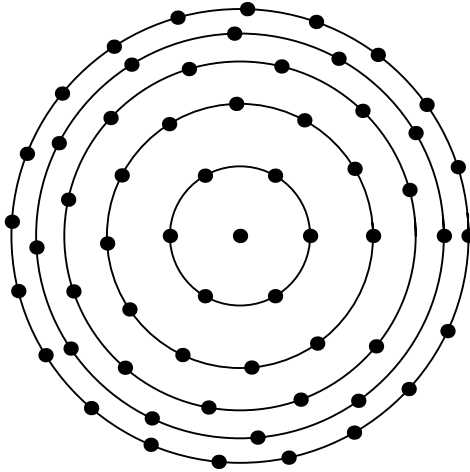
There are a number of improvements that may be made to the general construction. First, there may be points on the sphere that are not within d of any codepoint— and thus these points may be added to the codebook. For example, on shells 3 and 4 of $\text{LSC}(3, .3)$, it appears that an extra codepoint may be added without reducing the minimum distance. Also, the width of the annuli may be modified, which would alter the number of shells that may be fit on the sphere, as well as their placement. The annulus width used above was $d^{2/k} \approx .448$. If the annulus width is set to zero instead, the apple-peeling code results. When the annulus width is .5, a code of size 128 may be obtained. In fact, each annulus width can be optimized separately.

5.3 Asymptotic Density of the Laminated Spherical Code

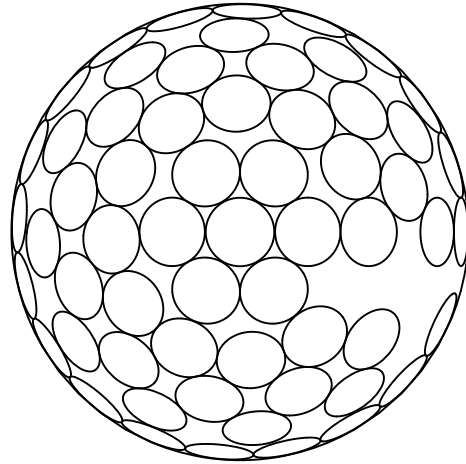
Let $\Delta_{\text{LSC}}(k, d)$ be the density of $\text{LSC}(k, d)$, let $\Delta_{\text{LSC}}(k) = \limsup_{d \rightarrow 0} \Delta_{\text{LSC}}(k, d)$, and let Δ_{Λ_k} be the density of the sphere packing with spheres of radius $1/2$ and centers in Λ_k . Within an annulus, layers of shells are stacked similarly to layers of lattices in a laminated lattice. Theorem 5.1 establishes that $\Delta_{\text{LSC}}(k)$ is asymptotically equal to the density of the sphere packing generated by Λ_{k-1} .



(a)

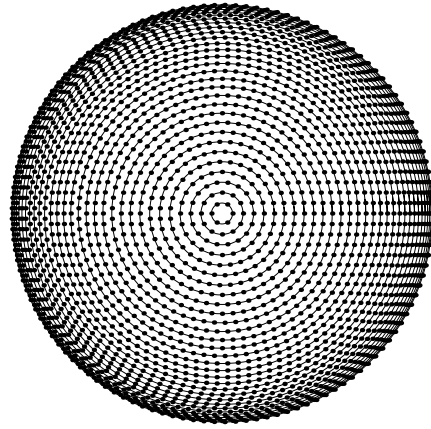


(b)

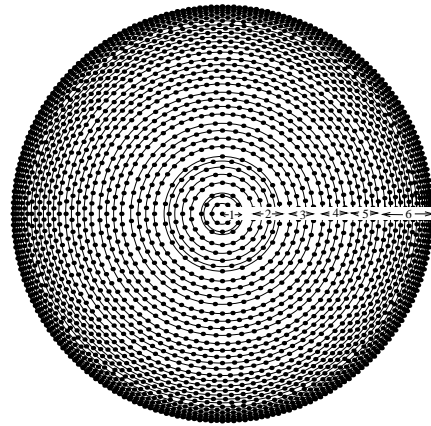


(c)

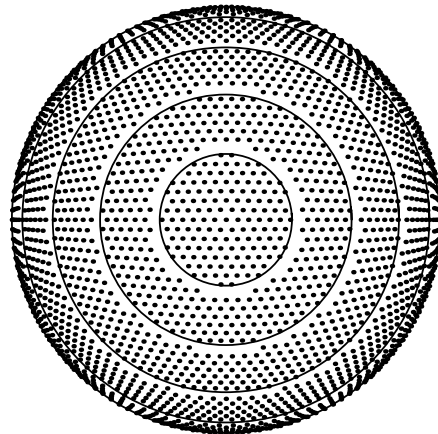
Figure 5.4 (a) A finite subset of A_2 . (b) $LSC(3, .3)$, before projection. (c) $LSC(3, .3)$ after projection.



(a)



(b)



(c)

Figure 5.5 Comparison of apple-peeling, laminated, and wrapped spherical codes. To obtain the spherical codes, the points shown in the circles are projected straight out of the page onto the surface of a sphere. (a) Apple-peeling code $\mathcal{C}^A(3, 0.05)$ has 4764 codepoints. (b) Laminated code $\text{LSC}(3, 0.05)$ has 5244 codepoints. (c) Wrapped code WA-SC constructed from the hexagonal lattice with minimum distance 0.05 has 4802 codepoints.

Theorem 5.1 *The density of a k -dimensional laminated spherical code $LSC(k, d)$ with minimum distance d is no more than $O(d^{1/k})$ less than the density of the $(k - 1)$ -dimensional laminated lattice Λ_{k-1} , for all $k \leq 49$. That is, $\Delta_{LSC}(k, d) = \Delta_{\Lambda_{k-1}} - O(d^{1/k})$.*

Proof: See Appendix D

Corollary 5.1 follows from Lemma 3.2, Theorem 5.1, and the fact that Λ_2 is the densest possible packing in two dimensions. It also establishes the fact that the Fejes Tóth upper bound in Lemma 3.2 is asymptotically tight.

Corollary 5.1 *The three-dimensional laminated spherical codes $LSC(3, d)$ are asymptotically optimal in the minimum distance sense as the minimum distance decreases.*

Figure 3.5 shows the laminated spherical code density $\Delta_{LSC}(3, d)$ versus d . All code densities are normalized by the Fejes Tóth upper bound, i.e., $\Delta_{LSC}(3, d)/\Delta_F(3, d)$ is plotted versus d , where $\Delta_F(3, d)$ is the upper bound on density $\Delta(3, d)$ for a three-dimensional spherical code with minimum distance d . For $d < 0.7$, the laminated spherical code $LSC(3, d)$ outperforms known codes derived from shells of lattices, and is comparable to the apple-peeling code. For $d < 0.02$, $LSC(3, d)$ is the best code known, and convergence to the upper bound is apparent as $d \rightarrow 0$.

In dimension four, the performance is similar to the performance in three dimensions: for small minimum distances, the best known spherical codes are produced. This is shown in Figure 3.6. In higher dimensions, the performance is not as good. In dimension eight, the performance of the laminated spherical code is significantly weaker than that of the wrapped spherical code and shells of lattices. However, from Theorem 5.1, the asymptotic density of the eight-dimensional laminated spherical code is the same as the density of the wrapped spherical code with an underlying Λ_7 lattice. Hence, for extremely small minimum distances, the laminated spherical code has equivalent performance to that for the wrapped spherical code. Figure 3.7 indicates that the convergence of the density of laminated spherical code to its asymptotic value is much slower in dimension eight than in the lower dimensions.

5.4 Decoding Laminated Spherical Codes

Two approaches to decoding are considered, reflecting a tradeoff in the time and space complexity of the decoding, namely, (I) the decoder stores the radii used to construct the code, or (II) the decoder stores only the dimension k and minimum distance d . For any $R \in \mathbb{R}^k$ and any spherical code $\mathcal{C}(k, d)$, the nearest codepoint of $\mathcal{C}(k, d)$ to R is the same as the nearest codepoint of $\mathcal{C}(k, d)$ to $R/\|R\|$. Hence, in the following, it is assumed that $R \in \Omega_k$. Recall from (5.2) that $N = \max \left\{ i: r_i \leq \sqrt{1 - d^2/4} \right\}$, i.e., N is the number of radii needed to construct a laminated spherical code (not counting the radii used to construct lower dimensional laminated codes).

Lemma 5.1 $N = O(|LSC(k, d)|^{1/(k-1)})$.

Proof: By construction of $LSC(k, d)$, codepoints arising from \mathcal{C}_i and $\mathcal{C}_{i-l_{k-1}}$ have angular separation at least θ , for all $i \geq l_{k-1}$. Thus, $(0, \dots, 0, r_i, \sqrt{1 - r_i^2})$ and $(0, \dots, 0, r_{i-l_{k-1}}, \sqrt{1 - r_{i-l_{k-1}}^2})$ also have angular separation θ (even though these points might not be codepoints). The intersection of Ω_k and the plane in \mathbb{R}^k spanned by $(0, \dots, 0, 1)$ and $(0, \dots, 1, 0)$ is a unit circle; thus, $l_{k-1}N \leq \pi/(2\theta)$. From the definition of density, $|LSC(k, d)| \cdot s(c(k, \theta/2)) = \Delta_{LSC}(k, d) \cdot S_k$. Using Equation (11) of [38] and the fact that $\Delta_{LSC}(k, d) \cdot S_k$ is bounded away from zero (in both k and d), it follows that $|LSC(k, d)| = O(1/d^{k-1})$; hence, $N = O(1/d) = O(|LSC(k, d)|^{1/(k-1)})$.

■

Lemma 5.2 *The sequences of radii needed to construct $LSC(k, d)$ can be written with storage complexity $O\left(\sqrt{|LSC(k, d)|}\right)$.*

Proof: Let $N(k, d)$ denote the *total* number of radii needed to construct $LSC(k, d)$, i.e., N plus the total number of radii needed to construct all of the $(k-1)$ -dimensional laminated spherical codes used in the recursive definition of $LSC(k, d)$. There are $O(d^{-2/k})$ annuli in $LSC(k, d)$, each of which has shells defined via a $(k-1)$ -dimensional laminated spherical code with minimum

distance at least d . Thus,

$$\begin{aligned}
N(k, d) &= O(d^{-1}) + O(d^{-2/k})N(k-1, d) \\
&= O(d^{-1}) + O(d^{-2/k}) \left(O(d^{-1}) + O(d^{2/(k-1)}) \right) N(k-2, d) \\
&= O(d^{-(1+(2/k))}) + O(d^{\frac{2}{k(k-1)}}) N(k-2, d) \\
&= O(d^{-(1+(2/k)+2/(k-1)+\dots+(2/4))}) \\
&= O\left(M^{\frac{1}{k-1}(1+2\sum_{i=4}^k 1/i)}\right) \\
&= O(\sqrt{M}).
\end{aligned}$$

■

Lemma 5.3 *For $k \leq 49$, the distance from any point on Ω_k to the nearest codepoint in $LSC(k, d)$ is $O(d)$.*

Proof: The width of any shell is no more than d . Thus, the distance from an arbitrary point $R \in \Omega_k$ to the nearest point, say R' , on the boundary of the shell containing R is at most d . This shell boundary contains a scaled spherical code $r_i \mathcal{C}_i(k-1, d/r_{s(i)})$, for some i . Since $r_i d/r_{s(i)} \leq 2d$, R' is at most $2d$ from the nearest point on the boundary of some shell *used to construct* $\mathcal{C}_i(k-1, r_i d/r_{s(i)})$. By computing the distance to the boundary of a shell in successively lower dimensions, it follows that R is at most a distance $d + 2d + 4d + \dots + 2^{k-2}d = O(d)$ from a codepoint of $LSC(k, d)$. ■

Let $R \in \Omega_k$. By construction of $LSC(k, d)$, codepoints arising from \mathcal{C}_i and $\mathcal{C}_{i-l_{k-1}}$ have angular separation at least θ , for all $i \geq l_{k-1}$. Hence, there are only a constant number of shells that contain points whose angular separation from R is $O(d)$. By Lemma 5.3, the nearest neighbor search may thus be restricted to a constant number of candidate shells, and the nearest neighbor distances may be found on each of those shells and compared to R . The algorithm may be written explicitly as follows:

Nearest_Neighbor($k, d, R, \{r_i\}$) {
 $(x_1, \dots, x_k) := R$;
 $i := \min \left\{ j : r_j > \sqrt{x_1^2 + \dots + x_{k-1}^2} \right\}$;
if ($k = 2$) {
 $X := (r_{i-1}, \sqrt{1 - r_{i-1}})$;

```

    if  $\left( \left\| \left( r_i, \sqrt{1 - r_i^2} \right) - R \right\| < \|X - R\| \right)$  then  $X := \left( r_i, \sqrt{1 - r_i^2} \right);$ 
  }
  if  $(k > 2)$  {
     $X := (3, \dots, 3);$ 
    for  $j := i - l_{k-1} \cdot 2^{k-1}$  to  $i + l_{k-1} \cdot 2^{k-1}$  {
       $\{r'_n\}$  := sequence of radii used to construct  $\mathcal{C}_{s(j)}(k-1, d/s(j));$ 
       $X' = (x'_1, \dots, x'_{k-1}) := \text{Nearest\_Neighbor} \left( k-1, d/r_{s(j)}, \frac{(x_1, \dots, x_{k-1})}{\|(x_1, \dots, x_{k-1})\|}, \{r'_n\} \right);$ 
      if  $\left( \left\| \left( x'_1, \dots, x'_{k-1}, \sqrt{1 - (x_1^2 + \dots + x_{k-1}^2)} \right) - R \right\| < \|X - R\| \right)$ 
        then  $X := \left( x'_1, \dots, x'_{k-1}, \sqrt{1 - (x_1^2 + \dots + x_{k-1}^2)} \right);$ 
    }
  }
  return  $(X);$ 
}

```

Theorem 5.2 *There exists a nearest codepoint algorithm for $LSC(k, d)$ using $O\left(\sqrt{|LSC(k, d)|}\right)$ space and $O(\log |LSC(k, d)|)$ time, and there exists a nearest codepoint algorithm using $O(1)$ space and $O\left(\sqrt{|LSC(k, d)|}\right)$ time.*

Proof: In the algorithm above, storing the sequences of radii requires $O(\sqrt{|LSC(k, d)|})$, by Lemma 5.2. To find the index i used in the algorithm requires

$$O(\log N) = O(\log |LSC(k, d)|^{1/(k-1)}) = O(\log |LSC(k, d)|)$$

time, by Lemma 5.1. The other lines of the algorithm require constant time plus a constant number of recursive calls to the decoding algorithm. Since the dimension k in $LSC(k, d)$ is a constant, the algorithm performs only a constant number of recursive calls. Thus, the algorithm uses $O\left(\sqrt{|LSC(k, d)|}\right)$ space and $O(\log |LSC(k, d)|)$ time.

Alternatively, the sequences of radii need not be stored. If only k and d are stored, $O(1)$ storage space is required. The algorithm may then generate a sequence of radii when needed, using the technique outlined in the construction of $LSC(k, d)$. This generation takes linear time in the size of the sequences, i.e., $O\left(\sqrt{|LSC(k, d)|}\right)$. ■

5.5 Conclusions

A new technique was presented that constructs laminated spherical codes in dimensions up to 49. The three-dimensional laminated spherical codes are asymptotically optimal, in the sense that the ratio of the minimum distance of the constructed code to the Fejes Tóth upper bound given in [23] approaches one as the number of codepoints increases. This proves that the upper bound is tight, asymptotically, and that previous lower bounds are not asymptotically optimal. The codes generated also compare favorably to other codes, for a wide variety of minimum distances. Good asymptotic performance is also achieved in higher dimensions, where the k -dimensional laminated spherical code density approaches the density of Λ_{k-1} . The question of whether the asymptotic density of the k -dimensional laminated spherical code is optimal is equivalent to the question of whether the Λ_{k-1} is the densest sphere packing.

Both wrapped spherical codes and laminated spherical codes presented in [38] improve the asymptotic performance of previous spherical codes. Similarly, the density of a wrapped spherical code with respect to a packing Λ approaches the density of Λ ; hence, any densest lattice Λ gives rise to an asymptotically optimal spherical code. The wrapped codes are not restricted to laminated lattices; any lattice or packing in \mathbb{R}^{k-1} may be used to construct a k -dimensional wrapped code.

The comparison of the nonasymptotic performance reveals that both the wrapped and laminated spherical codes perform better than other constructions, i.e., have larger code sizes for a given minimum distance. In three and four dimensions, the laminated spherical codes perform better than the wrapped codes. In higher dimensions, the advantages of wrapped spherical codes become more apparent: the wrapped codes are easier to construct than laminated spherical codes because an explicit mapping is specified instead of a recursive one, and the decoding algorithm reduces to a decoding algorithm for the underlying lattice, a well-studied problem. The decoding algorithm for the laminated codes is recursive, and though efficient for low dimensions, is in fact exponential in the number of dimensions. Additionally, the asymptotic density of wrapped spherical codes is higher than the asymptotic density of laminated spherical codes in any dimension for which the laminated lattice in the previous dimension is not the best packing, e.g., dimensions 10-13.

CHAPTER 6

WRAPPED SPHERICAL CODES AS VECTOR QUANTIZERS FOR A MEMORYLESS GAUSSIAN SOURCE

6.1 Introduction

A major goal in source coding theory is to design a quantizer that has both low implementation complexity and performance close to the rate-distortion function of the source. Scalar quantizers have low implementation complexity, but their distortion performance is usually much worse than the rate-distortion function. Shannon's source coding theorem shows that the performance of fixed-rate vector quantizers (VQs) can approach the rate-distortion function as the vector dimension tends to infinity [28], but the proof is nonconstructive. Constructive techniques for VQ, such as the generalized Lloyd algorithm [56] perform well, but their creation, storage, and encoding complexities each grow exponentially in both dimension and rate. There are other examples of VQs with good performance and exponential complexity as well [72, 94]. An exponential complexity is such a barrier to implementation that any quantizer exhibiting this behavior has been termed "noninstrumentable" [7].

A number of complexity constrained VQs have been proposed in an attempt to improve upon scalar quantization while retaining a low complexity implementation [31]. This chapter makes use of two of these methods: lattice quantizers and shape-gain quantizers. Our proposed quantizer does not have exponential complexity; in fact, the operating complexity grows linearly with the rate.

The quantizer presented in this chapter is optimized with respect to a memoryless Gaussian source. One reason for concentrating on a memoryless Gaussian source is that it naturally arises in numerous applications. For example, the prediction error signal in a DPCM (differential

pulse code modulation) coder for moving pictures is well-modeled as Gaussian using block activity classes with 8×8 -dimensional blocks [92]. Also, discrete Fourier transform coefficients and holographic data can often be considered to be the output of a Gaussian source [84], although some other aspects of images and speech are better modeled as Laplacian distributions [26, 88]. Furthermore, a known filtering technique tends to make any memoryless source appear Gaussian, which makes the system insensitive to errors in modeling the input [73]. Finally, the Gaussian source is easier mathematically to analyze compared to some other sources, because its distortion-rate function is known explicitly: $D = \sigma^2 2^{-2R}$. The literature is filled with results of quantizers with respect to a Gaussian source [2, 22, 24, 25, 46, 47, 61–63, 66, 68, 71–73, 76, 77, 84, 92–94].

In the following sections, it is shown how a lattice quantizer can be transformed into a shape-gain quantizer. For a memoryless Gaussian source, this shape-gain quantizer performs better than any quantizer in the literature at rates of three bits per sample or higher. For a memoryless Gaussian source. Section 6.2 presents properties of the Gaussian source, Section 6.3 gives the construction method for the wrapped shape-gain quantizer, Sections 6.4 and 6.5 give implementation complexity and distortion analysis, and Section 6.6 gives simulation results. Several extensions are discussed in Section 6.7, including the quantization of non-Gaussian sources.

6.2 Properties of Vectors from a Memoryless Gaussian Source

Let $X = (X_1, \dots, X_k)$, where each X_i is drawn from a memoryless $N(0, \sigma^2)$ source. The probability density function (pdf) of X is

$$f_X(Y) = f_X(y_1, \dots, y_k) = \prod_{i=1}^k \frac{\exp\left(\frac{-y_i^2}{2\sigma^2}\right)}{\sqrt{2\pi\sigma^2}} = \frac{\exp\left(\frac{-\|Y\|^2}{2\sigma^2}\right)}{(2\pi\sigma^2)^{k/2}}.$$

Since $f_X(Y)$ depends only on $\|Y\|$, the notations $f_X(\|Y\|)$ and $f_X(Y)$ will be used interchangeably.

Lemma 6.1 *The pdf of $g = \|X\|$ is $f_g(r) = \frac{2r^{k-1} \exp\left(\frac{-r^2}{2\sigma^2}\right)}{\Gamma(k/2)(2\sigma^2)^{k/2}}$.*

Proof:

$$\begin{aligned}
f_g(r) &= \lim_{h \rightarrow 0} \frac{1}{h} (\Pr[\|X\| \leq r+h] - \Pr[\|X\| \leq r]) \\
&= \lim_{h \rightarrow 0} \frac{1}{h} \int_{r < \|Y\| \leq r+h} f_X(Y) dY \\
&\leq \lim_{h \rightarrow 0} \frac{1}{h} \int_{r < \|Y\| \leq r+h} f_X(r) dY \\
&= f_X(r) \cdot \lim_{h \rightarrow 0} \frac{1}{h} \int_{r < \|Y\| \leq r+h} dY \\
&= f_X(r) \cdot \lim_{h \rightarrow 0} \frac{1}{h} (V_k(r+h)^k - V_k r^k) \\
&= f_X(r) k V_k r^{k-1} \\
&= f_X(r) S_k r^{k-1},
\end{aligned} \tag{6.1}$$

where, as in earlier chapters, V_k is the k -dimensional content (“volume”) of the unit-radius k -dimensional sphere Ω_k , and S_k is the $(k-1)$ -dimensional content (“surface area”) of Ω_k . On the other hand, from Equation (6.1),

$$\begin{aligned}
f_g(r) &\geq \lim_{h \rightarrow 0} \frac{1}{h} \int_{r < \|Y\| \leq r+h} f_X(r+h) dY \\
&= f_X(r) \cdot \lim_{h \rightarrow 0} \left(\frac{1}{h} \int_{r < \|Y\| \leq r+h} dY \right) \\
&= f_X(r) S_k r^{k-1}.
\end{aligned}$$

Thus,

$$f_g(r) = f_X(r) S_k r^{k-1} = \frac{2r^{k-1} \exp\left(\frac{-r^2}{2\sigma^2}\right)}{\Gamma(k/2)(2\sigma^2)^{k/2}}. \tag{6.2}$$

■

This derivation avoids the use of k -dimensional spherical coordinates, which were previously thought to be necessary [83, p. 258]. Using $f_g(\cdot)$, it is straightforward to verify the following.

Lemma 6.2 *The mean, second moment, and variance of $\|X\|$ are given by*

$$\begin{aligned}
E[\|X\|] &= \frac{\sqrt{2\sigma^2} \Gamma\left(\frac{k+1}{2}\right)}{\Gamma\left(\frac{k}{2}\right)} = \frac{\sqrt{2\pi\sigma^2}}{\beta\left(\frac{k}{2}, \frac{1}{2}\right)} \\
E[\|X\|^2] &= k\sigma^2 \\
\text{var}[\|X\|] &= k\sigma^2 - \frac{2\pi\sigma^2}{\beta^2\left(\frac{k}{2}, \frac{1}{2}\right)},
\end{aligned} \tag{6.3}$$

where $\Gamma(x) = \int_0^\infty e^{-t} t^{x-1} dt$ and $\beta(x, y) = \frac{\Gamma(x)\Gamma(y)}{\Gamma(x+y)}$.

Proof: See Section C.4.

Figure 6.1 shows the pdf of X and $\text{var}[\|X\|]$ when $\sigma^2 = 1$. Not surprisingly, $\text{var}[\|X\|]$ appears to be a strictly increasing function of its dimension k . This trend holds for all k .

Lemma 6.3 *$\text{var}[\|X\|]$ is a strictly increasing function of the vector dimension k .*

Proof: See Section C.5.

The following lemma demonstrates that the variance of the norm of X is bounded, for all k .

Lemma 6.4 *$\text{var}[\|X\|] \leq \sigma^2/2$, for every vector dimension k .*

Proof: From Lemma 6.3, it suffices to show that $\lim_{k \rightarrow \infty} \text{var}[\|X\|] \leq \sigma^2/2$.

$$\begin{aligned}
\lim_{k \rightarrow \infty} \text{var}[\|X\|] &= \lim_{k \rightarrow \infty} \left[k\sigma^2 - \frac{2\sigma^2\Gamma^2\left(\frac{k+1}{2}\right)}{\Gamma^2\left(\frac{k}{2}\right)} \right] \\
&= \sigma^2 \lim_{k \rightarrow \infty} \left[k - \frac{2\left(\frac{k+1}{2e}\right)^{k+1} \cdot \frac{2\pi}{\left(\frac{k+1}{2}\right)} \cdot (1 + O(1/k))^2}{\left(\frac{k}{2e}\right) \cdot \frac{2\pi}{\left(\frac{k}{2}\right)} (1 + O(1/k))} \right] \text{ by Stirling's formula} \\
&= \sigma^2 \lim_{k \rightarrow \infty} \left[k - \frac{k}{e} \cdot (1 + 1/k)^k \cdot \frac{(1 + O(1/k))}{(1 + O(1/k))} \right] \\
&= \sigma^2 \lim_{k \rightarrow \infty} \left[k - \frac{ke}{e} \left(1 - \frac{1}{2k} + O(1/k^2)\right) \cdot \frac{(1 + O(1/k))}{(1 + O(1/k))} \right] \tag{6.4} \\
&= \sigma^2 \lim_{k \rightarrow \infty} \left[\left(\frac{1}{2} + O(1/k^2)\right) \cdot \frac{(1 + O(1/k))}{(1 + O(1/k))} \right] \\
&= \frac{\sigma^2}{2}, \tag{6.5}
\end{aligned}$$

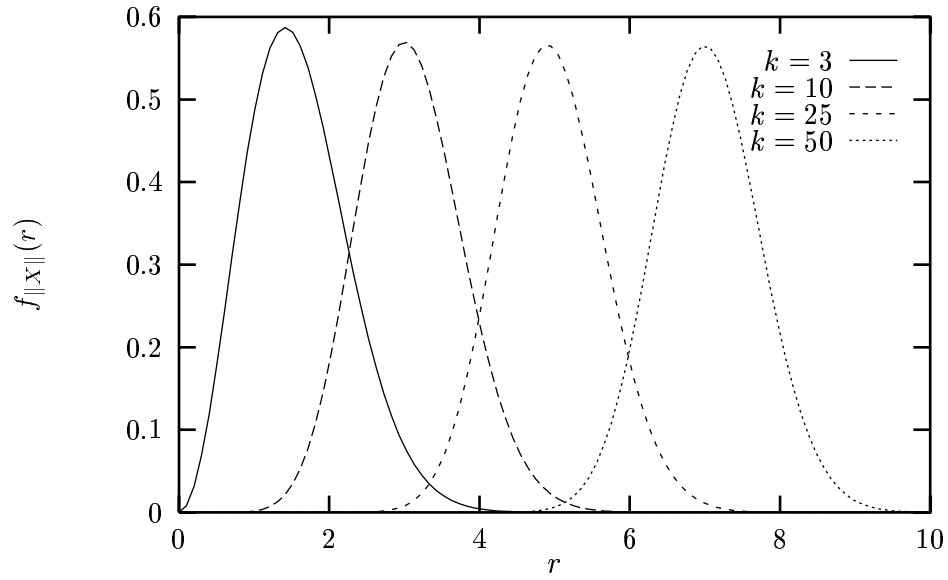
where in (6.4) we have used the fact that $(1 + 1/k)^k = e \cdot (1 - \frac{1}{2k} + O(\frac{1}{k^2}))$, as derived in the proof of Lemma 6.3. ■

Lemma 6.4 provides a tighter bound than the $\text{var}[\|X\|] \leq 5\sigma^2/6$, as reported by Sakrison [77].

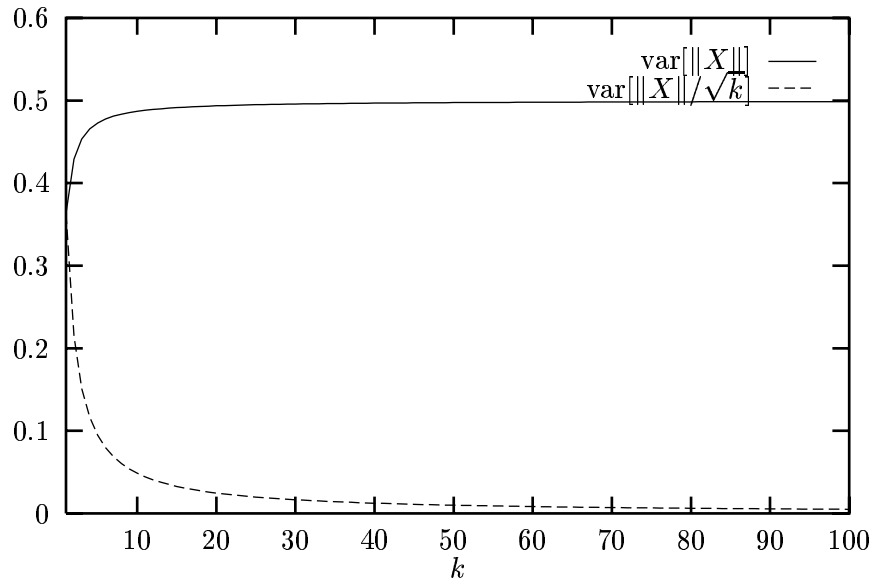
For ease of exposition, in the remainder of the chapter it is assumed that $\sigma^2 = 1$.

The analysis above brings to light a number of subtle points:

- The maximum value of $f_X(Y)$ occurs when $Y = 0$ and decreases monotonically as $\|Y\|$ increases; therefore, among all k -dimensional spheres of constant volume, the sphere centered on the origin has the highest probability of containing X . On the other hand, Figure 6.1(a) shows that X is not likely to be near the origin, even for small k . The high probability region of $\|X\|$ is near its expected value, which by Stirling's formula for Γ is approximated very well by $\sigma\sqrt{k - (1/2)}$ for $k > 1$.



(a)



(b)

Figure 6.1 $X = (X_1, \dots, X_k)$ is formed from an i.i.d. $N(0, 1)$ source. (a) The pdf of $\|X\|$. (b) The variance of $\|X\|$ and the variance of $\|X\|/\sqrt{k}$

- The “sphere hardening” that occurs as $k \rightarrow \infty$ (see, e.g., [32]), occurs on a *normalized* sphere only. That is, the high probability region of the random variable $\|X\|/\sqrt{k}$ converges to an infinitesimal interval about 1 as $k \rightarrow \infty$, but the high probability region of the unnormalized random variable $\|X\|$ is a cloud of roughly constant thickness, as derived in (6.5), and this thickness does not go to zero as $k \rightarrow \infty$.
- Since $f_X(Y)$ depends only on $\|Y\|$, it follows that $X/\|X\|$ is uniformly distributed on the unit sphere Ω_k . This provides the motivation for mapping lattices from \mathbb{R}^{k-1} to Ω_k . The excellent performance of lattice quantizers for a uniform source in \mathbb{R}^{k-1} is then transformed to excellent performance for a uniform source in Ω_k .

Recall from Chapter 2.2.4 that a spherical vector quantizer is one whose output points lie on a sphere. It is easy to show that if a spherical vector quantizer uses a nearest neighbor encoding rule and encodes X to \hat{X} , then it encodes cX to \hat{X} as well, for all $c > 0$. Sakrison showed that if a spherical vector quantizer with radius $E[\|X\|]$ is used to quantize a Gaussian random vector X to \hat{X} using a nearest neighbor encoding rule, then the resulting MSE distortion per dimension can be decomposed into shape and norm distortions [77]. For completeness, a derivation is included here. Let $X_p = E[\|X\|] \cdot \frac{X}{\|X\|}$. Then,

$$\begin{aligned}
D &= \frac{1}{k} E[\|X - \hat{X}\|^2] \\
&= \frac{1}{k} E\left[\|X - X_p + X_p - \hat{X}\|^2\right] \\
&= \frac{1}{k} E\left[\|X_p - \hat{X}\|^2\right] + \text{var}[\|X\|]/k,
\end{aligned} \tag{6.6}$$

where the cross term vanished because

$$\begin{aligned}
E\left[(X - X_p)^T (X_p - \hat{X})\right] &= E\left[E\left[(X - X_p)^T (X_p - \hat{X}) \mid X_p\right]\right] \\
&= E\left[E\left[(X - X_p)^T \mid X_p\right] (X_p - \hat{X})\right] \\
&= E\left[E\left[\frac{X^T}{\|X\|} (\|X\| - E[\|X\|]) \mid X_p\right] (X_p - \hat{X})\right] \\
&= E\left[\frac{X^T}{\|X\|} \cdot E[(\|X\| - E[\|X\|]) \mid X_p] (X_p - \hat{X})\right] \\
&= E\left[\frac{X^T}{\|X\|} \cdot E[(\|X\| - E[\|X\|])] (X_p - \hat{X})\right] \\
&= 0,
\end{aligned}$$

where the second to last step uses the fact that $\|X\|$ and X_p are independent random variables. Thus, for large k , the last term of Equation (6.6) is negligible (see dashed curve in Figure 6.1(b)), and an effective quantizer for X is a spherical vector quantizer for a source uniformly distributed on the k -dimensional sphere with radius $E[\|X\|]$. Sakrison designed such a quantizer using a random coding argument, which proved that the rate-distortion function can be approached, but this quantizer is noninstrumentable. This chapter provides a spherical vector quantizer that can be efficiently implemented and which also has excellent distortion performance. In the design no assumption is made that k is asymptotically large, and hence it is not assumed that the last term of the distortion is negligible. For example, when $k = 25$, the last term of Equation (6.6) dominates the overall distortion performance at rates of three or higher. This distortion is reduced in this chapter by the use of shape-gain quantization.

6.3 A Wrapped Spherical Vector Quantizer

6.3.1 Structure of the codebook

A shape-gain vector quantizer is used. Shape-gain VQ is a quantization technique in which a source vector X is decomposed into *gain* $g = \|X\|$ and *shape* $S = X/g$ components, g and S are quantized separately to \hat{g} and \hat{S} , respectively, and the VQ output is $\hat{g}\hat{S}$. One advantage of shape-gain quantization is that the storage complexity is the *sum* of the gain codebook size and shape codebook size, while the effective codebook size is the *product* of these quantities. In the new implementation, the gain codebook has fifteen or fewer codepoints for rates under 4, and the shape codebook is structured so that it need not be stored.

For the shape-gain quantizer presented here, \hat{g} depends only on g and \hat{S} depends only on S . This allows the gain and shape quantizers to operate in parallel and independently of each other, and it also greatly simplifies the analysis of the distortion. In the most general setting, \hat{g} and \hat{S} each depend on both g and S , and a small performance improvement can be realized. An extension to this type of quantizer will be discussed in Section 6.7. The gain codebook outputs are denoted by $\{g_1, \dots, g_{2^{R_g}}\}$, where the gain rate R_g is derived in the following section.

Using the gain pdf $f_g(r)$ from Equation (6.2), the gain codebook is optimized by the Lloyd-Max algorithm [58, 63]. No training vectors are needed for this since the pdf is known exactly. Furthermore, since $f_g(r)$ is a log-concave function, the Lloyd-Max algorithm converges to the

globally optimum gain codebook [27, 87]. The Lloyd-Max algorithm is terminated after a finite number of steps when successive iterations do not appreciably alter the codebook. Regardless of when terminated, the centroid condition holds and thus $E[\hat{g}] = E[g]$ and the MSE distortion is $E[g^2] - E[\hat{g}^2]$ [31]; these facts will be used in the distortion analysis in Section 6.5.

The shape codebook is generated by a wrapped spherical code as described in Chapter 4, except that the buffer zones are not used. Recall that the purpose of the buffer zones was to ensure that minimum distance violations did not occur between annuli, which is not a concern for the quantization problem. The wrapped spherical code construction is reviewed here. Let Λ be a sphere packing in \mathbb{R}^{k-1} with minimum distance d_Λ and density Δ_Λ . Λ may be either a lattice packing or a nonlattice packing. Using the same notation as in Chapter 4, let $N = \lceil \frac{\pi}{4\sqrt{d_\Lambda}} \rceil$, let $\alpha = \frac{\pi}{4N}$, let $\xi_i = \sin(i\alpha)$ for $0 \leq i \leq N$, and for $x \in [-1, 1]$, let $\underline{\xi}(x) \equiv \max\{\xi_i : \xi_i \leq |x|\}$ and $\bar{\xi}(x) \equiv \min\{\xi_i : \xi_i > |x|\}$. Define the many-to-one function $f': \Omega_k \rightarrow \mathbb{R}^{k-1}$ by

$$f'(x_1, \dots, x_k) = \left(\sqrt{1 - \underline{\xi}(x_k)^2} - \sqrt{(|x_k| - \underline{\xi}(x_k))^2 + \left(\sqrt{1 - \underline{\xi}(x_k)^2} - \sqrt{1 - x_k^2} \right)^2} \right)_+ \cdot \frac{(x_1, \dots, x_{k-1})}{\sqrt{1 - x_k^2}}$$

where $(x)_+ = \max(0, x)$. Let

$$f(x_1, \dots, x_k) = \begin{cases} f'(x_1, \dots, x_{k-2}, x_{k-1}, x_k) & \text{if } |x_k| \leq 1/\sqrt{2} \\ f'(x_1, \dots, x_{k-2}, x_k, x_{k-1}) & \text{if } |x_k| > 1/\sqrt{2} \end{cases}. \quad (6.8)$$

The wrapped spherical vector quantizer (SVQ) with respect to a packing Λ having minimum distance d_Λ is defined by

$$\text{WA-SVQ} = f^{-1}(\Lambda). \quad (6.9)$$

The use of WA-SVQ on a digital communication channel is accomplished using the algorithm in Table 6.1.

6.3.2 Shape-gain rate allocation

Let R be the desired total rate of the wrapped SVQ. The shape code rate R_s and gain code rate R_g must satisfy $R_s + R_g \leq R$. The rate R_s of the shape codebook defined in Equation

Table 6.1 Algorithmic description of WA–SVQ on a digital communication channel.

Step 1. Given k source samples, form vector $X \in \mathbb{R}^k$.	}	Encoder
Step 2. Compute $g = \ X\ $ and $S = X/g$.		
Step 3. Use gain codebook to quantize g as \hat{g} .		
Step 4. Compute $f(S)$ using Equation (6.8).		
Step 5. Find nearest neighbor $\hat{f}(S)$ to $f(S)$, using a nearest neighbor algorithm for Λ .		
Step 6. Compute $f^{-1}(\hat{f}(S))$ to identify quantized shape \hat{S} .	}	Channel
Step 7. Compute the index of $\hat{g}\hat{S}$ using Equation (6.11).		
Step 8. Transmit index of $\hat{g}\hat{S}$ across (noiseless) channel.	}	Decoder
Step 9. Identify $\hat{g}\hat{S}$ using Equation (6.11).	}	

(6.9) can be altered by rescaling Λ so that the minimum distance is some value d instead of the prescribed d_Λ . The optimal allocations for R_s and R_g are obtained by analyzing the distortion of the wrapped SVQ under varying allocations and performing a binary search for the optimal value of R_g . Since the gain codebook size is an integer, the values of R_g are restricted to a finite set and the optimal value of R_g can be found exactly.

For a given rate allocation, the gain codebook is optimized using the Lloyd algorithm with R_g bits. Λ is scaled by d/d_Λ before the shape codebook is constructed, where d is determined as follows. The image of an annulus on Ω_k under the mapping $f(\cdot)$ is a region \mathcal{A} bounded by two concentric spheres in \mathbb{R}^{k-1} (see explanation before Lemma 4.2); hence, the number of lattice points in \mathcal{A} is the number of lattice points on the corresponding annulus in Ω_k . As explained in Section 2.3, this number is obtained from the theta function of the lattice Λ .

In principle, specification of the theta function of a lattice allows one to efficiently count the number of codepoints in \mathcal{A} , but in practice the theta function often involves functions which are difficult to compute. This difficulty does not affect the operating complexity of the quantizer, because the optimization of the codebook is performed off-line. Nevertheless, it helps the design efficiency to use an *approximate* count of the codepoints in \mathcal{A} , and then perform an accurate count at the end of the design algorithm. The approximation is computed as follows. According to Theorem 4.1, the density of WA–SVQ is approximately Δ_Λ . Therefore, a $(k-1)$ -dimensional lattice Λ with minimum distance d and density Δ_Λ gives rise to a wrapped spherical code with

M codepoints, and M satisfies

$$M \approx \frac{\Delta_{\Lambda} S_k}{S(c(k, \sin^{-1}(d/2)))},$$

where $S(c(k, \sin^{-1}(d/2)))$ is the surface area of a spherical cap on Ω_k with angular radius $\sin^{-1}(d/2)$. Thus, the scale of Λ is chosen (heuristically) by

$$d = \arg \min_{d'} \left\{ \frac{\Delta_{\Lambda} S_k}{S(c(k, \sin^{-1}(d'/2)))} \leq 2^{kR_s} \right\}, \quad (6.10)$$

which will create a shape codebook that has 2^{kR_s} codepoints, i.e., a rate per sample of R_s bits. After optimization is complete, a one-time count of the actual number of codepoints is computed by evaluating the theta function.

6.3.3 Index assignment

Thus far, it has been assumed that a k -dimensional WA-SVQ with M codepoints and operating at rate R satisfies $M = 2^{kR}$. In order to be implemented in a communication system, the M quantizer codepoints must be uniquely identified by binary strings of length kR which are transmitted across the channel. Since each binary string represents a number between 0 and $M - 1$, an equivalent problem is the assignment of codepoints to unique integers.

The assignment is accomplished in a similar manner as for the pyramid vector quantizer for the Laplacian source [24]. First, the number of codepoints in each annulus of the shape codebook is counted, by the method of the previous section. This can be done with the theta function of Λ . For the WA₂₄-SVQ codes in this thesis, this involved a one-time computation of the first few hundred coefficients of the theta function of the Leech lattice, which were stored and used as needed.

It is assumed that there is an efficient method for assigning indices to the underlying lattice, and in particular, to those points in \mathcal{A} , as defined in Section 6.3.2. This is the case with many lattices, including for example, the Leech lattice Λ_{24} . The points of \mathcal{A} may be ordered using this index. For example, the l th point of \mathcal{A} could be that point that has the l th lowest index.

The codepoints of the wrapped spherical code are assigned to integers according to their quantized gain, annulus, and order within their annulus, as follows. Let N represent the number of annuli of the shape codebook. Let P_j be the number of points in the j th annulus of a shell, and let P be the total number of points in the shape codebook. Assuming all indices start at

0, the l th point within the j th annulus of the i th shell is assigned to the number

$$iP + \sum_{a=0}^{j-1} P_a + l. \quad (6.11)$$

The encoder and decoder each are required to perform the summation. This can be made efficient by storing in memory the partial summations $\sum_{a=0}^{j-1} P_a$, for $j = 0, 1, \dots, N - 1$. The memory required for this is equal to the total number of annuli in the codebook, which is generally not excessively large. For example, in the rate 4 $W\Lambda_{24}$ -SVQ, there are 36 total annuli.

6.4 Operational Complexity

The computational complexity of the operation of $W\Lambda$ -SVQ is analyzed in this section. The arithmetic functions needed are addition, multiplication, division, square root, and comparison. In our analysis, one operation is counted for any arithmetic function. If arithmetic functions take differing times to execute, this count could be decomposed into the number of operations of each type.

Refer now to the steps in Table 6.1. Step 1 requires no computation. Step 2 requires k squaring (multiplication) operations, $k - 1$ additions, and one square root to calculate the gain; k divisions to calculate the shape; and $3k$ operations altogether. Step 3 requires one scalar quantization operation, which can be performed by a binary search with R_g comparisons. Step 4 requires one comparison to determine if x_k is greater than $1/\sqrt{2}$; one multiplication to obtain x_k^2 ; one addition and one square root to determine $\sqrt{1 - x_k^2}$; $\log N \leq R_s$ comparisons in a binary search to identify $\underline{\xi}(x_k)$; one multiplication, one addition, and one square root to determine $\sqrt{1 - \underline{\xi}^2(x_k)}$; four additions, two multiplications, one square root, and one division to complete the computation of the scaling factor; and $k - 1$ multiplications to obtain $f(S)$. Thus, Step 4 requires no more than $k + R_s + 14$ operations. Step 5 requires the number of steps in a nearest neighbor algorithm for Λ . For the Leech lattice, the fastest known algorithm requires about 2955 operations on average [91]. Referring to Lemma 4.1, Step 6 requires one multiplication, one addition, and one square root to determine h_i ; one multiplication, one addition, and one square root to determine $\sqrt{4 - h_i^2}$; $k - 1$ multiplications, $k - 2$ additions, and one square root to determine $\|Y\|$; four multiplications and two additions to determine g_i ; one multiplication,

Table 6.2 Comparison of the operating complexity of $W\Lambda_{24}$ -SVQ to other quantization schemes for a memoryless Gaussian source. Data for other methods are taken from Table XII of [62].

Method	Operating complexity
$W\Lambda_{24}$ -SVQ	$127 + R/25$
TCQ (doubled alphabet)	$3S + 4R + 4$
TCQ (quadrupled alphabet)	$3S + 8R + 8$
GLA	2^{kR+1}
Wilson	$S 2^{R+1}$
Pearlman	$(S + 2)2^R$

k : dimension

R : rate

S : number of trellis states

one addition, and one square root to determine $\sqrt{1 - g_i^2}$; one division to determine $g_i/\|Y\|$; and $k - 1$ multiplications to determine the final result. Thus, Step 6 requires $3k + 13$ operations. Step 7 requires one multiplication and two additions to determine the index. Step 8 requires no computation. Step 9 requires one division to identify \hat{g} and a table lookup to identify \hat{S} . Altogether, this amounts to at most $7k + R + L + 32$ arithmetic operations, where k is the dimension, R is the rate, and L is the computational complexity of the nearest neighbor algorithm of Λ . Thus, per sample, the computational complexity is $7 + (R + L + 32)/k$. For the $W\Lambda_{24}$ -SVQ, the parameters are $k = 25$ and $L = 2955$, and the computational complexity is $127 + R/25$.

Thus, the operating complexity of $W\Lambda$ -SVQ grows linearly with rate, and is comparable to that of trellis-coded quantization (TCQ). As previously mentioned, the generalized Lloyd algorithm and several other methods are “noninstrumentable,” as they have operating complexity which grows exponentially with rate. See Table 6.2.

6.5 Performance Analysis

To design the quantizer, a measure of performance is needed. In particular, a method is needed to decide when one rate allocation is better than another. Finding an analytic expression for the distortion under varying allocations would be difficult; however, the distortion decomposes into gain and shape distortions in much the same way as Sakrison’s spherical vector

quantizer did in Equation (6.6). The gain distortion may be easily evaluated using numerical integration. The shape distortion is estimated using a heuristic technique that is motivated by reasonable assumptions about the mapping used in a wrapped spherical code. The estimate of the total distortion is validated by the simulated calculation of the actual distortion, which agrees closely with the estimate.

To compute the estimate of the distortion, it is first decomposed into shape and gain components. The MSE per dimension of the WA-SVQ is

$$\begin{aligned}
D &= \frac{1}{k} E[\|X - \hat{g}\hat{S}\|^2] \\
&= \frac{1}{k} E[\|X - \hat{g}S + \hat{g}S - \hat{g}\hat{S}\|^2] \\
&= \frac{1}{k} E[\|X - \hat{g}S\|^2] + \frac{2}{k} E[(X - \hat{g}S)^T(\hat{g}S - \hat{g}\hat{S})] + \frac{1}{k} E[\|\hat{g}S - \hat{g}\hat{S}\|^2] \quad (6.12) \\
&\equiv D_g + D_c + D_s, \quad (6.13)
\end{aligned}$$

where D_g , D_c , and D_s denote the first, second, and third terms, respectively. Thus,

$$D_g = \frac{1}{k} E[\|X - \hat{g}S\|^2] = \frac{1}{k} E\left[\left\|\left(1 - \frac{\hat{g}}{g}\right)X\right\|^2\right] = \frac{1}{k} E\left[\left(1 - \frac{\hat{g}}{g}\right)^2 \|X\|^2\right] = \frac{1}{k} E[(g - \hat{g})^2], \quad (6.14)$$

the per-dimension distortion due solely to the gain quantizer. Using repeated expectations and the fact that if $\hat{g}S$ is known, then \hat{g} , S , and \hat{S} are each also known, and it follows that

$$\begin{aligned}
D_c &= \frac{2}{k} E[E[(X - \hat{g}S)^T(\hat{g}S - \hat{g}\hat{S})|\hat{g}S]] \\
&= \frac{2}{k} E[E[(X - \hat{g}S)^T|\hat{g}S](\hat{g}S - \hat{g}\hat{S})] \\
&= \frac{2}{k} E[E[(g - \hat{g})S^T|\hat{g}S](\hat{g}S - \hat{g}\hat{S})] \\
&= \frac{2}{k} E[E[(g - \hat{g})|\hat{g}S]S^T(\hat{g}S - \hat{g}\hat{S})] \\
&= \frac{2}{k} E[E[(g - \hat{g})|\hat{g}]S^T(\hat{g}S - \hat{g}\hat{S})], \text{ by the independence of } g \text{ and } \hat{g} \text{ from } S \\
&= 0,
\end{aligned}$$

where the inner expectation is zero by the centroid condition of the gain quantizer. Thus, the crossterm does not contribute to the distortion. Finally,

$$\begin{aligned}
D_s &= \frac{1}{k} E[\|\hat{g}S - \hat{g}\hat{S}\|^2] \\
&= \frac{1}{k} E[\hat{g}^2 \|S - \hat{S}\|^2] \\
&= \frac{1}{k} \sum_{i=1}^{2^{R_g}} g_i^2 E[\|S - \hat{S}\|^2 | \hat{g} = g_i] \Pr[\hat{g} = g_i] \tag{6.15}
\end{aligned}$$

$$\begin{aligned}
&= \frac{1}{k} E[\hat{g}^2] E[\|S - \hat{S}\|^2], \text{ by the independence of } S \text{ and } \hat{S} \text{ from } g \\
&= \frac{1}{k} (E[g^2] - E[(g - \hat{g})^2]) E[\|S - \hat{S}\|^2], \text{ from the centroid condition of } \hat{g} \\
&\approx \frac{1}{k} E[g^2] E[\|S - \hat{S}\|^2], \tag{6.16}
\end{aligned}$$

where the final approximation follows from the fact that, by design, $E[(g - \hat{g})^2] \ll E[g^2]$. Hence, D_s may be accurately referred to as the shape distortion (multiplied by a constant).

In summary, the distortion of WA-SVQ is

$$\begin{aligned}
D &= D_g + D_s \\
&= \frac{1}{k} E[(g - \hat{g})^2] + \frac{1}{k} E[\hat{g}^2] E[\|S - \hat{S}\|^2] \\
&\approx \frac{1}{k} E[(g - \hat{g})^2] + \frac{1}{k} E[g^2] E[\|S - \hat{S}\|^2]. \tag{6.17}
\end{aligned}$$

Thus, the distortion of WA-SVQ may be partitioned into shape and gain components, just as Sakrison did for his quantizer [77]. This property holds despite the fact that the new quantizer presented here consists of multiple, structured, and concentric shape codebooks with various norms instead of one unstructured shape codebook of a fixed norm. This convenient decomposition of D into D_s and D_g allows us to optimize WA-SVQ by separately optimizing the shape and gain components.

Estimation of D_s

An analytical expression for D_s is difficult to obtain. Instead, an estimate for D_s is made; this estimate is used in the design algorithm and is validated by the observed shape distortion in the simulations of WA-SVQ.

Given $X = (x_1, \dots, x_k) \in \Omega_k$ and $x_k > 0$, let $\theta_X = \sin^{-1} \sqrt{1 - x_k^2}$ denote the latitudinal angle of X . Let X and Y be arbitrary points within the i th annulus and at some fixed distance $\|X - Y\| = \delta$. As in Chapter 4, let $X' = (x_1, \dots, x_{k-1})$ and let $Y' = (y_1, \dots, y_{k-1})$. If X

and Y have maximally differing latitudes given the constraints above, i.e., $|x_k - y_k|$ is as large as possible given that $\|X - Y\| = \delta$, then the distortion $\frac{\|X - Y\|}{\|f(X) - f(Y)\|}$ is less than the ratio of the arc length to the chord length shown in Figure 4.2. On the other hand, if X and Y have identical latitudes, i.e., $x_k = y_k$, then f scales the first $k - 1$ coordinates of X and Y by the same amount, and $\angle X'OY' = \angle f(X)0f(Y)$. Denote this common angle by ϕ . Note that the distances between X and Y and between $f(X)$ and $f(Y)$ now can be computed on a circle. It follows that

$$\begin{aligned}
\frac{\|X - Y\|}{\|f(X) - f(Y)\|} &= \frac{2\|X'\| \sin(\phi/2)}{2\|f(X)\| \sin(\phi/2)} \\
&= \frac{\|X'\|}{\|f(X)\|} \\
&= \frac{\cos \theta_X}{\cos(i\alpha) - 2 \sin(\frac{\theta_X - i\alpha}{2})}, \\
&\equiv h(\theta_X)
\end{aligned} \tag{6.18}$$

where Figure 4.2 has been used as a guide in obtaining (6.18). Under the assumption that $\frac{\|X - Y\|}{\|f(X) - f(Y)\|}$ is maximized when $x_k = y_k$, for all X and Y of the i th annulus, it follows that

$$\frac{\|X - Y\|}{\|f(X) - f(Y)\|} \leq h(\theta_X).$$

Although this assumption is not rigorously justified, it is intuitively appealing and leads to good quantizer performance. Thus,

$$\begin{aligned}
E[\|S - \hat{S}\|^2] &\leq E[h^2(\theta_S) \cdot \|f(S) - f(\hat{S})\|^2] \\
&= E[h^2(\theta_S)]E[\|f(S) - f(\hat{S})\|^2]
\end{aligned} \tag{6.19}$$

$$= E[h^2(\theta_S)](k - 1) \cdot G(\Pi) \cdot V(\Pi)^{\frac{2}{k-1}} \cdot (d/d_\Lambda)^2, \tag{6.20}$$

where (6.19) and (6.20) are accurate in high resolution (see Section 2.2.4). The first factor of (6.20) is the expected shape distortion due solely to the mapping $f(\cdot)$, while the second is the distortion due to the lattice being used. When the random point P is uniformly distributed on the part of Ω_k between latitudinal angles 0 and $\pi/4$, the pdf of the latitudinal angle θ_P is given

Table 6.3 Optimization algorithm for construction of WA-SVQ at rate R .

Step 1. Set $R_g = 0$ and $R_s = R$.
Step 2. Use Equation (6.10) to estimate minimum distance of underlying lattice Λ .
Step 3. Use the Lloyd algorithm to optimize gain scalar quantizer of size 2^{R_g} for pdf $f_g(r)$.
Step 4. Estimate distortion of WA-SVQ using Equations (6.14) and (6.21).
Step 5. Set $R_g = R$ and $R_s = 0$, and repeat steps 2-4 to compute a new distortion.
Step 6. Using a binary search, find the allocation of R_g and R_s which minimizes the distortion. For each allocation, use Steps 2-4 to compute the distortion.
Step 7. Compute R_s exactly using theta function of Λ .

by $S_{k-1} \cos^{k-2} \theta_S / (\int_0^{\pi/4} S_{k-1} \cos^{k-2} \theta' d\theta')$. Hence,

$$\begin{aligned} E[h^2(\theta_S)] &= \int_0^{\pi/2} h^2(\theta) \cdot \frac{\cos^{k-2} \theta}{\int_0^{\pi/4} \cos^{k-2} \theta' d\theta'} d\theta \\ &= \sum_{i=1}^N \int_{(i-1)\alpha}^{i\alpha} \left(\frac{\cos \theta}{\cos[(i-1)\alpha] - 2 \sin[(\theta - (i-1)\alpha]/2]} \right)^2 \frac{\cos^{k-2} \theta}{\int_0^{\pi/4} \cos^{k-2} \theta' d\theta'} d\theta \\ &= \int_0^\alpha \sum_{i=1}^N \left(\frac{\cos(\theta + (i-1)\alpha)}{\cos[(i-1)\alpha] - 2 \sin(\theta/2)} \right)^2 \frac{\cos^{k-2} \theta}{\int_0^{\pi/4} \cos^{k-2} \theta' d\theta'} d\theta \end{aligned}$$

which is easily calculated given d , since d uniquely determines N and α . Substituting into Equation (6.16),

$$D_s \leq \frac{k-1}{k} E[g^2] \cdot G(\Pi) \cdot V(\Pi)^{\frac{2}{k-1}} \cdot (d/d_\Lambda)^2 \int_0^\alpha \sum_{i=1}^N \left(\frac{\cos(\theta + (i-1)\alpha)}{\cos[(i-1)\alpha] - 2 \sin(\theta/2)} \right)^2 \frac{\cos^{k-2} \theta}{\int_0^{\pi/4} \cos^{k-2} \theta' d\theta'} d\theta. \quad (6.21)$$

Thus, the total distortion $D = D_g + D_s$ may be estimated using Equations (6.14) and (6.21).

This is used in the design algorithm in Table 6.3.

6.6 Simulations and Comparisons

6.6.1 Average distortion computation

The WA₂₄-SVQ was optimized according to the steps in Table 6.3. Its performance was evaluated with computer-generated i.i.d. Gaussian random samples. The random samples were encoded as described in Table 6.1; Step 5 was performed by an implementation of the Leech

lattice nearest neighbor algorithm in [6]. The average distortion was computed for 500,000 Gaussian samples, i.e., 20,000 25-dimensional vectors.

6.6.2 Confidence intervals of the simulations

Note that the codebook sizes for 25-dimensional VQ are extremely large: a codebook with a rate of R bits per sample has 2^{25R} points. For a codebook of rate one, the 500,000 random Gaussian samples amount to only one sample vector for every 1,677 codebook points. Thus, it is very important to detail why the simulations give meaningful results despite the fact that such a simulation cannot possibly test every Voronoi region of every codepoint.

The quality of the simulation results is expressed in terms of a 95% confidence interval. Let \tilde{D} be the true average distortion of the codebook, and let \bar{D} be the sample average distortion found by simulation. It is desired to find the value of δ such that $\Pr[|\bar{D} - \tilde{D}| < \delta] = 0.95$.

The simulation run of 20,000 vectors was broken down into 20 blocks that each contain 1,000 vectors. For the i th block, the average sample distortion D_i was determined. Since D_i is an average of 1,000 i.i.d. random variables, the central limit theorem may be applied to conclude that D_i has an approximately Gaussian distribution. The overall sample distortion was computed by $\bar{D} = \frac{1}{20} \sum_{i=1}^{20} D_i$, and the sample variance of the block averages was computed by $s^2 = \frac{1}{20} \sum_{i=1}^{20} (D_i - \bar{D})^2$.

The random variable

$$T = \frac{\sqrt{n}(\bar{D} - \tilde{D})}{s}$$

is distributed according to the student's t -distribution

$$F_n(t) = \frac{1}{\sqrt{n}\beta(\frac{n}{2}, \frac{1}{2})} \left(\frac{n}{n+t^2} \right)^{\frac{n+1}{2}},$$

where $n = 19$ is one less than the number of block samples [50]. Thus, the solution with respect to t of

$$0.95 = \int_{-t}^t F_{19}(t) dt$$

gives the value of t for which $\Pr[|\bar{D} - \tilde{D}| < \frac{st}{\sqrt{19}}] = 0.95$. From mathematical tables, it is found that $t \approx 2.093$, so that the 95% confidence interval is given by $\delta = \frac{2.093s}{\sqrt{19}}$. This may be converted to a confidence interval of the SQNR expressed in decibels by writing

$$\Pr[\bar{D} - \delta \leq \tilde{D} \leq \bar{D} + \delta] = 0.95,$$

which implies

$$\Pr \left[10 \log_{10} \left(\frac{\bar{D}}{\bar{D} + \delta} \right) \leq 10 \log_{10} \left(\frac{\bar{D}}{\bar{D}} \right) \leq 10 \log_{10} \left(\frac{\bar{D}}{\bar{D} - \delta} \right) \right] = 0.95.$$

Thus, with 95% confidence the absolute difference in decibels between the true and sample SQNR, i.e., $10 \log_{10} \left(\frac{\bar{D}}{\bar{D}} \right)$, is not more than $10 \log_{10} \left(\frac{\bar{D}}{\bar{D} - \delta} \right)$.

In all simulation results, $10 \log_{10} \left(\frac{\bar{D}}{\bar{D} - \delta} \right)$ was calculated and found to be less than 0.03 dB. Thus, with 95sample SQNR, which provides sufficient justification that the average distortions computed by the simulations accurately reflect the true performance of the codebook.

6.6.3 Comparisons

WA-SVQ was designed to have good performance for asymptotically large rates. This good performance for high rates holds for surprisingly small rates as well. As indicated in Figure 6.2 and Table 6.4, $W\Lambda_{24}$ -SVQ performs within one dB of the distortion-rate function for rates in the range of two to seven. For this range, it performs better than some of the best quantizers in the literature, including 256-state trellis coded quantization (TCQ) [62], two-dimensional four-state trellis coded vector quantization (TCVQ) [93], Fischer's spherical vector quantization [24], and Lloyd-Max scalar quantization. With an increasing number of trellis states, TCQ and TCVQ perhaps would outperform WA-SVQ; however, the reports of results in the literature have thus far been limited to trellises with 256 or fewer states because the design complexity of TCQ and TCVQ is somewhat prohibitive for larger trellises. Trellis-based scalar-vector quantization [53] performs slightly better than $W\Lambda_{24}$ -SVQ at a rate of two, but is outperformed at rates three and higher.

The SQNR gap between $W\Lambda_{24}$ -SVQ and the rate-distortion function is roughly constant for all rates. This property is shared neither by Lloyd-Max quantization, nor by trellis quantizers (either scalar or vector) having a fixed number of states. The performance reported by Fischer [24] for a spherical vector quantizer formed from lattice shells is constant but lower than for $W\Lambda_{24}$ -SVQ; furthermore, it is an estimate only and depends on the assumption that points from high-dimensional lattice shells are approximately uniformly distributed on the sphere. This assumption requires justification in view of the fact that shells of lattices appear to be mostly clustered and sparsely located about the surface of the sphere (see Figures 2.9 and 2.10).

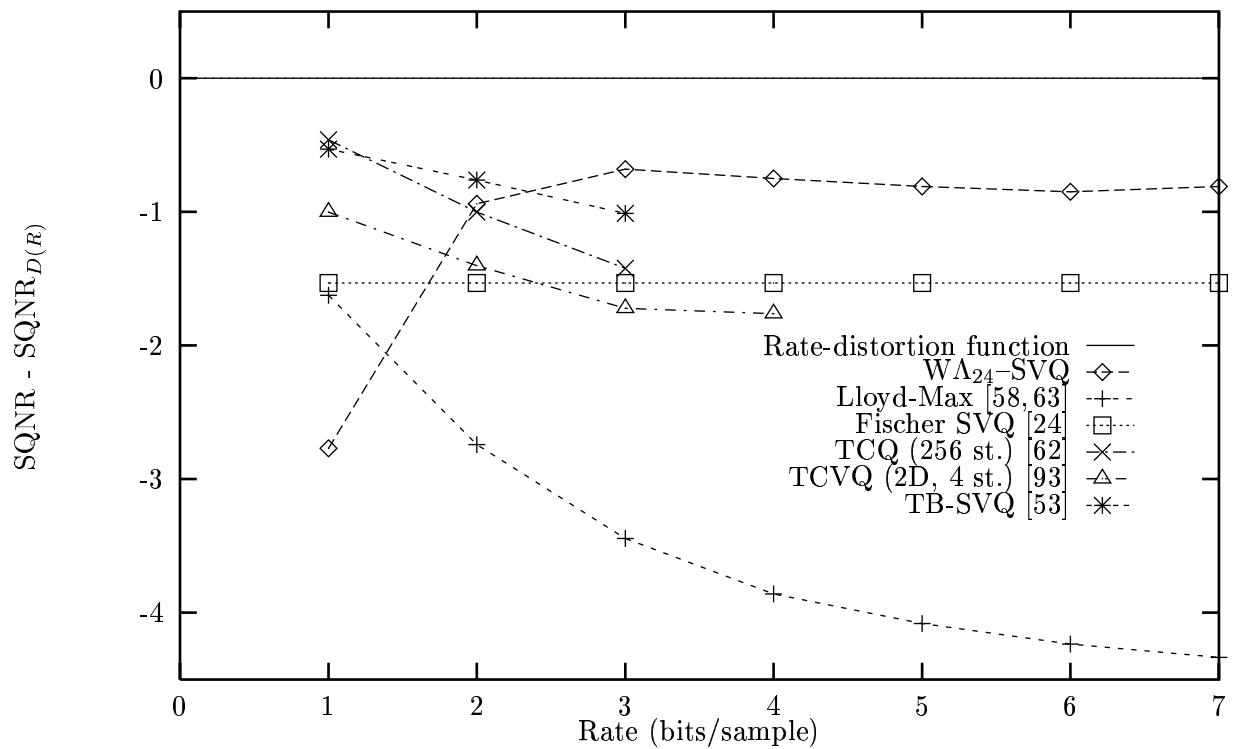


Figure 6.2 Comparison of VQs for the memoryless Gaussian source. The number of decibels below the SQNR of the rate-distortion function is plotted as a function of rate, for various quantization schemes.

Table 6.4 Comparison of various quantization schemes for a memoryless Gaussian source. Values are listed as SQNR in decibels.

Method	Rate:	1	2	3	4	5	6	7
D(R)		6.02	12.04	18.06	24.08	30.10	36.12	42.14
WL ₂₄ -SVQ(acc,ind,sim)		2.44	11.02	17.36	23.33	29.29	35.27	41.33
GLA (kR=8)			10.65		20.98			
Lloyd-Max Scalar		4.40	9.30	14.62	20.22	26.02	31.89	37.81
Uniform scalar		4.40	9.25	14.27	19.38	24.57	29.83	35.13
Ent. coded scalar		4.64	10.55	16.56	22.55	28.57	34.59	40.61
UPQ		4.40	9.63					
Fischer SVQ (estimated)		4.49	10.51	16.53	22.55	28.57	34.59	40.61
TCQ (256 state)		5.56	11.04	16.64				
Wilson (128 state)		5.47	10.87	16.78				
TB-SVQ (4 state)		5.14	11.11	16.77				
TB-SVQ (64 dim.,16 state)		5.49	11.28	17.05				

6.7 Improvements and Extensions of the Basic Construction

6.7.1 Vector quantization of the gain

Thus far, the shape-gain approach has used a scalar quantizer for the gain and a wrapped spherical code as a vector quantizer for the shape. Improvement in the distortion can be made by blocking together the gains of L consecutive k -dimensional vectors. Using this method, the shape codebook is used L times for the L vectors, and a single L -dimensional VQ is used for the block of gains.

To evaluate the performance of this scheme, let $Y = (X^{(1)}, \dots, X^{(L)})$, where for each i , $X^{(i)} = (X_1^{(i)}, \dots, X_k^{(i)})$, and where $X_j^{(i)}$ is drawn from a memoryless Gaussian source, for all i, j . As before, each k -dimensional vector is decomposed into its gain and shape by letting $g^{(i)} = \|X^{(i)}\|$ and $S^{(i)} = X^{(i)}/g^{(i)}$. Let

$$\hat{Y} = (\hat{g}^{(1)}\hat{S}^{(1)}, \dots, \hat{g}^{(L)}\hat{S}^{(L)})$$

be the quantized value of Y , where for all i , $\hat{S}^{(i)}$ is the quantized value of $S^{(i)}$ using the shape codebook as before, and where $\hat{G} = (\hat{g}^{(1)}, \dots, \hat{g}^{(L)})$ is the quantized value of the vector $(g^{(1)}, \dots, g^{(L)})$. \hat{G} is the output of an L -dimensional VQ optimized by the generalized Lloyd algorithm. In particular, the VQ satisfies the centroid condition. The MSE distortion per dimension is

$$\begin{aligned}
D &= \frac{1}{kL} E[\|Y - \hat{Y}\|^2] \\
&= \frac{1}{kL} E \left[\sum_{i=1}^L \|X^{(i)} - \hat{g}^{(i)} \hat{S}^{(i)}\|^2 \right] \\
&= \frac{1}{kL} E \left[\sum_{i=1}^L \|X^{(i)} - \hat{g}^{(i)} S^{(i)} + \hat{g}^{(i)} S^{(i)} - \hat{g}^{(i)} \hat{S}^{(i)}\|^2 \right] \\
&= \frac{1}{kL} \sum_{i=1}^L E[\|X^{(i)} - \hat{g}^{(i)} S^{(i)}\|^2] + 2E[(X^{(i)} - \hat{g}^{(i)} S^{(i)})^T (\hat{g}^{(i)} S^{(i)} - \hat{g}^{(i)} \hat{S}^{(i)})] \\
&\quad + E[\|\hat{g}^{(i)} S^{(i)} - \hat{g}^{(i)} \hat{S}^{(i)}\|^2] \\
&\equiv \frac{1}{L} \sum_{i=1}^L D_g^{(i)} + D_c^{(i)} + D_s^{(i)}.
\end{aligned}$$

Following the same analysis as in Equations (6.14)-(6.16),

$$\begin{aligned}
D_g^{(i)} &= \frac{1}{k} E[(g^{(i)} - \hat{g}^{(i)})^2] \\
D_c^{(i)} &= 0 \\
D_s^{(i)} &= \frac{1}{k} E[(\hat{g}^{(i)})^2] E[\|S^{(i)} - \hat{S}^{(i)}\|^2].
\end{aligned}$$

Thus,

$$\begin{aligned}
D &= \frac{1}{L} \sum_{i=1}^L \left(\frac{1}{k} E[(g^{(i)} - \hat{g}^{(i)})^2] + \frac{1}{k} E[(\hat{g}^{(i)})^2] E[\|S^{(i)} - \hat{S}^{(i)}\|^2] \right) \\
&= \frac{1}{kL} E[\|G - \hat{G}\|^2] + \frac{1}{kL} \sum_{i=1}^L E[(\hat{g}^{(i)})^2] E[\|S^{(i)} - \hat{S}^{(i)}\|^2] \\
&= \frac{1}{k} E[\|G - \hat{G}\|^2] + \frac{1}{kL} E[\|S^{(1)} - \hat{S}^{(1)}\|^2] \sum_{i=1}^L E[(\hat{g}^{(i)})^2] \\
&= \frac{1}{k} E[\|G - \hat{G}\|^2] + \frac{1}{kL} E[\|\hat{G}\|^2] E[\|S^{(1)} - \hat{S}^{(1)}\|^2], \\
&= \frac{1}{k} E[\|G - \hat{G}\|^2] + \frac{1}{kL} (E[\|G\|^2] - E[\|G - \hat{G}\|^2]) E[\|S^{(1)} - \hat{S}^{(1)}\|^2], \text{ by centroid condition} \\
&\approx \frac{1}{k} E[\|G - \hat{G}\|^2] + \frac{1}{kL} E[\|G\|^2] E[\|S^{(1)} - \hat{S}^{(1)}\|^2] \tag{6.22}
\end{aligned}$$

which is the same as Equation (6.17) except that the scalar quantizer output \hat{g} has been replaced by the VQ output \hat{G} . For all $i \neq j$, g_i is independent of g_j , and thus the pdf of G is given by $f_G(r_1, \dots, r_L) = \prod_{i=1}^L f_g(r_i)$. The design algorithm in Table 6.3 remains the same, except that Steps 3 and 4 are replaced by:

Step 3'. Use the generalized Lloyd algorithm to optimize gain VQ of size 2^{LR_g} for pdf f_G .

Step 4'. Estimate distortion using Equation (6.22)

6.7.2 Allowing the shape codebook to depend on the gain

The codebook of the shape-gain quantizer may be viewed as a set of concentric shells on which all codepoints lie. Each shell in this set has exactly the same number of codepoints on it, and is a scaling of every other shell. Consequently, larger shells have more space between codepoints compared to smaller shells. Also, the pdf of X is not equal among all shells. This leads us to believe that performance may be improved by allowing shells to have a differing number of codepoints. This implies having a different shape codebook corresponding to each output \hat{g} of the gain quantizer, and that the shape quantizer depends on \hat{g} and S , instead of just S . The different shape codebook sizes are obtained by scaling the underlying lattice a different amount.

Nothing in the analysis of $D = D_g + D_s$ from Equations (6.12) to (6.15) assumed that the shape codebooks were all the same. In particular, Equation (6.15) still holds. Let M_i denote the number of codepoints on the i th shell, and define its partial distortion by

$$D_i[M_i] = \frac{1}{k} g_i^2 E \left[\|S - \hat{S}\|^2 | \hat{g} = g_i \right] \cdot \Pr[\hat{g} = g_i], \quad (6.23)$$

so that $D_s = \sum_i D_i[M_i]$. If the gain codebook is of sufficiently high resolution, then the partial distortion theorem [31] implies that the optimal allocation of M_1, \dots, M_N is such that

$$D_1[M_1] = D_2[M_2] = \dots = D_N[M_N],$$

as $N \rightarrow \infty$. Usually, however, the gain codebook is too small to justify use of the theorem.

An alternate optimization method for M_i is as follows. For a fixed gain codebook, the partial distortion $D_i[M_i]$ is a monotonically nonincreasing function of a discrete argument, it can be extended to a continuous and piecewise linear function which is also monotonically

nonincreasing. For ease of notation, let us also refer to this function as $D_i[M_i]$, with the understanding that M_i is now real-valued. Left- and right-hand derivatives exist for all $M_i > 0$; let $\frac{\partial^- D_i}{\partial M_i}$ and $\frac{\partial^+ D_i}{\partial M_i}$ denote these derivatives, respectively. Then a necessary condition for the optimality of M_1, \dots, M_N is

$$\text{for all } i \neq j, \frac{\partial^+ D_i}{\partial M_i} \geq \frac{\partial^- D_j}{\partial M_j}.$$

That is, removing a point from shell j and adding a point to i cannot lower the distortion.

For moderate rates, the left- and right-hand derivatives of each partial distortion are approximately equal. For example, if $R = 3$ in $\text{WL}_{24}\text{-SVQ}$, then $M = 2^{3 \cdot 25} = 3.78 \times 10^{22}$, the gain codebook is size 7, and so $M_i \gg 1$ for all i . Therefore, for each i

$$\frac{\partial^- D_i}{\partial M_i} \approx \frac{\partial^+ D_i}{\partial M_i} \tag{6.24}$$

and the ‘+’ and ‘-’ may be dropped from the notation. A necessary condition for optimality of M_1, \dots, M_N is

$$\frac{\partial D_i}{\partial M_i} = \frac{\partial D_j}{\partial M_j}, \tag{6.25}$$

for all i and j .

Using this condition, M_1, \dots, M_N may be optimized, i.e., M_1, \dots, M_N are chosen to minimize $\sum_i D_i[M_i]$ subject to the constraint that $\sum_i M_i = 2^{R_s}$. The optimization is begun with an initial assignment of $M_1 = \dots = M_N$. Then, $\frac{\partial D_i}{\partial M_i}$ is computed for each i . Let i and j be the indices of the maximum and minimum partial derivatives, respectively. M_i is reduced and M_j is increased by equal amounts, and the partial derivatives are recalculated. This is repeated until the condition in (6.25) holds. The number of points moved at each iteration does not have to be constant. Faster convergence to the optimal allocation would occur if a larger number were moved during early iterations, and a gradual reduction is made throughout the algorithm. The algorithm is summarized in Table 6.5.

The operating complexity of the quantizer is not affected very much by having gain-dependent shape quantizers. The encoder and decoder need only store the minimum distance of each shape code, which increases the storage complexity by a factor of two (only the gain codebook previously was stored). Using these stored minimum distances, decoding complexity remains the same as before.

Table 6.5 Iterative algorithm to allocate number of points per shell.

Step 1. Set $M_1 = \dots = M_N = \frac{2^{R_s}}{N}$.
Step 2. Adjust design parameter m .
Step 3. For each i , compute an estimate of $\frac{\partial D_i}{\partial M_i}$ by calculating $D_i[M_i]$ and $D[M_i + m]$ using Equation (6.23).
Step 4. Let $i = \arg \max_l \frac{\partial D_l[M_l]}{\partial M_l}$ and $j = \arg \min_l \frac{\partial D_l[M_l]}{\partial M_l}$.
Step 5. Set $M_i := M_i - m$ and $M_j := M_j + m$.
Step 6. Go to Step 2.

If each shell has a differing number of points and/or shells, the index assignment must also be modified. Let $\text{Ann}(i)$ be the number of annuli in the i th shell, and let $M(i, j)$ be the number of codepoints on the j th annulus of the i th shell. The codepoints of the first annulus of the first shell are assigned to the integers $(0, \dots, M(1, 1) - 1)$, the codepoints of the second annulus of the first shell are assigned to the integers $(M(1, 1), \dots, M(1, 1) + M(1, 2) - 1)$, and in general, the l th point within the j th annulus of the i th shell is assigned to the integer

$$\left(\sum_{a=1}^{i-1} \sum_{b=1}^{\text{Ann}(a)} M(a, b) \right) + \left(\sum_{b=1}^{j-1} M(i, b) \right) + l.$$

6.7.3 Allowing the gain codebook to depend on the shape

The shape-gain quantizers can be improved by allowing \hat{g} to depend not only on g , but on S as well [31]. This is accomplished by first encoding S and then choosing \hat{g} to minimize $\|X - \hat{g}\hat{S}\|$, instead of $\|g - \hat{g}\|$. Using this approach makes the optimization problem much more difficult, since the two quantizers are now coupled. In particular, the gain codebook cannot be designed based solely on the pdf of g . The analysis of the distortion also becomes more involved, as the distortion does not separate neatly into shape and gain components, because $D_c \neq 0$. In any case, using a training sequence to design g , and simulating the performance of the dependent shape-gain wrapped spherical vector quantizer, it was found that this more general approach results in improvements of 0.02 dB or less for rates above 3. For this reason and because the analysis and implementation of the quantizer is less complex if the two quantizers operate independently, it was assumed in the rest of the chapter that \hat{g} depends only on g .



Figure 6.3 A universal quantizer.

6.7.4 Non-Gaussian sources

Inherent in the treatment thus far is that the source has a Gaussian distribution, for if the source is not Gaussian then the high probability region is not a sphere, but some other shape [60], and the wrapped SVQ cannot be effectively used. This section presents a method to obtain the performance above for any source. The method consists of transform coding the source. Typically, transform coding is done to remove dependencies between consecutive samples of the source; here, it is used to change the distribution of the source, which may or may not already be i.i.d., to be roughly Gaussian and i.i.d., so that wrapped SVQ may still be used. This same intuition was used in [73] to quantize an arbitrary source and obtain distortion performance that approximates that of a scalar quantizer for a Gaussian source. Unlike the approach in [73], in this section the source is transformed in blocks, instead of using FIR filters.

Let $Q(\cdot)$ be the output of any k -dimensional vector quantizer. Let

$$X \equiv \begin{pmatrix} X_1 & X_{m+1} & & X_{(k-1)m+1} \\ \vdots & \vdots & \dots & \vdots \\ X_m & X_{2m} & & X_{km} \end{pmatrix}.$$

Let \mathcal{H}_m be a Hadamard matrix of order m , i.e., an $m \times m$ matrix with $+1$ and -1 entries only such that $\mathcal{H}_m^T \mathcal{H}_m = mI$. Such matrices are known to exist when the order is any power of 2, and for many other orders as well.¹ Let $H_m \equiv (1/\sqrt{m})\mathcal{H}_m$. Given X , the vector quantizer output is: $H_m^T Q(H_m X)$. This is illustrated in Figure 6.3. If $Y \equiv H_m X$, $\hat{Y} \equiv Q(Y)$, and $e \equiv \hat{Y} - Y$,

¹Hadamard matrices are known to exist for orders equal to every multiple of 4 up to 268. It is an open question as to whether they exist for orders equal to all multiples of 4. It is known that if m is a multiple of 4 and $m = p + 1$ for some prime p , then a Hadamard matrix of order m exists.

then it follows that

$$\begin{aligned}
\hat{X} &= H_m^T \hat{Y} \\
&= H_m^T (Y + e) \\
&= H_m^T (H_m X + e) \\
&= H_m^T H_m X + H_m^T e \\
&= X + H_m^T e.
\end{aligned}$$

The end-to-end distortion of this system is

$$\begin{aligned}
E[\|\hat{X} - X\|^2] &= E[(\hat{X} - X)^T (\hat{X} - X)] \\
&= E[(H_m^T e)^T (H_m^T e)] \\
&= E[e^T H_m H_m^T e] \\
&= E[e^T e] \\
&= E[(\hat{Y} - Y)^T (\hat{Y} - Y)] \\
&= E[\|\hat{Y} - Y\|^2]
\end{aligned}$$

Thus, the end-to-end distortion of the system is equal to the distortion due to the quantization of the intermediary signal Y alone. Most importantly, the Hadamard transform modifies the distribution of the input to the vector quantizer. A row Y_i of Y is an k -vector, each component of which is the sum of m different samples (or their negation) from $\{X_i\}$; hence, as $m \rightarrow \infty$ the probability distribution of each component of Y_i approaches the Gaussian distribution, by the central limit theorem. Thus, the internal k -dimensional quantizer Q may be optimized with respect to the Gaussian distribution, even if k is fixed and small.

6.8 Conclusions

The wrapped spherical vector quantizer for the memoryless Gaussian source achieves excellent distortion performance, in some cases better than any other published results. The operating complexity of the quantizer grows linearly with the rate, and for moderate rates is dominated by the complexity of the nearest neighbor algorithm of the underlying lattice. This complexity is comparable or slightly less than other efficient quantization techniques such

as pyramid vector quantization of the Laplacian source [24], trellis coded quantization [62], and trellis coded vector quantization [93]. Thus, the wrapped spherical vector quantizer is instrumentable, unlike full-search quantization techniques which have exponential operational complexity.

The codepoints of the wrapped spherical vector quantizer lie in the high probability region of the source in a pattern that, locally, is only a small distortion of the underlying lattice. It is worth remarking that packings other than lattices may be used to create the shape codebook. In this case, more than one type of Voronoi cell results, and an average over all the different Voronoi cells is necessary to compute the MSE of the scaled packing as in (2.2).

This work might be extendible to trellis coded quantization of wrapped spherical codes. A trellis coded quantizer based on a lattice is designed using a partition of the lattice into subsets, where each subset has a larger minimum distance than the lattice itself. This same partition may be used in the wrapped spherical vector quantizer, and the trellis may operate in the same manner as it would for the underlying lattice.

CHAPTER 7

CONCLUSIONS

The characteristics of asymptotically optimal codes with respect to minimum distance, quantization coefficient, and covering thickness have been related to the corresponding parameter for sphere packings in one lower dimension. The wrapped spherical codes presented in this thesis are asymptotically optimal with respect to minimum distance; the laminated spherical codes are asymptotically optimal whenever the laminated lattice of the previous dimension is the densest sphere packing in that dimension. This represents the first work that has produced asymptotically optimal spherical codes. An extensive review of other methods of constructing spherical codes has been given in Chapter 3. Some of these techniques produce the best known spherical codes for particular minimum distances, but it was shown that none of them is asymptotically optimal for small minimum distances.

In addition to being asymptotically optimal, the spherical codes presented in the thesis are also the best known codes for a large range of moderate minimum distances. The codes are also highly structured. This structure allows extremely large codes to be used in communication applications with very modest implementation complexity. In particular, it was shown that the wrapped spherical code may be used as a vector quantizer for the memoryless Gaussian source. Despite the fact that the spherical code is optimal only in an asymptotic sense, the wrapped spherical vector quantizer outperforms other quantizers found in the literature for rates as low as $R = 2$ bits per sample. For example, its performance compares favorably with Lloyd-Max scalar quantization, 256-state trellis coded quantization, and many other schemes. This is accomplished by using a 25-dimensional spherical code with 2^{25R} points, which is an extremely large number even for moderate R .

The wrapped spherical vector quantizer opens up a number of new questions. Just as a memoryless Gaussian source naturally gives rise to a high-probability region near the surface of a sphere, other sources have high-probability regions with other geometries. For example, the high-probability region of a Gaussian source with memory is a hyperellipse, and the high-probability region of a Laplacian source is a hyperpyramid. The mapping used for wrapped spherical codes may be altered to match these or other geometries.

Since the wrapped spherical code has many of its properties in common with its underlying lattice, many quantization techniques for a memoryless uniform source may be converted to quantization techniques for a memoryless Gaussian source. This is based on the principle that the wrapped spherical codes map \mathbb{R}^{k-1} to Ω_k with little distortion and the fact that a vectorized memoryless Gaussian source is spherically symmetric and heavily concentrated near the surface of a sphere. As an example, consider a trellis-coded quantizer for the uniform source based on the \mathbb{Z}^2 lattice. It is formed by a partition of \mathbb{Z}^2 into subsets in which each has a larger minimum distance than \mathbb{Z}^2 ; the partition gives rise to a trellis whose paths correspond to sequences of subsets. This may be converted to a trellis-coded wrapped spherical vector quantizer as follows. First, $\text{W}\mathbb{Z}^2\text{-SVQ}$ is constructed using the definition of the wrapped spherical code. The codepoints are then partitioned according to the partition of \mathbb{Z}^2 . The trellis for $\text{W}\mathbb{Z}^2\text{-SVQ}$ may choose a sequence of subsets in the identical manner as the original trellis-coded quantizer.

APPENDIX A

GENERATOR MATRICES OF LATTICES

$$M_{\mathbb{Z}^k} = \begin{bmatrix} 1 & 0 & 0 & \cdots & 0 \\ 0 & 1 & 0 & \cdots & 0 \\ 0 & 0 & 1 & \cdots & 0 \\ \vdots & \vdots & \vdots & \ddots & \vdots \\ 0 & 0 & 0 & \cdots & 1 \end{bmatrix}$$

$$M_{A_k} = \begin{bmatrix} -1 & 1 & 0 & 0 & \cdots & 0 & 0 \\ 0 & -1 & 1 & 0 & \cdots & 0 & 0 \\ 0 & 0 & -1 & 1 & \cdots & 0 & 0 \\ \vdots & \vdots & \vdots & \vdots & \ddots & \vdots & \vdots \\ 0 & 0 & 0 & 0 & \cdots & -1 & 1 \end{bmatrix}$$

$$M_{A_k^*} = \begin{bmatrix} 1 & -1 & 0 & 0 & \cdots & 0 & 0 \\ 1 & 0 & -1 & 0 & \cdots & 0 & 0 \\ 1 & 0 & 0 & -1 & \cdots & 0 & 0 \\ \vdots & \vdots & \vdots & \vdots & \ddots & \vdots & \vdots \\ 1 & 0 & 0 & 0 & \cdots & -1 & 0 \\ \frac{-k}{k+1} & \frac{1}{k+1} & \frac{1}{k+1} & \frac{1}{k+1} & \cdots & \frac{1}{k+1} & \frac{1}{k+1} \end{bmatrix}$$

$$M_{D_k} = \begin{bmatrix} -1 & -1 & 0 & \cdots & 0 & 0 \\ 1 & -1 & 0 & \cdots & 0 & 0 \\ 0 & 1 & -1 & \cdots & 0 & 0 \\ \vdots & \vdots & \vdots & \ddots & \vdots & \vdots \\ 0 & 0 & 0 & \cdots & 1 & -1 \end{bmatrix}$$

$$M_{D_k^*} = \begin{bmatrix} 1 & 0 & \cdots & 0 & 0 \\ 0 & 1 & \cdots & 0 & 0 \\ \vdots & \vdots & \ddots & \vdots & \vdots \\ 0 & 0 & \cdots & 1 & 0 \\ 1/2 & 1/2 & \cdots & 1/2 & 1/2 \end{bmatrix}$$

$$M_{E_8} = \begin{bmatrix} 2 & 0 & 0 & 0 & 0 & 0 & 0 & 0 \\ -1 & 1 & 0 & 0 & 0 & 0 & 0 & 0 \\ 0 & -1 & 1 & 0 & 0 & 0 & 0 & 0 \\ 0 & 0 & -1 & 1 & 0 & 0 & 0 & 0 \\ 0 & 0 & 0 & -1 & 1 & 0 & 0 & 0 \\ 0 & 0 & 0 & 0 & -1 & 1 & 0 & 0 \\ 0 & 0 & 0 & 0 & 0 & -1 & 1 & 0 \\ 1/2 & 1/2 & 1/2 & 1/2 & 1/2 & 1/2 & 1/2 & 1/2 \end{bmatrix}$$

APPENDIX B

THE ASYMPTOTIC NATURE OF PARAMETERS OTHER THAN DENSITY

B.1 Quantization Coefficient

In this section it is shown that the quantization coefficient for vectors having a uniform distribution in \mathbb{R}^{k-1} is $k/(k-1)$ times the spherical quantization coefficient for vectors having a uniform distribution on Ω_k .

Let $X \in \mathbb{R}^k$ be a random vector with pdf $f(X)$, let Q_N denote an N -point vector quantizer for X , and let

$$D(r, k, N, f) \triangleq \inf_{Q_N} \frac{1}{k} E[\|X - Q_N(X)\|^r].$$

From Zador [99],

$$\lim_{N \rightarrow \infty} N^{r/k} D(r, k, N, f) = G_{r,k} \|f\|_{\frac{k}{k+r}}, \quad (\text{B.1})$$

where $\|f\|_\rho = [\int f^\rho]^{1/\rho}$, and where $G_{r,k}$ is a constant depending only on r and k . If f is uniform inside an open, bounded region $R \subset \mathbb{R}^k$, i.e.,

$$f(X) = U_{R \subset \mathbb{R}^k}(X) \triangleq \begin{cases} 1/V(R) & \text{if } X \in R \\ 0 & \text{otherwise,} \end{cases}$$

where $V(R)$ is the k -dimensional content of R , then (B.1) can be written as

$$G_{r,k} = \lim_{N \rightarrow \infty} \left(\frac{N}{V(R)} \right)^{r/k} D(k, N, r, U_{R \subset \mathbb{R}^k}).$$

$G_{r,k}$ is referred to as the *quantization coefficient* for vectors with a uniform source in \mathbb{R}^k , under the r th norm distortion measure; $G_{r,k}$ may be regarded as the normalized r th norm distortion

of a uniformly distributed source in \mathbb{R}^k when optimal quantization and a large number of points are used.

Let X be uniform in an open region $T \subseteq \Omega_k$, i.e.,

$$f(X) = U_{T \subseteq \Omega_k}(X) \triangleq \begin{cases} 1/S(T) & \text{if } X \in T \\ 0 & \text{otherwise,} \end{cases}$$

where $S(T)$ is the $(k-1)$ -dimensional content of T . The *spherical quantization coefficient* for vectors uniform in $T \subseteq \Omega_k$ under the r th norm distortion measure is defined by

$$H_{r,k} \triangleq \lim_{N \rightarrow \infty} \left(\frac{N}{S(T)} \right)^{r/(k-1)} D(r, k, N, U_{T \subseteq \Omega_k}).$$

Lemma B.1 *Under the r th distortion measure, the spherical quantization coefficient for vectors uniformly distributed in a subset of Ω_k is $(k-1)/k$ times the quantization coefficient for vectors uniformly distributed in a bounded, open region within \mathbb{R}^{k-1} . That is,*

$$H_{r,k} = \frac{k-1}{k} G_{r,k-1}.$$

Proof: Define a mapping $F : \Omega_k \rightarrow \mathbb{R}^{k-1}$ by $F(x_1, \dots, x_k) = (x_1, \dots, x_{k-1})$, and let

$$T \equiv \{(x_1, \dots, x_k) \in \Omega_k : \forall i \leq k-1, |x_i| < c, \text{ and } x_k > 0\},$$

where $c \geq 0$ is a constant to be chosen later. Let $R = F(T)$. For all $X, Y \in T$, it is the case that $\|X - Y\| \geq \|F(X) - F(Y)\|$, and hence $V(R) \leq S(T)$. In the other direction, the surface area of T is less than the surface area of a superscribing hypercube in \mathbb{R}_k with $k-1$ sides of length c and one side of length $O(c^2)$:

$$S(T) \leq c^{k-1} + 2^{k-1} \cdot c^{k-1} \cdot O(c^2) = V(R) + O(c^{k+1}).$$

Also,

$$\begin{aligned} \|X - Y\|^r &= (\|X - Y\|^2)^{r/2} \\ &= \left(\sum_{i=1}^k (x_i - y_i)^2 \right)^{r/2} \\ &= (\|F(X) - F(Y)\|^2 + O(c^4))^{r/2} \\ &= \|F(X) - F(Y)\|^r (1 + O(c^2)). \end{aligned}$$

Thus,

$$\begin{aligned}
H_{r,k} &= \lim_{N \rightarrow \infty} \left(\frac{N}{S(T)} \right)^{\frac{r}{k-1}} D(r, k, N, U_{T \subseteq \Omega_k}) \\
&= \lim_{N \rightarrow \infty} \left(\frac{N}{S(T)} \right)^{\frac{r}{k-1}} \inf_{Q_n} \frac{1}{k} \int_T \|X - Q_N(X)\|^r \frac{1}{S(T)} dX \\
&\geq \lim_{N \rightarrow \infty} \left(\frac{N}{V(R) + O(c^{k+1})} \right)^{\frac{r}{k-1}} \inf_{Q_n} \frac{1}{k} \int_T \|F(X) - F(Q_N(X))\|^r \frac{1}{V(R) + O(c^{k+1})} dX \\
&= \frac{k-1}{k} \lim_{N \rightarrow \infty} \left(\frac{N}{V(R)} \right)^{\frac{r}{k-1}} [1 - O(c^2)] \inf_{Q_n} \frac{1}{k-1} \int_R \|X - Q_N(X)\|^r \frac{1}{V(R)} \cdot (1 - O(c)) \\
&= \frac{k-1}{k} \left[\lim_{N \rightarrow \infty} \left(\frac{N}{V(R)} \right)^{\frac{r}{k-1}} \inf_{Q_n} \frac{1}{k-1} \int_R \|X - Q_N(X)\|^r \frac{1}{V(R)} dX \right] \cdot (1 - O(c)) \\
&= \frac{k-1}{k} G_{r,k-1} [1 - O(c + c^{\frac{r}{k-1}})]
\end{aligned}$$

and

$$\begin{aligned}
H_{r,k} &\leq \lim_{N \rightarrow \infty} \left(\frac{N}{V(R)} \right)^{\frac{r}{k-1}} \inf_{Q_n} \frac{1}{k} \int_T [\|F(X) - F(Q_N(X))\|^r (1 + O(c^2))] \frac{1}{V(R)} dX \\
&= \frac{k-1}{k} \left[\lim_{N \rightarrow \infty} \left(\frac{N}{V(R)} \right)^{\frac{r}{k-1}} \inf_{Q_n} \frac{1}{k-1} \int_R \|X - Q_N(X)\|^r \frac{1}{V(R)} dX \right] \cdot [1 + O(c^2)] \\
&= \frac{k-1}{k} G_{r,k-1} [1 + O(c^2)].
\end{aligned}$$

Thus,

$$1 - O(c) \leq \frac{kH_{r,k}}{(k-1)G_{r,k-1}} \leq 1 + O(c^2).$$

Since c may be chosen arbitrarily small, $H_{r,k} = \frac{k-1}{k} G_{r,k-1}$. ■

B.2 Covering Thickness

The *covering thickness* (or *covering density*) of an arrangement of unit-radius spheres that covers \mathbb{R}^k is defined as the average number of spheres that contain a point of \mathbb{R}^k . Denote the minimum covering thickness for \mathbb{R}^k by $\Theta_{\mathbb{R}^k}$. If \mathcal{A} is the set of unit-radius spheres in the arrangement and $N(\mathcal{A}, R)$ is the number of spheres in \mathcal{A} whose center lies inside the k -dimensional hypercube centered about the origin and with edge length R , the covering thickness is

$$\Theta_{\mathbb{R}^k} = \lim_{R \rightarrow \infty} \inf_{\mathcal{A} \supset \mathbb{R}^k} N(\mathcal{A}, R) V_k / R^k.$$

Similarly, suppose an arrangement of spherical caps with angular radius ϕ covers Ω_k . Let $\mathcal{C}(\phi)$ denote the set of caps, and define $\Theta_{\Omega_k}(\phi)$ as the average number of spherical caps that contain a point of Ω_k , i.e.,

$$\Theta_{\Omega_k}(\phi) \triangleq \frac{|\mathcal{C}(\phi)| \cdot S(c(k, \phi))}{S_k}.$$

Let the thinnest asymptotic covering thickness for Ω_k be defined by

$$\Theta_{\Omega^k} \triangleq \lim_{\phi \rightarrow 0} \inf_{\mathcal{C}(\phi) \supseteq \Omega_k} \Theta_{\Omega_k}(\phi).$$

Lemma B.2 *The thinnest asymptotic covering thickness of Ω_k equals the thinnest covering thickness of \mathbb{R}_{k-1} , i.e., $\Theta_{\Omega_k} = \Theta_{\mathbb{R}^{k-1}}$.*

Proof: Define a mapping $F : \Omega_k \rightarrow \mathbb{R}^{k-1}$ by $F(x_1, \dots, x_k) = (x_1, \dots, x_{k-1})$, and let

$$T \equiv \{(x_1, \dots, x_k) \in \Omega_k : \forall i \leq k-1, |x_i| < c, \text{ and } x_k > 0\},$$

where $c \geq 0$ is a constant to be chosen later. Let $\{\mathcal{C}(\phi)\}$ be a family of coverings of Ω_k whose thicknesses converge to Θ_{Ω_k} as $\phi \rightarrow 0$. Construct an arrangement of unit-radius spheres in \mathbb{R}^{k-1} with centers from the set

$$\mathcal{A}(\phi) \triangleq \frac{F(\mathcal{C}(\phi) \cap T) \oplus c\mathbb{Z}^{k-1}}{\phi}.$$

Then the arrangement covers \mathbb{R}^{k-1} .

$$\begin{aligned} \Theta_{\Omega_k} &= \lim_{\phi \rightarrow 0} \inf_{\mathcal{C}(\phi) \supseteq \Omega_k} \Theta_{\Omega_k}(\phi) \\ &= \lim_{\phi \rightarrow 0} \inf_{\mathcal{C}(\phi) \supseteq \Omega_k} \frac{|\mathcal{C}(\phi)| \cdot S(c(k, \phi))}{S_k} \\ &= \lim_{\phi \rightarrow 0} \inf_{\mathcal{C}(\phi) \supseteq T} \frac{|\mathcal{C}(\phi) \cap T| \cdot S(c(k, \phi))}{S(T)} \\ &= \lim_{\phi \rightarrow 0} \inf_{\mathcal{C}(\phi) \supseteq T} \frac{|\mathcal{A}(\phi) \cap (F(T)/\phi)| \cdot (V_{k-1}\phi^{k-1} - O(\phi^{k+1}))}{c^{k-1} + O(c^{k+1})} \\ &= \lim_{\phi \rightarrow 0} \inf_{\mathcal{C}(\phi) \supseteq T} \frac{|\mathcal{A}(\phi) \cap (F(T)/\phi)| \cdot V_{k-1}\phi^{k-1}}{c^{k-1}} \cdot \frac{1 - O(\phi^2)}{1 + O(c^2)} \\ &= \lim_{R \rightarrow \infty} \inf_{\mathcal{A}(1/R) \supseteq \mathbb{R}^{k-1}} \frac{|\mathcal{A}(1/R) \cap (R \cdot F(T))| \cdot V_{k-1}}{c^{k-1} R^{k-1}} \cdot \frac{1}{1 + O(c^2)} \\ &= \lim_{R \rightarrow \infty} \inf_{\mathcal{A}(1/R) \supseteq \mathbb{R}^{k-1}} N(\mathcal{A}(1/R), R) V_{k-1} \cdot (1 - O(c^2)) / R^{k-1} \\ &= \Theta_{\mathbb{R}^{k-1}} \cdot (1 - O(c^2)) \end{aligned}$$

Since c can be chosen as small as desired, $\Theta_{\Omega_k} = \Theta_{\mathbb{R}^{k-1}}$. ■

APPENDIX C

PROOF OF LEMMAS

C.1 Proof of Lemma 3.1

Proof: First, suppose that $\Delta_k^{s.c.} > \Delta_{k-1}^{pack}$. Then there exists a family of spherical codes $\{\mathcal{C}(k, d)\}$ such that

$$\lim_{d \rightarrow 0} \Delta_{\mathcal{C}(k, d)} = \Delta_k^{s.c.} > \Delta_{k-1}^{pack}.$$

Define a mapping $F : \Omega_k \rightarrow \mathbb{R}^{k-1}$ by $F(x_1, \dots, x_k) = (x_1, \dots, x_{k-1})$ and let

$$R \equiv \left\{ (x_1, \dots, x_k) \in \Omega_k : |x_i| < \frac{d^{2/3}}{2}, \quad \forall i \leq k-1 \right\}.$$

This is illustrated in Figure C.1. We construct a $(k-1)$ -dimensional sphere packing with density greater than Δ_{k-1}^{pack} . Define the packing by the sphere centers described by the direct sum

$$\mathcal{P} \equiv F(R \cap \mathcal{C}(k, d)) \oplus (d^{2/3} + d)\mathbb{Z}^{k-1}.$$

Denote two arbitrary distinct points in $\mathcal{P}, Q \in \mathcal{P}$ by

$$P = X + (d^{2/3} + d)(i_1, \dots, i_{k-1})$$

and

$$Q = Y + (d^{2/3} + d)(j_1, \dots, j_{k-1}),$$

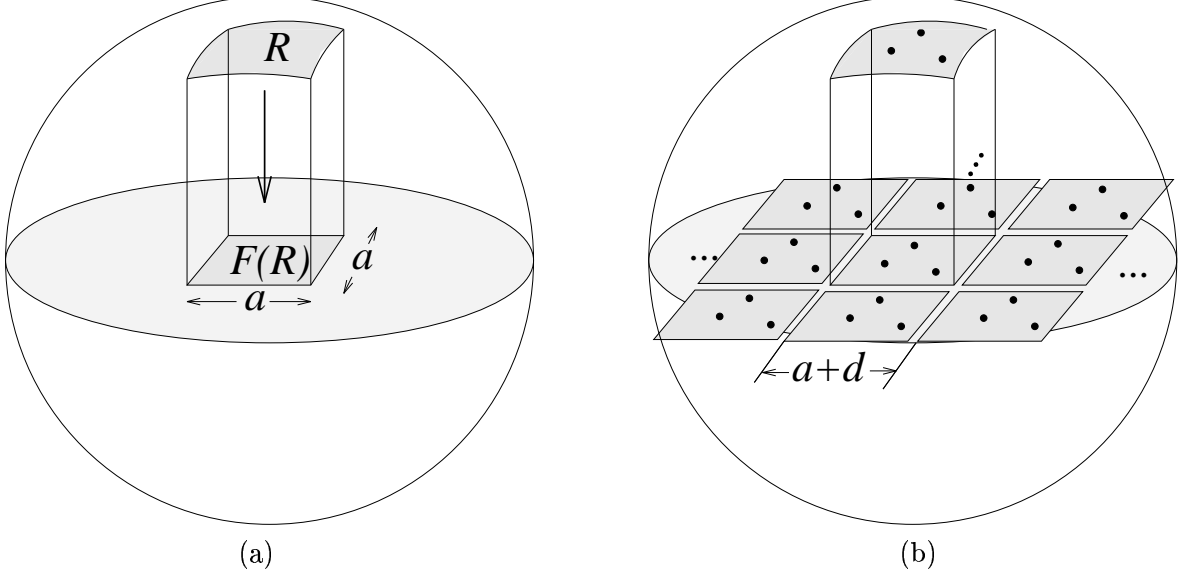


Figure C.1 Mapping part of Ω_k to \mathbb{R}^{k-1} . (a) R is the set of points whose image under F lies in a hypercube of edge length $a = d^{2/3}$. (b) A packing is constructed by shifting copies of $F(R)$.

where $X, Y \in F(R \cap \mathcal{C}(k, d))$. If $(i_1, \dots, i_{k-1}) \neq (j_1, \dots, j_{k-1})$, then clearly $\|P - Q\| > d$. If $(i_1, \dots, i_{k-1}) = (j_1, \dots, j_{k-1})$, then

$$\begin{aligned} \|P - Q\| &= \|X - Y\| \\ &\geq d - \|F^{-1}(X) - F^{-1}(Y)\| + \|X - Y\| \end{aligned} \tag{C.1}$$

$$\begin{aligned} &= d - \sqrt{\sum_{i=1}^k (x_i - y_i)^2} + \sqrt{\sum_{i=1}^{k-1} (x_i - y_i)^2} \\ &\geq d - \sqrt{\sum_{i=1}^{k-1} (x_i - y_i)^2} - |x_k - y_k| + \sqrt{\sum_{i=1}^{k-1} (x_i - y_i)^2} \\ &= d - |x_k - y_k| \\ &\geq d - \left(1 - \sqrt{1 - (k-1)d^{4/3}/4}\right) \\ &> d - O(d^{4/3}), \end{aligned} \tag{C.2}$$

where (C.1) follows because $F^{-1}(X), F^{-1}(Y) \in \mathcal{C}(k, d)$, and (C.2) follows by the triangle inequality. Thus, the packing radius is at least $(d/2) - O(d^{4/3})$. By the choice of the family $\{\mathcal{C}(k, d)\}$, for any $\epsilon > 0$ there is a sufficiently small d such that

$$|R \cap \mathcal{C}(k, d)| \geq \frac{(\Delta_k^{s.c.} - \epsilon)S(R)}{S(c(k, \theta/2))},$$

where $S(R)$ is the $(k-1)$ -dimensional content of R . Since the $(k-1)$ -dimensional content of a $(k-1)$ -dimensional sphere of radius r is $V_{k-1}r^{k-1}$ and using (2.7),

$$\begin{aligned} \frac{V_{k-1}(\frac{d}{2} - O(d^{4/3}))^{k-1}}{S(c(k, \theta/2))} &= \frac{V_{k-1}(\frac{d}{2} - O(d^{4/3}))^{k-1}}{V_{k-1}(d/2)^{k-1} + O(d^{k+1})} \\ &= (1 - O(d^{1/3}))^{k-1}. \end{aligned} \quad (\text{C.3})$$

Also, since $F(R)$ is a $(k-1)$ -dimensional hypercube with edge length $d^{2/3}$, we have $S(R) \geq S(F(R)) = d^{2(k-1)/3}$, and thus

$$\begin{aligned} \frac{S(R)}{(d^{2/3} + d)^{k-1}} &\geq \frac{S(F(R))}{d^{2(k-1)/3}(1 + O(d^{1/3}))} \\ &= \frac{1}{1 + O(d^{1/3})} \\ &= 1 - O(d^{1/3}). \end{aligned} \quad (\text{C.4})$$

The density of the sphere packing \mathcal{P} is (for sufficiently small $d, \epsilon > 0$)

$$\begin{aligned} \Delta_{\mathcal{P}} &\geq |R \cap \mathcal{C}(k, d)| \cdot \frac{V_{k-1}(\frac{d-O(d^{4/3})}{2})^{k-1}}{(d^{2/3} + d)^{k-1}} \\ &\geq \frac{(\Delta_k^{s.c.} - \epsilon)S(R)}{S(c(k, \theta/2))} \cdot \frac{V_{k-1}(\frac{d-O(d^{4/3})}{2})^{k-1}}{(d^{2/3} + d)^{k-1}} \\ &= (\Delta_k^{s.c.} - \epsilon) \left(\frac{S(R)}{(d^{2/3} + d)^{k-1}} \right) \cdot \left(\frac{V_{k-1}(\frac{d-O(d^{4/3})}{2})^{k-1}}{S(c(k, \theta/2))} \right) \\ &\geq (\Delta_k^{s.c.} - \epsilon)(1 - O(d^{1/3}))(1 - O(d^{1/3}))^{k-1} \end{aligned} \quad (\text{C.5})$$

$$\begin{aligned} &\geq (\Delta_k^{s.c.} - \epsilon)(1 - O(d^{1/3}))^k \\ &> \Delta_{k-1}^{pack}, \end{aligned} \quad (\text{C.6})$$

where (C.5) follows from (C.3) and (C.4), and (C.6) is true for sufficiently small ϵ and d . This is a contradiction, since Δ_{k-1}^{pack} is by definition the highest density possible. Thus, $\Delta_k^{s.c.} \leq \Delta_{k-1}^{pack}$.

It remains to show that $\Delta_k^{s.c.} \geq \Delta_{k-1}^{pack}$. Let $\mathcal{P}(d)$ be the set of centers of spheres of radius $d/2$ which belong to a $(k-1)$ -dimensional sphere packing with density Δ_{k-1}^{pack} . From $\mathcal{P}(d)$, we shall construct a family of spherical codes whose asymptotic density is Δ_{k-1}^{pack} . For any $\epsilon > 0$, Ω_k can be partitioned into sets (called ‘‘cells’’) whose diameters are at most ϵ by uniformly quantizing each coordinate separately. Let L be an arbitrary cell, and define axes such that if $(x_1, \dots, x_k) \in L$ then $|x_i| \leq \epsilon$ for all $i \leq k-1$ and $x_k > 0$. Let

$$\mathcal{C}_L \equiv \{ X \in \Omega_k : F(X) \in \mathcal{P}(d) \cap F(L) \text{ and } c_X(k, \sin^{-1}(d/2)) \subset L \},$$

and define a spherical code by $\mathcal{C} \equiv \cup_L \mathcal{C}_L$.

Let $X, Y \in \mathcal{C}$, with $X \neq Y$. If X and Y belong to the same cell, then $\|X - Y\| \geq d$, since points in $\mathcal{P}(d)$ are separated by at least distance d . If X and Y do not belong to the same cell, then $c_X(k, \sin^{-1}(d/2))$ and $c_Y(k, \sin^{-1}(d/2))$ are disjoint and again $\|X - Y\| \geq d$. Thus, \mathcal{C} has minimum distance at least d .

The density of $(k-1)$ -dimensional spheres of $\mathcal{P}(d)$ with centers in $F(\mathcal{C}_L)$ (i.e., the percentage of volume within $F(L)$ covered by such spheres) approaches Δ_{k-1}^{pack} as $d \rightarrow 0$, by the choice of $\mathcal{P}(d)$. As in the first part of the proof, the ratio of the $(k-1)$ -dimensional content of L to that of $F(L)$ can be made arbitrarily close to 1 and the ratio of the $(k-1)$ -dimensional content of a spherical cap $c(k, \sin^{-1}(d/2))$ to the $(k-1)$ -dimensional content of a $(k-1)$ -dimensional sphere of radius $d/2$ can be made arbitrarily close to one, by the choice of ϵ . Thus, the asymptotic density of cell L , and hence \mathcal{C} , can be made arbitrarily close to Δ_{k-1}^{pack} . ■

C.2 Proof of Lemma 3.7

Proof: Let $\gamma \in (0, \pi/2)$ and

$$R \equiv \{ (x_1, \dots, x_k) \in \Omega_k : \sin \gamma < x_k < \sin(\gamma + \theta) \},$$

and let $S(R)$ be the $(k-1)$ -dimensional content of R . Then,

$$\begin{aligned} S(R) &= S_{k-1} \int_{\gamma}^{\gamma+\theta} \cos^{k-2} x \, dx \\ &= S_{k-1} \int_{\gamma}^{\gamma+\theta} (\cos \gamma - O(x - \gamma))^{k-2} \, dx \\ &= S_{k-1} \int_{\gamma}^{\gamma+\theta} \cos^{k-2} \gamma - O(x - \gamma) \, dx \\ &= S_{k-1} \theta \cos^{k-2} \gamma - O(\theta^2). \end{aligned}$$

Since the k th coordinate of every codepoint in $\mathcal{C}^A(k, d)$ is of the form $\sin[(i + 1/2)\theta]$, every codepoint in $\mathcal{C}^A(k, d) \cap R$ has the same k th coordinate, say, $\sin \eta$. Thus,

$$|\mathcal{C}^A(k, d) \cap R| = M(k-1, d/\cos \eta). \quad (\text{C.7})$$

By the definition of $\Delta_{k-1}^{s.c.}$, given any $\epsilon > 0$ there exists a sufficiently small $d_0 > 0$ such that

$$\frac{M(k-1, d/\cos \eta) S(c(k-1, \sin^{-1}(d/(2 \cos \eta))))}{S_{k-1}} \leq \Delta_{k-1}^{s.c.} + \epsilon$$

for all $d \leq d_0$. Since

$$\sin^{-1}\left(\frac{d}{2\cos\eta}\right) = \sin^{-1}\left(\frac{\sin(\theta/2)}{\cos\eta}\right) = \frac{\theta}{2\cos\eta} - O(\theta^3),$$

one can apply (2.6) and obtain

$$S(c(k-1, \sin^{-1}(d/(2\cos\eta)))) = V_{k-2} \left(\frac{\theta}{2\cos\eta}\right)^{k-2} - O(\theta^k). \quad (\text{C.8})$$

Hence,

$$\begin{aligned} \Delta_{\mathcal{C}^A(k,d)} &\leq \frac{|\mathcal{C}^A(k,d) \cap R| \cdot S(c(k, \theta/2))}{S(R)} \\ &= \frac{M(k-1, d/\cos\eta) S(c(k, \theta/2))}{S(R)} \\ &\leq \frac{(\Delta_{k-1}^{s.c.} + \epsilon) S_{k-1} S(c(k, \theta/2))}{S(c(k-1, \sin^{-1}(d/(2\cos\eta)))) S(R)} \end{aligned} \quad (\text{C.9})$$

$$\begin{aligned} &= \frac{(\Delta_{k-1}^{s.c.} + \epsilon) (V_{k-1} (\frac{\theta}{2})^{k-1} - O(\theta^{k+1}))}{\left(V_{k-2} \left(\frac{\theta}{2\cos\eta}\right)^{k-2} - O(\theta^k)\right) (\theta \cos^{k-2} \gamma - O(\theta^2))} \\ &\leq \frac{(\Delta_{k-1}^{s.c.} + \epsilon) V_{k-1} (\frac{\theta}{2})^{k-1}}{\theta (\cos^{k-2} \gamma) V_{k-2} (\frac{\theta}{2\cos\eta})^{k-2} (1 - O(\theta)) (1 - O(\theta^2))} \\ &= \frac{(\Delta_{k-1}^{s.c.} + \epsilon) V_{k-1}}{2V_{k-2}} + O(\theta), \quad (\text{C.10}) \\ &= \frac{\Delta_{k-2}^{pack} V_{k-1}}{2V_{k-2}} + O(\epsilon + \theta), \end{aligned}$$

where (C.9) follows from (C.8), and where (C.10) follows from

$$\frac{\cos\gamma}{\cos\eta} = \frac{\cos\gamma}{\cos\gamma - O(\theta)} = 1 + O(\theta).$$

By letting $\epsilon \rightarrow 0$ and $\theta \rightarrow 0$, the result is obtained. ■

C.3 Proof of Lemma 4.1

Proof: Let $Y \in \mathbb{R}^{k-1}$, $Y \neq 0$, and let $J(Y)$ be the set claimed to equal $f^{-1}(Y)$. Let $X = (x_1, \dots, x_k) \in J(Y)$, and define $X' = (x_1, \dots, x_{k-1})$. Let i be such that

$$0 \leq h_i \leq \sqrt{(\xi_{i+1} - \xi_i)^2 + \left(\sqrt{1 - \xi_i^2} - \sqrt{1 - \xi_{i+1}^2}\right)^2}.$$

Then $x_k = \sqrt{1 - g_i^2}$, $\|X'\| = g_i$, and

$$\begin{aligned} f(X) &= \left(\sqrt{1 - \xi_i^2} - \sqrt{(x_k - \xi_i)^2 - \left(\sqrt{1 - \xi_i^2} - \sqrt{1 - x_k^2} \right)^2} \right)_+ \cdot \frac{X'}{\sqrt{1 - x_k^2}} \\ &= \left(\sqrt{1 - \xi_i^2} - \sqrt{\left(\sqrt{1 - g_i^2} - \xi_i \right)^2 + \left(\sqrt{1 - \xi_i^2} - g_i \right)^2} \right)_+ \cdot \frac{g_i Y}{g_i \|Y\|} \end{aligned}$$

Hence,

$$\begin{aligned} f(X) = Y &\Leftrightarrow \left(\sqrt{1 - \xi_i^2} - \sqrt{\left(\sqrt{1 - g_i^2} - \xi_i \right)^2 + \left(\sqrt{1 - \xi_i^2} - g_i \right)^2} \right)_+ = \|Y\| \\ &\Leftrightarrow 2 \left(1 - \xi_i \sqrt{1 - g_i^2} - g_i \sqrt{1 - \xi_i^2} \right) = h_i^2 \end{aligned} \quad (\text{C.11})$$

$$\Leftrightarrow g_i = \left(1 - \frac{h_i^2}{2} \right) \sqrt{1 - \xi_i^2} - \frac{h_i \xi_i}{2} \sqrt{4 - h_i^2}, \quad (\text{C.12})$$

where (C.11) follows because $Y \neq 0$, and (C.12) follows from simplification and the quadratic formula. The condition is always satisfied, by the definition of g_i ; therefore, $X \in f^{-1}(Y)$, i.e., $J(Y) \subseteq f^{-1}(Y)$.

Now let $X = (x_1, \dots, x_k) \in f^{-1}(Y)$, and let i be such that $\xi_i = \underline{\xi}(x_k)$. Since $f^{-1}(Y)$ can have at most one element corresponding to each ξ_i , from the above it only has to be shown that

$$0 \leq h_i \leq \sqrt{(\xi_{i+1} - \xi_i)^2 + \left(\sqrt{1 - \xi_i^2} - \sqrt{1 - \xi_{i+1}^2} \right)^2}.$$

The left inequality is implied by $0 \leq \|Y\| = \|f(X)\| \leq \sqrt{1 - \xi_i^2}$. On the other hand, $\xi_i = \underline{\xi}(x_k)$ implies $\xi_{i+1} > |x_k|$, and thus

$$\begin{aligned} \sqrt{(\xi_{i+1} - \xi_i)^2 + \left(\sqrt{1 - \xi_i^2} - \sqrt{1 - \xi_{i+1}^2} \right)^2} &> \sqrt{(x_{k-1} - \xi_i)^2 + \left(\sqrt{1 - x_k^2} - \sqrt{1 - \xi_i^2} \right)^2} \\ &= \sqrt{1 - \xi_i^2} - \|Y\|, \end{aligned}$$

which is the right inequality. Therefore, $f^{-1}(Y) \subseteq J(Y)$. ■

C.4 Proof of Lemma 6.2

Proof: The derivation involves an integral which can be massaged to the form of the Gamma function:

$$\begin{aligned}
 E[\|X\|] &= \int_0^\infty x f_g(x) dx \\
 &= \int_0^\infty \frac{2x^k e^{-\frac{x^2}{2\sigma^2}}}{\Gamma(\frac{k}{2})(2\sigma^2)^{k/2}} dx \\
 &= \int_0^\infty \frac{2t^{k/2} e^{-t}}{\Gamma(\frac{k}{2})} \cdot \sqrt{\frac{\sigma^2}{2t}} dt, \text{ by setting } t = \frac{x^2}{2\sigma^2} \\
 &= \frac{\sqrt{2\sigma^2}}{\Gamma(\frac{k}{2})} \int_0^\infty t^{(\frac{k+1}{2})-1} e^{-t} dt \\
 &= \frac{\sqrt{2\sigma^2} \Gamma(\frac{k+1}{2})}{\Gamma(\frac{k}{2})} \\
 &= \frac{\sqrt{2\pi\sigma^2}}{\beta(\frac{k}{2}, \frac{1}{2})}, \text{ since } \Gamma(1/2) = \sqrt{\pi}.
 \end{aligned}$$

Also,

$$E[\|X\|^2] = E[X_1^2 + \dots + X_k^2] = E[X_1^2] + \dots + E[X_k^2] = k\sigma^2,$$

and

$$\text{var}[\|X\|] = E[\|X\|^2] - E[\|X\|]^2 = k\sigma^2 - \frac{2\pi\sigma^2}{\beta^2(\frac{k}{2}, \frac{1}{2})}$$

■

C.5 Proof of Lemma 6.3

Proof: Let $f(k) = \text{var}[\|X\|]$, where X is a k -dimensional vector formed from an i.i.d. $N(0, \sigma^2)$ source. It suffices to show that $f(k+1) - f(k) > 0$ for all $k > 0$. From Equation (6.3),

$$f(k) = k\sigma^2 - \frac{2\pi\sigma^2}{\beta^2(\frac{k}{2}, \frac{1}{2})}.$$

Thus, $f(1) = \sigma^2 - \frac{2\sigma^2\Gamma^2(2)}{\Gamma(1/2)} = \sigma^2(1 - \frac{2}{\pi}) \approx 0.363$ and it is readily computed that the sequence continues $0.429, 0.453, 0.466, 0.473, 0.478, \dots$. Hence, attention may be restricted to $k > 6$.

$$\begin{aligned}
f(k+1) - f(k) &= \left[(k+1)\sigma^2 - \frac{2\pi\sigma^2}{\beta^2(\frac{k+1}{2}, \frac{1}{2})} \right] - \left[k\sigma^2 - \frac{2\pi\sigma^2}{\beta^2(\frac{k}{2}, \frac{1}{2})} \right] \\
&= \sigma^2 \left[1 + 2\pi \left(\frac{1}{\beta^2(\frac{k}{2}, \frac{1}{2})} - \frac{1}{\beta^2(\frac{k+1}{2}, \frac{1}{2})} \right) \right] \\
&= \sigma^2 \left[1 + 2 \left(\frac{\Gamma^2(\frac{k+1}{2})}{\Gamma^2(\frac{k}{2})} - \frac{\Gamma^2(\frac{k+2}{2})}{\Gamma^2(\frac{k+1}{2})} \right) \right] \\
&= \sigma^2 \left[1 + 2 \left(\frac{\Gamma^2(\frac{k+1}{2})}{\Gamma^2(\frac{k}{2})} - \frac{k^2\Gamma^2(\frac{k}{2})}{4\Gamma^2(\frac{k+1}{2})} \right) \right] \dots
\end{aligned}$$

Let $g(k) = 2\Gamma^2(\frac{k+1}{2}) / (k\Gamma^2(\frac{k}{2}))$. From Stirling's asymptotic series [36],

$$\begin{aligned}
\Gamma\left(\frac{k+1}{2}\right) &\geq \left(\frac{k+1}{2e}\right)^{\frac{k+1}{2}} \sqrt{\frac{2\pi}{\frac{k+1}{2}}} \left(1 + \frac{1}{12\left(\frac{k+1}{2}\right)}\right) \\
\Gamma\left(\frac{k}{2}\right) &\leq \left(\frac{k}{2e}\right)^{\frac{k}{2}} \sqrt{\frac{2\pi}{\frac{k}{2}}} \left(1 + \frac{1}{12\left(\frac{k}{2}\right)} + \frac{1}{288\left(\frac{k}{2}\right)^2}\right).
\end{aligned}$$

Thus,

$$\begin{aligned}
g(k) &\geq \frac{2\left(\frac{k+1}{2e}\right)^{k+1} \cdot \frac{4\pi}{k+1} \cdot \left(1 + \frac{1}{6k+6}\right)^2}{k\left(\frac{k}{2e}\right)^k \cdot \frac{4\pi}{k} \cdot \left(1 + \frac{1}{6k} + \frac{1}{72k^2}\right)^2} \\
&= \left(1 + \frac{1}{k}\right)^k \cdot \frac{1}{e} \cdot \left(\frac{1 + \frac{1}{6k+6}}{1 + \frac{1}{6k} + \frac{1}{72k^2}}\right)^2.
\end{aligned}$$

If a function $h(x)$ has a continuous $(n+1)$ st derivative for all $x \in [0, t]$ and satisfies $h^{(n+1)}(x) \geq 0$ for all x in that range, then [4]

$$h(x) \geq \sum_{i=0}^n \frac{h^{(i)}(0)x^i}{i!}$$

for all $x \in [0, t]$. Thus, $e^{-u} \geq 1 - u$ for all $u \in [0, 1]$, since $\frac{d^2}{du^2}e^{-u} = e^{-u} \geq 0$ for all $u \in [0, 1]$.

Also,

$$\ln(1+x) \geq x - \frac{x^2}{2} + \frac{x^3}{3} - \frac{x^4}{4}$$

for all $x \in [0, 1]$, since $\frac{d^5}{dx^5}\ln(1+x) = \frac{24}{(1+x)^5} \geq 0$ for all $x \in [0, 1]$. This implies

$$\frac{1}{x}\ln(1+x) \geq 1 - \frac{x}{2} + \frac{x^2}{3} - \frac{x^3}{4}$$

for all $x \in (0, 1]$, and

$$\begin{aligned}
(1+x)^{1/x} &= \exp\left[\frac{1}{x}\ln(1+x)\right] \\
&\geq \exp\left[1 - \frac{x}{2} + \frac{x^2}{3} - \frac{x^3}{4}\right] \\
&= e \cdot \exp\left[-\frac{x}{2} + \frac{x^2}{3} - \frac{x^3}{4}\right] \\
&\geq e \cdot \left(1 - \frac{x}{2} + \frac{x^2}{3} - \frac{x^3}{4}\right)
\end{aligned}$$

for all $x \in (0, 1]$. Note that $x \in (0, 1]$ implies $u = \frac{x}{2} - \frac{x^2}{3} + \frac{x^3}{4} > 0$, which meets the requirement for the inequality $e^{-u} \geq 1 - u$. Setting $k = 1/x$, it follows that

$$\left(1 + \frac{1}{k}\right)^k \geq e \cdot \left(1 - \frac{1}{2k} + \frac{1}{3k^2} - \frac{1}{4k^3}\right) \tag{C.13}$$

for all $k \geq 1$. Also, for all $k \geq 1$,

$$\begin{aligned}
6k + 7 &> 6k + 7 - \frac{85}{72k^2} - \frac{169}{864k^3} - \frac{13}{864k^4} \\
&= (6k + 6) \left(1 - \frac{13}{72k^2}\right) \left(1 + \frac{1}{6k} + \frac{1}{72k^2}\right).
\end{aligned}$$

Dividing both sides by the first factor on the right-hand side and then dividing by the last factor on the right-hand side give

$$\left(\frac{1 + \frac{1}{6k+6}}{1 + \frac{1}{6k} + \frac{1}{72k^2}}\right)^2 \geq 1 - \frac{13}{72k^2} \tag{C.14}$$

for all $k \geq 1$. Using Equations (C.13) and (C.14),

$$\begin{aligned}
g(k) &\geq \left(1 - \frac{1}{2k} + \frac{1}{3k^2} - \frac{1}{4k^3}\right) \left(1 - \frac{13}{72k^2}\right) \\
&= 1 - \frac{1}{2k} + \frac{11}{72k^2} - \frac{23}{144k^3} - \frac{13}{216k^4} + \frac{13}{288k^5} \\
&> 1 - \frac{1}{2k} + \frac{1}{8k^2},
\end{aligned} \tag{C.15}$$

where the last inequality holds for all $k \geq 7$, as can be verified by using the quadratic formula on the third through fifth terms of (C.15). Therefore,

$$\begin{aligned}
 f(k+1) - f(k) &\geq \sigma^2 \left(1 + kg(k) - \frac{k}{g(k)} \right) \\
 &= \frac{k\sigma^2}{g(k)} \left(g(k)^2 + \frac{g(k)}{k} - 1 \right) \\
 &\geq \frac{k\sigma^2}{g(k)} \left(\left(1 - \frac{1}{2k} + \frac{1}{8k^2} \right)^2 + \frac{1 - \frac{1}{2k} + \frac{1}{8k^2}}{k} - 1 \right) \\
 &= \frac{\sigma^2}{64k^3g(k)} \\
 &> 0,
 \end{aligned}$$

which was what was wanted. ■

APPENDIX D

PROOF OF THEOREM 5.1

Proof: Use induction on the dimension k . The claim holds for $k = 2$, since $\Delta_{\text{LSC}}(2, d) > 1 - \frac{d}{2\pi}$ and $\Delta_{\Lambda_1} = 1$. Now suppose $k \geq 3$ and let

$$J \equiv \left\{ i: d^{1/k} < r_i < 1 - d^{1/k}, \text{ where } r_i \text{ is determined by (5.5)} \right\}.$$

For each $i \in J$, the density Δ_{T_i} of gap T_i of LSC shall be computed. The $(k-1)$ -dimensional content (surface area) of T_i is

$$S(T_i) = \int_{\sqrt{1-r_i^2}}^{\sqrt{1-r_{i-1}^2}} S_{k-1} (1-x^2)^{(k-3)/2} dx. \quad (\text{D.1})$$

The integrand in (D.1) is monotonically nonincreasing in x , and hence

$$\left(\sqrt{1-r_{i-1}^2} - \sqrt{1-r_i^2} \right) r_{i-1}^{k-3} \leq \frac{S(T_i)}{S_{k-1}} \leq \left(\sqrt{1-r_{i-1}^2} - \sqrt{1-r_i^2} \right) r_i^{k-3}. \quad (\text{D.2})$$

Using (5.5), the occurrences of r_i in (D.2) shall be removed. First (5.5) will be put into an asymptotic form. In the following, constants encompassed by the O -notation do *not* depend on i . Since $r_i > d^{1/k}$ for all $i \in J$, $r_{s(i)} \geq d^{1/k} - d^{2/k} = \Omega(d^{1/k})$, and so

$$\left(1 - \frac{d^2}{2} \right) \sqrt{1 - \left(\frac{c_{k-2}}{r_{s(i)}} \right)^2} = \left(1 - \frac{d^2}{2} \right) \sqrt{1 - O(d^{2(1-(1/k))})} = 1 - O(d^{2(k-1)/k}).$$

Also,

$$\begin{aligned} \sqrt{1 - \frac{d^2}{4} - \frac{c_{k-2}^2 r_{i-1}^2}{r_{s(i)}^2}} &= \sqrt{1 - \frac{c_{k-2}^2 r_{i-1}^2}{r_{s(i)}^2}} \sqrt{1 - \frac{d^2}{4 \left(1 - \frac{c_{k-2}^2 r_{i-1}^2}{r_{s(i)}^2} \right)}} \\ &= \sqrt{1 - \frac{c_{k-2}^2 r_{i-1}^2}{r_{s(i)}^2} - O(d^2)}, \end{aligned}$$

where the fact that

$$\begin{aligned}
\frac{c_{k-2}^2 r_{i-1}^2}{r_{s(i)}^2} &\leq c_{k-2}^2 \left[\frac{r_{s(i)} + d^{2/k}}{r_{s(i)}} \right]^2 \\
&= c_{k-2}^2 \left[1 + O(d^{1/k}) \right]^2 \\
&= c_{k-2}^2 + O(d^{1/k}) \\
&< 0.99,
\end{aligned} \tag{D.3}$$

has been used, where (D.3) holds for sufficiently small d because $c_{k-2}^2 \leq 31/32$ for $k \leq 49$ [14].

Similarly,

$$\frac{r_{i-1}^2 d^2}{r_{s(i)}^2} = O(d^2(1 + d^{(2/k)-(1/k)})^2) = O(d^2),$$

and thus, (5.5) can be rewritten as

$$\begin{aligned}
r_i &= \frac{r_{i-1}(1 - O(d^{2(k-1)/k})) + d\sqrt{1 - r_{i-1}^2} \left(\sqrt{1 - \frac{c_{k-2}^2 r_{i-1}^2}{r_{s(i)}^2}} - O(d^2) \right)}{1 - O(d^2)} \\
&= r_{i-1} + d\sqrt{(1 - r_{i-1}^2) \left(1 - \frac{c_{k-2}^2 r_{i-1}^2}{r_{s(i)}^2} \right) - O(d^{2(k-1)/k})},
\end{aligned}$$

and

$$\begin{aligned}
\sqrt{1 - r_i^2} &= \left(1 - \left(r_{i-1} + d\sqrt{(1 - r_{i-1}^2) \left(1 - \frac{c_{k-2}^2 r_{i-1}^2}{r_{s(i)}^2} \right) - O(d^{2(k-1)/k})} \right)^2 \right)^{1/2} \\
&= \sqrt{1 - r_{i-1}^2} \left(1 - \frac{2r_{i-1}d\sqrt{1 - \frac{c_{k-2}^2 r_{i-1}^2}{r_{s(i)}^2}}}{\sqrt{1 - r_{i-1}^2}} + \frac{O(d^{2(k-1)/k})}{1 - r_{i-1}^2} \right)^{1/2} \\
&= \sqrt{1 - r_{i-1}^2} - r_{i-1}d\sqrt{1 - \frac{c_{k-2}^2 r_{i-1}^2}{r_{s(i)}^2}} + O(d^{2(k-1)/k}).
\end{aligned}$$

Hence, the left- and right-hand sides of (D.2) differ by $O(d^2)$. This gives

$$\begin{aligned}
\frac{S(T_i)}{S_{k-1}} &= \left(\sqrt{1 - r_{i-1}^2} - \sqrt{1 - r_i^2} \right) r_{i-1}^{k-3} + O(d^2) \\
&= r_{i-1}^{k-2} d \sqrt{1 - \frac{c_{k-2}^2 r_{i-1}^2}{r_{s(i)}^2}} - O(d^{2(k-1)/k}) \\
&\leq r_{i-1}^{k-2} d \sqrt{1 - c_{k-2}^2},
\end{aligned} \tag{D.4}$$

where (D.4) holds for sufficiently small d . From Equation (11) of [38],

$$S(c(k, \theta/2)) = V_{k-1}(d/2)^{k-1} (1 - O(d^2)). \quad (\text{D.5})$$

and thus the number of codepoints in each of shell $\mathcal{C}_{i-1}(k-1, d/r_{s(i)})$ and shell $\mathcal{C}_i(k-1, d/r_{s(i)})$ is

$$\begin{aligned} N_{s(i)} &= \frac{\Delta_{\text{LSC}}\left(k-1, \frac{d}{r_{s(i)}}\right) \cdot S_{k-1}}{S\left(c\left(k-1, \sin^{-1}\left(\frac{d}{2r_{s(i)}}\right)\right)\right)} \\ &\geq \frac{\Delta_{\text{LSC}}\left(k-1, \frac{d}{r_{s(i)}}\right) \cdot S_{k-1}}{V_{k-2}\left(\frac{d}{2r_{s(i)}}\right)^{k-2}} \\ &= \frac{\Delta_{\text{LSC}}(k-1, O(d^{(k-1)/k})) S_{k-1}}{V_{k-2}\left(\frac{d}{2r_{s(i)}}\right)^{k-2}}, \end{aligned} \quad (\text{D.6})$$

where (D.6) holds for sufficiently small d , by (D.5). The density of spherical caps in T_i is thus

$$\Delta_{T_i} = \frac{N_{s(i)} S(c(k, \theta/2))}{S(T_i)} \quad (\text{D.7})$$

$$\begin{aligned} &\geq \frac{\left(\frac{\Delta_{\text{LSC}}(k-1, O(d^{(k-1)/k})) \cdot S_{k-1}}{V_{k-2}\left(\frac{d}{2r_{s(i)}}\right)^{k-2}}\right) \cdot V_{k-1}(d/2)^{k-1} \cdot (1 - O(d^2))}{S_{k-1} r_{i-1}^{k-2} d \sqrt{1 - c_{k-2}^2}} \end{aligned} \quad (\text{D.8})$$

$$= \frac{\Delta_{\text{LSC}}(k-1, O(d^{(k-1)/k})) V_{k-1}}{2V_{k-2} \sqrt{1 - c_{k-2}^2}} - O(d^{1/k}) \quad (\text{D.9})$$

$$= \frac{\Delta_{\Lambda_{k-2}} V_{k-1}}{2V_{k-2} \sqrt{1 - c_{k-2}^2}} (1 - O(d^{1/k})) - O(d^{1/k}) \quad (\text{D.10})$$

$$= \frac{\Delta_{\Lambda_{k-2}} V_{k-1}}{2V_{k-2} \sqrt{1 - c_{k-2}^2}} - O(d^{1/k}), \quad (\text{D.11})$$

where (D.10) follows by induction on k . The above density applies for all $i \in J$, i.e., all i determined by (5.5) that are not in a wasted region. Now the argument is repeated for r_i determined by (5.7). Let

$$J' \equiv \left\{ i : d^{1/k} < r_i < 1 - d^{1/k}, \text{ where } r_i \text{ is determined by (5.7)} \right\}. \quad (\text{D.12})$$

If $J' \neq \emptyset$, let $i \in J'$, and let

$$R_i \equiv \bigcup_{j=i-l_{k-1}+1}^i T_j. \quad (\text{D.13})$$

Then from (5.7),

$$r_i = r_{i-l_{k-1}} + d\sqrt{1 - r_{i-l_{k-1}}^2} - O(d^2),$$

and

$$\begin{aligned} \sqrt{1 - r_i^2} &= \sqrt{1 - r_{i-l_{k-1}}^2 - 2r_{i-l_{k-1}}d\sqrt{1 - r_{i-l_{k-1}}^2} \pm O(d^2)} \\ &= \sqrt{1 - r_{i-l_{k-1}}^2} \left(1 - \frac{r_{i-l_{k-1}}d}{\sqrt{1 - r_{i-l_{k-1}}^2}} \pm \frac{O(d^2)}{1 - r_{i-l_{k-1}}^2} \right) \\ &= \sqrt{1 - r_{i-l_{k-1}}^2} - r_{i-l_{k-1}}d \pm O(d^{(2k-1)/k}). \end{aligned}$$

From (D.2), with r_{i-1} replaced by $r_{i-l_{k-1}}$, it follows that

$$\left(\sqrt{1 - r_{i-l_{k-1}}^2} - \sqrt{1 - r_i^2} \right) r_{i-l_{k-1}}^{k-3} \leq \frac{S(R_i)}{S_{k-1}} \leq \left(\sqrt{1 - r_{i-l_{k-1}}^2} + \sqrt{1 - r_i^2} \right) r_i^{k-3}.$$

Again, the left- and right-hand side differ by $O(d^2)$. Thus,

$$\begin{aligned} \frac{S(R_i)}{S_{k-1}} &= \left(\sqrt{1 - r_{i-l_{k-1}}^2} - \sqrt{1 - r_i^2} \right) r_{i-l_{k-1}}^{k-3} + O(d^2) \\ &= r_{i-l_{k-1}}^{k-2} d \pm O(d^{(2k-1)/k}) \\ &\leq r_{i-l_{k-1}}^{k-2} d (1 \pm O(d^{1/k})). \end{aligned}$$

The density of spherical caps in R_i is thus

$$\Delta_{R_i} = \frac{l_{k-1} N_{s(i)} S(c(k, \theta/2))}{S(R_i)} \tag{D.14}$$

$$\begin{aligned} & l_{k-1} \left(\frac{\Delta_{\text{LSC}}(k-1, O(d^{(k-1)/k})) \cdot S_{k-1}}{V_{k-2} \left(\frac{d}{2r_{s(i)}} \right)^{k-2}} \right) \cdot V_{k-1} (d/2)^{k-1} \cdot (1 - O(d^2)) \\ & \geq \frac{l_{k-1} \left(\frac{\Delta_{\text{LSC}}(k-1, O(d^{(k-1)/k})) \cdot S_{k-1}}{V_{k-2} \left(\frac{d}{2r_{s(i)}} \right)^{k-2}} \right) \cdot V_{k-1} (d/2)^{k-1} \cdot (1 - O(d^2))}{S_{k-1} r_{i-l_{k-1}}^{k-2} d (1 \pm O(d^{1/k}))} \\ & \geq \frac{\left(\frac{\Delta_{\text{LSC}}(k-1, O(d^{(k-1)/k})) \cdot S_{k-1}}{V_{k-2} \left(\frac{d}{2r_{s(i)}} \right)^{k-2}} \right) \cdot V_{k-1} (d/2)^{k-1} \cdot (1 \pm O(d^{1/k}))}{S_{k-1} r_{i-l_{k-1}}^{k-2} d \sqrt{1 - c_{k-2}^2}} \\ & \geq \frac{\Delta_{\Lambda_{k-2}} V_{k-1}}{2\sqrt{1 - c_{k-2}^2} V_{k-2}} - O(d^{1/k}), \end{aligned} \tag{D.15}$$

where (D.15) follows from $l_{k-1} \geq 1/\sqrt{1 - c_{k-2}^2}$ and (D.15) follows from (D.8)-(D.11).

Since (D.11) and (D.15) are independent of i , the density of T can be bounded as

$$\Delta_T \geq \frac{\Delta_{\Lambda_{k-2}} V_{k-1}}{2\sqrt{1 - c_{k-2}^2} V_{k-2}} - O(d^{1/k}). \tag{D.16}$$

Since $r_j - r_{j-1} < d$, for all j , the $(k-1)$ -dimensional content of any buffer zone is bounded above by $S_{k-1}d$. The number of buffer zones in this region is no more than $2\lceil d^{-2/k} \rceil$, where buffer zones with both positive and negative k th coordinates are included. Hence, the total $(k-1)$ -dimensional content of $B = \cup_i B_i$ is bounded as

$$S(B) < 2S_{k-1}d\lceil d^{-2/k} \rceil = O(d^{(k-2)/k}),$$

and $S(W) = O(d^{1/k})$. Thus,

$$\begin{aligned} \Delta_{\text{LSC}}(k, d) &\geq \frac{\Delta_T S(T)}{S_k} \\ &= \Delta_T \frac{S_k - S(W) - S(B)}{4\pi} \\ &= \left(\frac{\Delta_{\Lambda_{k-2}} V_{k-1}}{2V_{k-2} \sqrt{1 - c_{k-2}^2}} - O(d^{1/k}) \right) \left(\frac{S_k - O(d^{1/k})}{S_k} \right) \\ &= \frac{\Delta_{\Lambda_{k-2}} V_{k-1}}{2V_{k-2} \sqrt{1 - c_{k-2}^2}} - O(d^{1/k}), \end{aligned} \tag{D.17}$$

where (D.17) follows from (D.16). Since layers of Λ_{k-1} within Λ_k are separated by a distance of $\sqrt{1 - c_{k-1}^2}$ and each lattice point is distance 1 from an adjacent point, it follows that

$$\Delta_{\Lambda_k} = \frac{\Delta_{\Lambda_{k-1}} V_k (\frac{1}{2})^k}{V_{k-1} (\frac{1}{2})^{k-1} \sqrt{1 - c_{k-1}^2}} = \frac{\Delta_{\Lambda_{k-1}} V_k}{2V_{k-1} \sqrt{1 - c_{k-1}^2}}. \tag{D.18}$$

Thus, $\Delta_{\text{LSC}}(k, d) \geq \Delta_{\Lambda_{k-1}} - O(d^{1/k})$. ■

REFERENCES

- [1] J.-P. Adoul and M. Barth, "Nearest neighbor algorithm for spherical codes from the Leech lattice," *IEEE Trans. Inform. Theory*, vol. 34, no. 5, pp. 1188–1202, Sept. 1988.
- [2] J.-P. Adoul, C. Lamblin, and A. Leguyader, "Base-band speech coding at 2400 bps using spherical vector quantization," in *IEEE Int. Conf. Acoustics, Speech, Signal Processing*, 1984, pp. 1.12.1–1.12.4.
- [3] T. J. Aird and J. R. Rice, "Systematic search in high dimensional sets," *SIAM J. Numer. Alg.*, vol. 14, pp. 296–312, 1977.
- [4] T. M. Apostol, *Calculus*. New York, NY: John Wiley & Sons, 1967.
- [5] J. T. Astola, "The Tietäväinen bound for spherical codes," *Discrete Appl. Math.*, vol. 7, no. 1, pp. 17–21, 1984.
- [6] Y. Be'ery, B. Shahar, and J. Snyders, "Fast decoding of the Leech lattice," *IEEE J. Select. Area Commun.*, vol. 7, no. 6, pp. 959–966, Aug. 1989.
- [7] T. Berger, *Rate Distortion Theory*. Englewood Cliffs, NJ: Prentice-Hall, 1971.
- [8] E. M. Biglieri and M. Elia, "Optimum permutation modulation codes and their asymptotic performance," *IEEE Trans. Inform. Theory*, vol. 22, pp. 751–753, Nov. 1976.
- [9] R. E. Blahut, "Computation of channel capacity and rate-distortion functions," *IEEE Trans. Inform. Theory*, vol. IT-18, no. 4, July 1972.
- [10] K. Böröczky, "Packing of spheres in spaces of constant curvature," *Acta Math. Acad. Scient. Hung.*, vol. 32, pp. 243–261, 1978.
- [11] P. G. Boyvalenkov, D. P. Danev, and S. P. Bumova, "Upper bounds on the minimum distance of spherical codes," *IEEE Trans. Inform. Theory*, vol. 42, no. 5, pp. 1576–1581, Sept. 1996.
- [12] A. G. Burr, "Spherical codes for m -ary code shift keying," in *2nd IEE Nat. Conf. Telecomm.*, Apr. 1989, pp. 67–72.
- [13] J. H. Conway and N. J. A. Sloane, "A lower bound on the average error of vector quantizers," *IEEE Trans. Inform. Theory*, vol. IT-31, no. 1, pp. 106–109, Jan. 1985.
- [14] J. H. Conway and N. J. A. Sloane, *Sphere Packings, Lattices, and Groups*. New York, NY: Springer-Verlag, 1993.
- [15] J. H. Conway and N. J. A. Sloane, "The antipode construction for sphere packings," *Inventiones Math.*, 1995, submitted.

- [16] H. S. M. Coxeter, *Twelve Geometric Essays*. Carbondale, IL: Southern Illinois University Press, 1968.
- [17] P. Delsarte, J. M. Goethals, and J. J. Seidel, "Spherical codes and designs," *Geom. Dedicata*, vol. 6, pp. 363–388, 1977.
- [18] A. A. El Gamal, L. A. Hemachandra, I. Shperling, and V. K. Wei, "Using simulated annealing to design good codes," *IEEE Trans. Inform. Theory*, vol. IT-33, no. 1, pp. 116–123, Jan. 1987.
- [19] T. Ericson and V. Zinoviev, "On spherical codes generating the kissing number in dimensions 8 and 24," *Discrete Math.*, vol. 106/107, pp. 199–207, 1992.
- [20] T. Ericson and V. Zinoviev, "Spherical codes from the hexagonal lattice," in *Communications and Cryptography, Two Sides of One Tapestry*, R. E. Blahut, D. J. Costello, Jr., U. Maurer, and T. Mittelholzer, Eds., Dordrecht, The Netherlands: Kluwer Academic Publishers, 1994, pp. 109–114.
- [21] T. Ericson and V. Zinoviev, "Spherical codes generated by binary partitionings of symmetric pointsets," *IEEE Trans. Inform. Theory*, vol. 41, no. 1, pp. 107–129, Jan. 1995.
- [22] M. V. Eyuboğlu and G. D. Forney, "Lattice and trellis quantization with lattice- and trellis-bounded codebooks—high-rate theory for memoryless sources," *IEEE Trans. Inform. Theory*, vol. 39, no. 1, pp. 46–59, Jan. 1993.
- [23] L. Fejes Tóth, "Kugelunterdeckungen und Kugelüberdeckungen in Räumen konstanter Krümmung," *Archiv Math.*, vol. 10, pp. 307–313, 1959.
- [24] T. R. Fischer, "A pyramid vector quantizer," *IEEE Trans. Inform. Theory*, vol. IT-32, no. 4, pp. 568–583, July 1986.
- [25] T. R. Fischer, "Geometric source coding and vector quantization," *IEEE Trans. Inform. Theory*, vol. 35, no. 1, pp. 137–145, Jan. 1989.
- [26] T. R. Fischer and K. Malone, "Transform coding of speech with pyramid vector quantization," in *Conf. Rec. MILCOM*, 1985, pp. 620–623.
- [27] P. E. Fleischer, "Sufficient conditions for achieving minimum distortion in a quantizer," *IEEE Int. Conv. Rec., Part 1*, pp. 104–111, 1964.
- [28] R. Gallager, *Information Theory and Reliable Communication*. New York, NY: Wiley, 1968.
- [29] J. Gao, "Iteratively maximum likelihood decodable spherical codes," Ph.D. dissertation, Syracuse University, Dec. 1984.
- [30] J. Gao, L. D. Rudolph, and C. R. P. Hartmann, "Iteratively maximum likelihood decodable spherical codes and a method for their construction," *IEEE Trans. Inform. Theory*, vol. 34, no. 3, pp. 480–485, May 1988.
- [31] A. Gersho and R. M. Gray, *Vector Quantization and Signal Compression*. Boston, MA: Kluwer Academic Publishers, 1993.
- [32] J. D. Gibson and K. Sayood, "Lattice quantization," in *Adv. Electronics Electron Phys.*, P. Hawkes, Ed., vol. 72, New York: Academic, 1988, pp. 259–330.

- [33] M. Goldberg, "Packing of 18 equal circles on a sphere," *Elem. Math.*, vol. 20, pp. 59–61, 1965.
- [34] M. Goldberg, "An improved packing of 33 equal circles on a sphere," *Elem. Math.*, vol. 22, pp. 110–112, 1967.
- [35] M. Goldberg, "Packing of 19 equal circles on a sphere," *Elem. Math.*, vol. 22, pp. 108–110, 1967.
- [36] I. S. Gradshteyn and I. M. Ryzhik, *Table of Integrals, Series, and Products*. Orlando, FL: Academic Press, Inc., 1980.
- [37] T. C. Hales, "The status of the Kepler conjecture," *The Mathematical Intelligencer*, vol. 16, no. 3, pp. 47–58, 1994.
- [38] J. Hamkins and K. Zeger, "Asymptotically efficient spherical codes—Part I: Wrapped spherical codes." Submitted to *IEEE Trans. Inform. Theory*, Dec. 1995.
- [39] J. Hamkins and K. Zeger, "Asymptotically efficient spherical codes—Part II: Laminated spherical codes." Submitted to *IEEE Trans. Inform. Theory*, Dec. 1995.
- [40] J. Hamkins and K. Zeger, "Asymptotically optimal spherical codes," in *Proc. IEEE Conf. Inform. Sci. Syst.*, Mar. 1995, pp. 52–57.
- [41] J. Hamkins and K. Zeger, "Asymptotically optimal spherical codes," in *IEEE Int. Symp. Inform. Theory*, Sept. 1995, p. 184.
- [42] J. Hamkins and K. Zeger, "Wrapped spherical codes," in *Proc. IEEE Conf. Inform. Sci. Syst.*, Mar. 1996.
- [43] W.-Y. Hsiang, "Sphere packings and spherical geometry—Kepler's conjecture and beyond." preprint, Center for Pure and Applied Mathematics, University of California, Berkeley, July 1991.
- [44] W.-Y. Hsiang, "On the sphere packing problem and the proof of Kepler's conjecture," *Int. J. Math.*, vol. 4, no. 5, pp. 739–831, 1993.
- [45] W.-Y. Hsiang, "A rejoinder to Hales's article," *Math. Intelligencer*, vol. 17, no. 1, pp. 35–42, 1995.
- [46] N. S. Jayant and P. Noll, *Digital Coding of Waveforms*. Englewood Cliffs, NJ: Prentice-Hall, 1984.
- [47] D. G. Jeong and J. D. Gibson, "Uniform and piecewise uniform lattice vector quantization for memoryless Gaussian and Laplacian sources," *IEEE Trans. Inform. Theory*, vol. 39, no. 3, pp. 786–803, May 1993.
- [48] G. A. Kabatyanskii and V. I. Levenšteĭn, "Bounds for packings on a sphere and in space (English translation)," *Prob. Pered. Inform.*, vol. 14, no. 1, pp. 3–25, 1978.
- [49] J. K. Karlof, "Decoding spherical codes for the Guassian channel," *IEEE Trans. Inform. Theory*, vol. 39, no. 1, pp. 60–65, Jan. 1993.
- [50] J. F. Kenney, *Mathematics of Statistics*, 6th ed. New York, NY: D. Van Nostrand Company, Inc., 1941.

- [51] D. A. Kottwitz, "The densest packing of equal circles on a sphere," *Acta Cryst.*, vol. A47, pp. 158–165, 1991.
- [52] G. Lachaud and J. Stern, "Polynomial-time construction of codes ii," *IEEE Trans. Inform. Theory*, vol. 40, no. 4, pp. 1140–1146, 1994.
- [53] R. Laroia and N. Farvardin, "Trellis-based scalar-vector quantizer for memoryless sources," *IEEE Trans. Inform. Theory*, vol. 40, no. 3, pp. 860–870, May 1994.
- [54] V. I. Levenšteĭn, "On bounds for packing in n -dimensional Euclidean space," *Sov. Math. Dokl.*, vol. 20, no. 2, pp. 417–421, 1979.
- [55] V. I. Levenšteĭn, "Bounds on the maximal cardinality of a code with bounded modules of the inner product," *Soviet Math. Dokl.*, vol. 25, no. 2, pp. 526–531, 1982.
- [56] Y. L. Linde, A. Buzo, and R. M. Gray, "An algorithm for vector quantizer design," *IEEE Trans. Commun.*, vol. COM-28, pp. 84–95, Jan. 1980.
- [57] J. H. Lindsey II, "Sphere-packing in R^3 ," *Mathematika*, vol. 33, pp. 137–147, 1986.
- [58] S. P. Lloyd, "Least squares quantization in PCM," tech. rep., Bell Laboratories, 1957. Republished in the March 1982 special issue on quantization of *IEEE Trans. Inform. Theory*.
- [59] A. Lowry, S. Hossain, and W. Millar, "Binary search trees for vector quantisation," in *IEEE Int. Conf. Acoustics, Speech, Signal Processing*, 1987, pp. 51.8.1–51.8.3.
- [60] K. T. Malone and T. R. Fischer, "Contour-gain vector quantization," *IEEE Trans. Acoust. Speech Sig. Process.*, vol. 36, no. 6, pp. 862–870, June 1988.
- [61] M. W. Marcellin, "On entropy-constrained trellis coded quantization," *IEEE Trans. Commun.*, vol. 42, no. 1, pp. 14–16, Jan. 1994.
- [62] M. W. Marcellin and T. Fischer, "Trellis coded quantization of memoryless and Gauss-Markov sources," *IEEE Trans. Commun.*, vol. 38, no. 1, pp. 82–93, Jan. 1990.
- [63] J. Max, "Quantizing for minimum distortion," *IRE Trans. Inform. Theory*, vol. 6, pp. 7–12, March 1960.
- [64] A. D. McLaren, "Optimal numerical integration on a sphere," *Math. Comp.*, vol. 17, pp. 361–383, 1963.
- [65] T. W. Melnyk, O. Knop, and W. R. Smith, "Extremal arrangements of points and unit charges on a sphere: Equilibrium configurations revisited," *Can. J. Chem.*, vol. 55, pp. 1745–1761, 1977.
- [66] D. Miller, K. Rose, and P. A. Chou, "Deterministic annealing for trellis quantizer and HMM design using Baum-Welch re-estimation," in *IEEE Int. Conf. Acoustics, Speech, Signal Processing*, Apr. 1994, pp. V–261–V–264.
- [67] N. Moayeri and D. L. Neuhoff, "Theory of lattice-based fine-coarse vector quantization," *IEEE Trans. Inform. Theory*, vol. 37, no. 4, pp. 1072–1084, July 1991.
- [68] P. Noll and R. Zelinski, "Bounds on quantizer performance in the low bit-rate region," *IEEE Trans. Commun.*, vol. COM-26, no. 2, pp. 300–304, Feb. 1978.

- [69] K. J. Nurmella, “Constructing spherical codes by global optimization methods,” Tech. Rep. 32, Helsinki University of Technology, Otaniemi, Finland, Feb. 1995.
- [70] A. M. Odlyzko and N. J. A. Sloane, “New bounds on the number of unit spheres that can touch a unit sphere in n dimensions,” *J. Combinatorial Theory, Series A*, vol. 26, pp. 210–214, 1979.
- [71] J. Pan and T. R. Fischer, “Two-stage vector quantization—lattice vector quantization,” *IEEE Trans. Inform. Theory*, vol. 41, no. 1, pp. 155–163, Jan. 1995.
- [72] W. A. Pearlman, “Sliding-block and random source coding with constrained size reproduction alphabets,” *IEEE Trans. Commun.*, vol. COM-30, no. 8, pp. 1859–1867, Aug. 1982.
- [73] K. Popat and K. Zeger, “Robust quantization of memoryless sources using dispersive FIR filters,” *IEEE Trans. Commun.*, vol. 40, no. 11, pp. 1670–1674, Nov. 1992.
- [74] R. A. Rankin, “The closest packing of spherical caps in n dimensions,” *Proc. Glasgow Math. Assoc.*, vol. 2, pp. 139–144, 1955.
- [75] C. A. Rogers, “The packing of equal spheres,” *Proc. London Math. Soc.*, vol. 8, pp. 609–620, 1958.
- [76] M. C. Rost and K. Sayood, “The root lattices as low bit rate vector quantizers,” *IEEE Trans. Inform. Theory*, vol. 34, no. 5, pp. 1053–1058, Sept. 1988.
- [77] D. J. Sakrison, “A geometric treatment of the source encoding of a Gaussian random variable,” *IEEE Trans. Inform. Theory*, vol. IT-14, no. 3, pp. 481–486, May 1968.
- [78] D. G. Sampson and M. Ghanbari, “Fast lattice-based gain-shape vector quantization for image-sequence coding,” *IEE Proc.*, vol. 140, no. 1, pp. 56–66, Feb. 1993.
- [79] L. Schläfli, “Réduction d’une intégrale multiple, qui comprend l’arc de cercle et l’aire du triangle sphérique comme cas particuliers,” *Gesammelte mathematische Abhandlungen*, vol. 2, pp. 164–190, 219–258, 1885.
- [80] D. Slepian, “Permutation modulation,” *Proc. IEEE*, vol. 53, pp. 228–236, Mar. 1965.
- [81] N. J. A. Sloane, “Tables of sphere packings and spherical codes,” *IEEE Trans. Inform. Theory*, vol. IT-27, no. 3, pp. 327–338, May 1981.
- [82] N. J. A. Sloane. Anonymous ftp from netlib.att.com in directory netlib/att/math/sloane/doc, 1994.
- [83] H. Stark and J. W. Woods, *Probability, Random Processes, and Estimation Theory for Engineers*, 2nd ed. Englewood Cliffs, NJ: Prentice Hall, 1994.
- [84] P. F. Swaszek and J. B. Thomas, “Multidimensional spherical coordinates quantization,” *IEEE Trans. Inform. Theory*, vol. IT-29, no. 4, pp. 570–576, July 1983.
- [85] E. Székely, “Sur le problème de Tammes,” *Ann. Univ. Sci. Budapest. Eötvös, Sect. Math.*, vol. 17, pp. 157–175, 1974.
- [86] P. M. L. Tammes, “On the origin of number and arrangement of the places of exit on the surface of pollen-grains,” *Recueil des travaux botaniques néerlandais*, vol. 27, pp. 1–84, 1930.

- [87] A. V. Trushkin, "Sufficient conditions for uniqueness of a locally optimal quantizer for a class of convex error weighting functions," *IEEE Trans. Inform. Theory*, vol. IT-28, pp. 187–198, Mar. 1982.
- [88] H.-C. Tseng and T. R. Fischer, "Transform and hybrid transform/DPCM coding of images using pyramid vector quantization," *IEEE Trans. Commun.*, vol. COM-35, pp. 79–86, 1987.
- [89] G. Ungerboeck, "Channel coding with multilevel/phase signals," *IEEE Trans. Inform. Theory*, vol. IT-28, no. 1, pp. 55–67, 1981.
- [90] A. Vardy, "A new sphere packing in 20 dimensions," *Inventiones Math.*, vol. 121, no. 1, pp. 119–133, July 1995.
- [91] A. Vardy and Y. Be'ery, "Maximum likelihood decoding of the Leech lattice," *IEEE Trans. Inform. Theory*, vol. 39, no. 4, pp. 1435–1444, July 1993.
- [92] P. Vogel, "Analytical coding of Gaussian sources," *IEEE Trans. Inform. Theory*, vol. 40, no. 5, pp. 1639–1645, Sept. 1994.
- [93] H. S. Wang and N. Moayeri, "Trellis coded vector quantization," *IEEE Trans. Commun.*, vol. 40, no. 8, pp. 1273–1276, Aug. 1992.
- [94] S. G. Wilson and D. W. Lytle, "Trellis encoding of continuous-amplitude memoryless sources," *IEEE Trans. Inform. Theory*, vol. IT-23, pp. 404–409, May 1977.
- [95] A. Wyner, "Capabilities of bounded discrepancy decoding," *The Bell System Technical Journal*, vol. 44, pp. 1061–1122, July-Aug. 1965.
- [96] A. Wyner, "Random packings and coverings of the unit n -sphere," *Bell Syst. Tech. J.*, pp. 2111–2118, Nov. 1967.
- [97] I. M. Yaglom, "Some results concerning distributions in n -dimensional space." Appendix to Russian edition of Fejes Tóth's *Lagerungen in der Ebene, auf der Kugel und in Raum*, 1958.
- [98] Z. Yu, "On spherical codes and coded modulation," M.S. thesis, University of Hawaii at Manoa, 1992.
- [99] P. L. Zador, "Asymptotic quantization error of continuous signals and the quantization dimension," *IEEE Trans. Inform. Theory*, vol. IT-28, no. 2, pp. 139–149, Mar. 1982.

VITA

Jon Hamkins was born on September 21, 1968, in Racine, Wisconsin. He received the B.S. degree with honor from the California Institute of Technology in 1990 and the M.S. degree from the University of Illinois at Urbana-Champaign in 1993. In 1990 he was a Teaching Assistant at the California Institute of Technology. From 1990 to 1993, he was a Teaching Assistant at the University of Illinois at Urbana-Champaign. From 1994 to 1996 he was a Research Assistant at the University of Illinois at Urbana-Champaign. He has co-authored the following papers:

J. Hamkins and K. Zeger, Asymptotically Efficient Spherical Codes—Part I: Wrapped Spherical Codes, *IEEE Trans. Inform. Theory*, (submitted Dec. 1995).

J. Hamkins and K. Zeger, Asymptotically Efficient Spherical Codes—Part II: Laminated Spherical Codes, *IEEE Trans. Inform. Theory*, (submitted Dec. 1995).

J. Hamkins and K. Zeger, Improved Bounds on Maximum Size Binary Radar Arrays, *IEEE Trans. Inform. Theory*, (to appear), May 1997.

J. Hamkins and K. Zeger, Wrapped Spherical Codes, *Proc. IEEE Conf. Inform. Sci. Syst.*, March 1996, p. 290-295.

J. Hamkins and K. Zeger, Asymptotically Optimal Spherical Codes, *Proc. Int. Symp. Inform. Theory*, British Columbia, Canada, Sept. 1995, p. 184.

J. Hamkins and K. Zeger, Asymptotically Optimal Spherical Codes, *Proc. Conf. Inform. Sci. Syst.*, Johns Hopkins University, March 1995, p. 52-57.

J. Hamkins and D. Brown, Switchbox Routing with Movable Terminals, *Proc. Great Lakes Symp. VLSI*, Kalamazoo, MI, p. 57-61, March 1993.

J. Hamkins, Routing in a Convex Grid with k -ary Overlap, M.S. thesis, University of Illinois at Urbana-Champaign, Jan. 1993.

J. Hamkins and D. Brown, Routing in a Rectangle with k -ary Overlap, *Proc. Great Lakes Symposium on VLSI*, Kalamazoo, MI, p. 144-151, Feb. 1992.